



■ International Telecommunication Union



Handbook

Terrestrial land mobile radiowave propagation in the VHF/UHF bands

THE RADIOPHONIC SECTOR OF ITU

The role of the Radiophonic Sector is to ensure the rational, equitable, efficient and economical use of the radio-frequency spectrum by all radiocommunication services, including satellite services, and carry out studies without limit of frequency range on the basis of which Recommendations are adopted.

The regulatory and policy functions of the Radiocommunication Sector are performed by World and Regional Radiocommunication Conferences and Radiocommunication Assemblies supported by Study Groups.

Inquiries about radiocommunication matters

Please contact:

ITU
Radiocommunication Bureau
Place des Nations
CH-1211 Geneva 20
Switzerland

Telephone:	+41 22 730 5800
Fax:	+41 22 730 5785
E-mail:	brmail@itu.int
Web:	www.itu.int/itu-r

Placing orders for ITU publications

Please note that orders cannot be taken over the telephone. They should be sent by fax or e-mail.

ITU
Sales and Marketing Division
Place des Nations
CH-1211 Geneva 20
Switzerland

Telephone:	+41 22 730 6141 English
Telephone:	+41 22 730 6142 French
Telephone:	+41 22 730 6143 Spanish
Fax:	+41 22 730 5194
Telex:	421 000 uit ch
Telegram:	ITU GENEVE
E-mail:	sales@itu.int

The Electronic Bookshop of ITU: www.itu.int/publications



International Telecommunication Union

Handbook
***Terrestrial land mobile
radiowave propagation
in the VHF/UHF bands***

Edition 2002

Radiocommunication Bureau

TABLE OF CONTENTS

	Page
FOREWORD.....	vii
ACKNOWLEDGEMENTS	ix
CHAPTER 1 – INTRODUCTION.....	1
1.1 Purpose	1
1.2 How to use this Handbook	1
1.3 Applicable ITU-R texts	2
CHAPTER 2 – APPLICATIONS TO LAND MOBILE RADIO SYSTEMS.....	5
2.1 General network architecture	5
2.2 Private mobile radio (dispatch) systems.....	7
2.3 Public radio paging networks.....	9
2.4 Public cordless telephony systems	10
2.5 Public cellular mobile telephony systems	12
2.6 Useful references	15
CHAPTER 3 – FUNDAMENTAL PROPAGATION PRINCIPLES.....	17
3.1 Propagation mechanisms.....	17
3.1.1 Free space.....	17
3.1.2 Reflections.....	17
3.1.3 Reflection from ground	18
3.1.4 Reflection from buildings.....	18
3.1.5 Diffraction	19
3.1.6 Refraction	20
3.2 Shadowing and rapid fading.....	20
3.2.1 Shadowing	20
3.2.2 Rapid fading	21
3.3 The statistics of location variability	21
3.4 References	23

	Page
CHAPTER 4 – MODELLING TECHNIQUES FOR PROPAGATION PREDICTION ..	25
4.1 Generalized point-to-area models	25
4.1.1 Okumura and Hata models	26
4.1.2 Testing and tuning of generalized empirical point-to-area models	28
4.2 Methods using terrain and ground cover information	33
4.3 Ray tracing, GTD-UTD, parabolic and integral equation methods	35
4.3.1 Ray tracing and geometric theory of diffraction (GTD) – uniform theory of diffraction (UTD) methods	35
4.3.2 Parabolic equation (PE) methods	36
4.3.3 Integral equation (IE) methods	36
4.4 Diffraction modelling	37
4.4.1 Summary of earlier methods, spherical Earth, knife-edge, and cylinder models..	37
4.4.2 Recommendation ITU-R P.526	44
4.5 Propagation model considerations	45
4.5.1 System planning	47
4.5.2 Interference assessment and spectrum management	47
4.5.3 Comparison of measurements and predictions	48
4.6 References	48
CHAPTER 5 – TERRAIN DATABASES (AVAILABILITY AND USE).....	51
5.1 Terrain height	51
5.2 Ground cover	53
5.3 Use of databases in available modelling and planning methods	55
5.3.1 Area metaphor	56
5.3.2 Profile considerations	56
5.4 References	57
CHAPTER 6 – PROPAGATION WITHIN AND INTO BUILDINGS AND UNDERGROUND	59
6.1 Site-specific approaches	59

	Page
6.2 Site-general approaches.....	60
6.3 Combined (indoor-outdoor and outdoor-indoor) propagation	63
6.4 References	64
CHAPTER 7 – ANTENNA CONSIDERATIONS.....	67
7.1 Emission of radiowaves	67
7.2 Reference isotropic radiator and dipole antenna	68
7.3 Antenna characteristics	70
7.4 Base station antennas	71
7.5 Mobile station antennas.....	72
7.6 Impact of the land mobile environment	72
7.6.1 Depolarization phenomena in the land mobile environment	72
7.6.2 Antenna height gain: base and mobile	73
7.6.3 Correlation/space diversity.....	74
7.6.4 Realizable antenna gain of the vehicular mobile station.....	74
7.6.5 Body loss	74
7.7 References	75
CHAPTER 8 – ENVIRONMENTAL NOISE	77
8.1 Radio system performance factors	77
8.2 Noise terms and background	77
8.2.1 Noise components	77
8.2.2 Noise power and noise temperature	77
8.2.3 Noise factor	78
8.2.4 Noise factor for cascaded components.....	79
8.2.5 Noise factor for receiving systems	81
8.3 Antenna noise figure information in Recommendation ITU-R P.372	83
8.4 Noise measurements for specific applications	85
8.5 References	85
CHAPTER 9 – CHANNEL CHARACTERISTICS FOR DIGITAL MODULATION SCHEMES	87
9.1 Characterization in time domain	87
9.2 Characterization in frequency domain	88
9.3 Characterization in angular domain and Doppler spectra	89
9.4 WSSUS channels.....	89

	Page
9.5 Modelling the wideband channel	90
9.5.1 Site-specific channel models.....	90
9.5.2 Site general channel models for system simulation	90
9.6 References	92
BIBLIOGRAPHY	93
ITU-R texts.....	93
Books	93
Data-sets, online	93
Monographs and reports.....	94
Conference and journal papers.....	94
APPENDIX A – PRACTICAL EXAMPLES	101
A.1 Example of testing and tuning generalized empirical point-to-area models (see also § 4.1.2).....	101
A.1.1 Model testing (see also § 4.1.2.2).....	101
A.1.2 Choosing the best model (see also § 4.1.2.2).....	103
A.1.3 Model tuning (see also § 4.1.2.3)	103
APPENDIX B – UNIT CONVERSIONS	105
B.1 Propagation losses versus field strength.....	105
B.2 Decibel units and logarithmic scale	105
B.3 Unit conversions.....	107
B.4 References	107

FOREWORD

Much of modern life, in developing and developed countries, is predicated on the expectation that radiocommunication will be available, mobile, and immediate. Telecommunication agencies and businesses around the world have to be able to establish and maintain mobile communication infrastructure that will meet the quality of communication required.

An understanding of the propagation mechanisms through natural and man-made environments is a basic element of the culture of a telecommunications engineer. That knowledge is needed in planning and optimizing the technical support for mobile radiocommunications to meet customer needs. Natural variability, both spatial and temporal, and the effects of terrain and topography cannot be controlled but they can be accommodated provided that the effect they have on systems is known.

In the case of terrestrial land mobile services, recent years have seen an extraordinary increase in customer demand and use. In establishing terrestrial mobile networks many technical innovations have been developed, one of these being an increase in the understanding of radiowave propagation. The International Telecommunication Union (ITU-R) is dedicated to providing standard methods (Recommendations) for calculating the performance of radio systems within a variable environment. This ITU-R Handbook gives the technical basis for predicting the radio propagation in point-to-point, point-to-area, and point-to-multipoint mobile networks. The Handbook focuses on the use of ITU-R Recommendations for the regulating, planning, engineering and deployment of land mobile services. The reader is encouraged to seek further information from the ITU-R (<http://www.itu.int/ITU-R>).

David G. Cole
Chairman, Radiocommunication Study Group 3,
Radiowave Propagation

ACKNOWLEDGEMENTS

The material in this Handbook was developed by a group of participants in ITU-R Working Party 3K. The Rapporteur for this work wishes to thank the following individuals who made substantial contributions to the Handbook:

Mr. Richard Biby, United States of America
Mr. Eldon J. Haakinson, United States of America
Dr. Thomas Kürner, Germany
Mr. Paul McKenna, United States of America
Dr. Artūras Medešis, Lithuania
Mr. Ian Pullen, United Kingdom
Prof. Mauro Soares de Assis, Brazil
Dr. James Whitteker, Canada

In addition, the Rapporteur wishes to thank Mr. Eldon J. Haakinson and Mr. Rainer Großkopf in their capacities as successive Chairmen of Working Party 3K for their support and encouragement.

Thomas N. Rubinstein
Rapporteur

CHAPTER 1

INTRODUCTION

1.1 Purpose

The purpose of this Handbook is to introduce the engineer or network designer who has little or no experience in radiowave propagation to those concepts that are necessary to understand how radiowave propagation principles are applied to the design of terrestrial land mobile radio systems.

1.2 How to use this Handbook

The primary intended audience for this Handbook is users of ITU-R electromagnetic propagation Recommendations who require additional information concerning the background and application of the methods found in these Recommendations, particularly the Recommendations applying to terrestrial, land mobile services in the VHF and UHF bands. The ITU-R radiowave propagation Recommendations are delineated by a Recommendation number and a version number (e.g. P.1144-2). In this Handbook Recommendation will generally be referenced without the latest version number but the reader is advised to use the latest version for practical work. The Working Parties of Study Group 3 are constantly engaged in studies intended to improve and broaden existing Recommendations, as well as the development of new Recommendations. Therefore, additional materials have been included with a view toward the future.

Chapter 2 of the Handbook discusses common land mobile radio system applications, broadly subdivided into vehicular- and hand-portable systems. The emphasis of this Chapter is to place these applications within the context of the expected communication range(s), environment(s) and channel characteristics of each application. The final section of the Chapter addresses the choices of method by which information is transmitted, i.e., modulation methods, and the impacts of the channel characteristics on these methods. A user can place the land mobile system that he is designing or planning within the framework of these applications and identify the important considerations that affect his system by reading this Chapter.

Chapter 3 discusses the fundamentals of terrestrial electromagnetic wave propagation. The first section of the Chapter introduces the deterministic concepts of electromagnetic wave reflection, refraction, diffraction and multipath. For the case of a fixed transmitter and receiver and a well-mixed atmosphere, these govern the long-term (hourly) median signal strengths. The remaining two sections of this Chapter then introduce the seemingly random nature of the fluctuations of the signal strength about the long-term median as the mobile transmitter or receiver (or both) move about over short distances. A user should read this Chapter to become acquainted with the fundamental concepts of a broad range of radio propagation models.

Chapter 4 discusses modelling techniques for outdoor radio propagation predictions. These are broadly subdivided into site-general, empirically-based models and more deterministic, site-specific models. Also included in this Chapter are brief sections on modelling techniques such as ray tracing, GTD-UTD methods and parabolic equation and integral equation methods. Due to their importance, diffraction modelling methods are revisited and finally, a section on the considerations on the choice of which propagation models to use is included. The user should read this section to obtain details of the various modelling methods available for use in propagation predictions.

Chapter 5 discusses the availability and use of terrain and land-use/land-cover databases. These are particularly helpful when using a site-specific propagation model, but also useful for some types of site-general models.

Chapter 6 discusses considerations for propagation within and into/out of buildings. Here again, models are subdivided into site-general and site-specific models. Users desiring methods for propagation predictions for these increasingly important cases should read this Chapter.

Chapter 7 covers antenna considerations as these relate to the propagation problem, while **Chapter 8** covers the effects of environmental radio noise on radio system performance. Both are important in designing or planning a detailed radio communication system. **Chapter 9** treats the important case of the channel transfer function/channel impulse response for digital modulation methods. These are very important in determining the expected performance of a digitally modulated system bit error ratio or symbol error rate in the presence of noise and/or interference. The Handbook concludes with a Bibliography and two Appendices on practical examples and unit conversions.

1.3 Applicable ITU-R texts

The following ITU-R texts cover areas relevant to the scope of this Handbook. A bibliography of non-ITU-R texts follows Chapter 9.

Recommendation ITU-R P.833-3 – Attenuation in vegetation, International Telecommunication Union, Geneva, 2001.

Recommendation ITU-R P.525-2 – Calculation of free space attenuation, International Telecommunication Union, Geneva, 2000.

Recommendation ITU-R P.341-5 – The concept of transmission loss for radio links, International Telecommunication Union, Geneva, 2000.

Recommendation ITU-R P.1058-2 – Digital topographic databases for propagation studies, International Telecommunication Union, Geneva, 2000.

Recommendation ITU-R P.368-7 – Ground-wave propagation curves for frequencies between 10 kHz and 30 MHz, International Telecommunication Union, Geneva, 2000.

Recommendation ITU-R P.1144-2 – Guide to the application of the propagation methods of Radiocommunication Study Group 3, International Telecommunication Union, Geneva, 2001.

Handbook on radiowave propagation information for predictions for terrestrial path communications, International Telecommunication Union, Geneva, in preparation.

Handbook on radio spectrum monitoring, International Telecommunication Union , Geneva, 1995.

Recommendation ITU-R P.1407 – Multipath propagation and parameterization of its characteristics, International Telecommunication Union, 2000.

Recommendation ITU-R P.529-3 – Prediction methods for the terrestrial land mobile service in the VHF and UHF bands, International Telecommunication Union, Geneva, 2000. (Superseded by Recommendation ITU-R P.1546)

Recommendation ITU-R P.452-10 – Prediction procedure for the evaluation of microwave interference between stations on the surface of the Earth at frequencies above about 0.7 GHz, International Telecommunication Union, Geneva, 2001.

Volume 2 of Handbook on Land Mobile – Principles and approaches on evolution to IMT-2000/FPLMTS, International Telecommunication Union, Geneva, 1997.

Recommendation ITU-R P.1057-1 – Probability distributions relevant to radiowave propagation modelling, International Telecommunication Union, Geneva, 2001.

Recommendation ITU-R P.526-7 – Propagation by diffraction, International Telecommunication Union, Geneva, 2001.

Recommendation ITU-R P.1411-1 – Propagation data and prediction methods for the planning of short range outdoor radiocommunication systems and radio local area networks in the frequency range 300 MHz to 100 GHz, International Telecommunication Union, Geneva, 2001.

Recommendation ITU-R P.1238-2 – Propagation data and prediction models for the planning of indoor radiocommunication systems and radio local area networks in the frequency range 900 MHz to 100 GHz, International Telecommunication Union, Geneva, 2001.

Recommendation ITU-R P.1406 – Propagation effects relating to terrestrial land mobile service in the VHF and UHF bands, International Telecommunication Union, Geneva, 2000.

Ex-CCIR Report 902 – Radiating/leaky cable systems in the land mobile service.

Handbook on land mobile (Volume 3) – Radio dispatch systems, International Telecommunication Union, Geneva (in preparation).

ITU-R P.372-7 – Radio noise, International Telecommunication Union, Geneva, 2001.

Recommendation ITU-R P.453-8 – The radio refractive index: Its formula and refractivity data, International Telecommunication Union, Geneva, 2001.

Ex-CCIR Report 880-1 – Short distance radio-wave propagation in special environments.

Report ITU-R M.2014 – Spectrum efficient digital land mobile systems for dispatch traffic, International Telecommunication Union, Geneva, 1998.

Recommendation ITU-R P.1546 – Method for point-to-area predictions for terrestrial services in the frequency range 30 to 3 000 MHz, Geneva, 2001.

Handbook on land mobile (Volume 1) – Wireless access local loop, International Telecommunication Union, Geneva, 1997.

CHAPTER 2

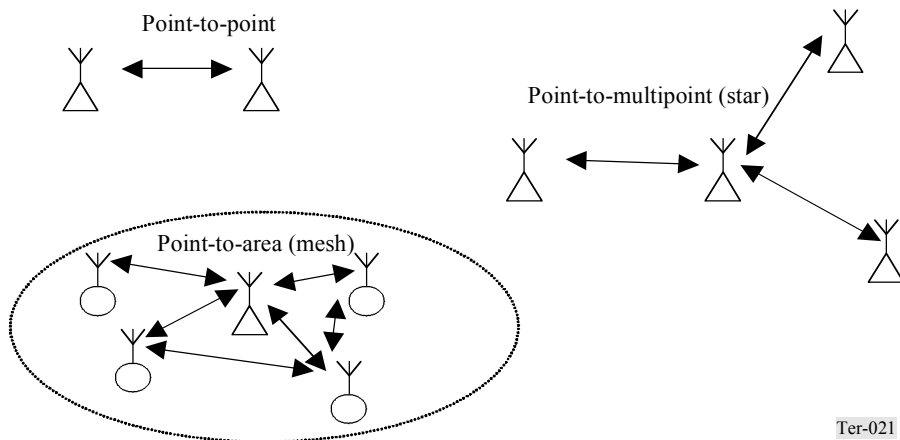
APPLICATIONS TO LAND MOBILE RADIO SYSTEMS

This Chapter provides a brief overview of typical applications in the land mobile services. Giving only a general presentation of system structure, it highlights those system features which may impact upon the scope, aims or choice of relevant propagation studies. Special attention is paid to the necessary coverage and communication range considerations.

2.1 General network architecture

One of the primary points to consider when discussing any radiocommunication system is its general network architecture. This describes the way in which communication links are established in the network and which terminals are actually communicating among themselves. Such consideration gives very important ideas on necessary propagation paths, ranges and directivities. Three of the most typical radiocommunication network architectures are shown in Fig. 2.1.

FIGURE 2.1
Typical network architectures of radiocommunication systems



Ter-021

It may be noted, that from the three architectures shown in Fig. 2.1, a point-to-area network may be considered as most representative of land mobile systems. However the other two architectures are also relevant for certain modes of operation in land mobile systems.

Point-to-point operation is most typical for fixed radiocommunication networks but may be used also in land mobile networks when mobile (transportable) terminals operate while not in motion, from some temporary fixed locations. Examples of such applications include mobile tactical radio-relay links, temporary electronic news gathering systems, etc. It is also likely that such a mode of operation may further spread within mobile systems with the introduction of advanced steerable antennas. This technique allows the tracking of a mobile remote terminal while in motion with a rotating beam of a base station antenna.

The exceptional advantage of such point-to-point mode of operation is that it allows the use of highly directional antennas, which increases the range of communication and reduces multipath effects. In such cases the propagation path is well defined, so it is often possible and advisable to use path-specific propagation prediction models.

Point-to-multipoint network architecture, also known as a star configuration, contains a central node which acts as a managing and switching point for communication with the remote stations, as well as for communications between remote stations. When only one-way communication is involved, such networks become what is well known as a broadcasting network. Although primarily a domain of fixed networks, star architectures are now often employed in radiocommunication systems, which stand on the boundary between fixed and mobile services. A good example of such application may be the so called wireless local loop (WLL) systems, often having both fixed and mobile user terminals in their structure. But even fixed terminals in WLL systems are being deployed in a simplified flexible way (sometimes even by the end subscribers themselves), without prior knowledge of terminal locations and appropriate path consideration.

Due to heavy traffic load expectations in WLL systems, they are usually planned in the frequency bands above the UHF range. However in sparsely populated areas WLL systems are often deployed at UHF frequencies, typically around 900 MHz, 1.5 GHz or 2 GHz frequency bands. In such cases, it is expected that communication ranges will be comparable with those of land mobile systems and possibly even greater, up to some 50-100 km. Therefore, if circular coverage is necessary, UHF band WLL systems employ directional antennas at base stations, arranged in several sectors over the whole 360°.

Therefore in coverage prediction of such WLL point-to-multipoint systems it is often possible to use point-to-area coverage prediction methods, but care should be taken to account for the higher antenna gain at base and remote stations. The height of remote antennas is usually taken as 10 m above ground, because they are often mounted on rooftops along with antennas for broadcast reception.

Point-to-area architecture is the essential mode of operation of traditional land mobile systems. It provides coverage of an entire area from one or more base stations on the assumption that mobile stations may appear at any time in any point of a given coverage area and may maintain a communication channel while moving within the limits of that entire coverage area. Such architecture may become a mesh network, when mobile stations may communicate directly among themselves. This is the case in traditional private mobile radio networks. In public cellular networks mobile terminals may communicate only via the central node (actually via the relevant base station and central network switching facility), hence from a pure network perspective they act as if in a star configuration. But even in the latter case, from a radio planning perspective they should be treated as point-to-area systems.

Planning of coverage areas in the point-to-area mode is a difficult task, because it is in principle impossible to foresee the exact path that radiowaves will travel. Therefore path-general models are usually employed for propagation prediction, with the assumption that the field strength will be subject to variations which may be described using statistical methods. In such planning, it is important to plan for the most reliable coverage of the entire intended coverage area, minimizing the number of “shadow” areas.

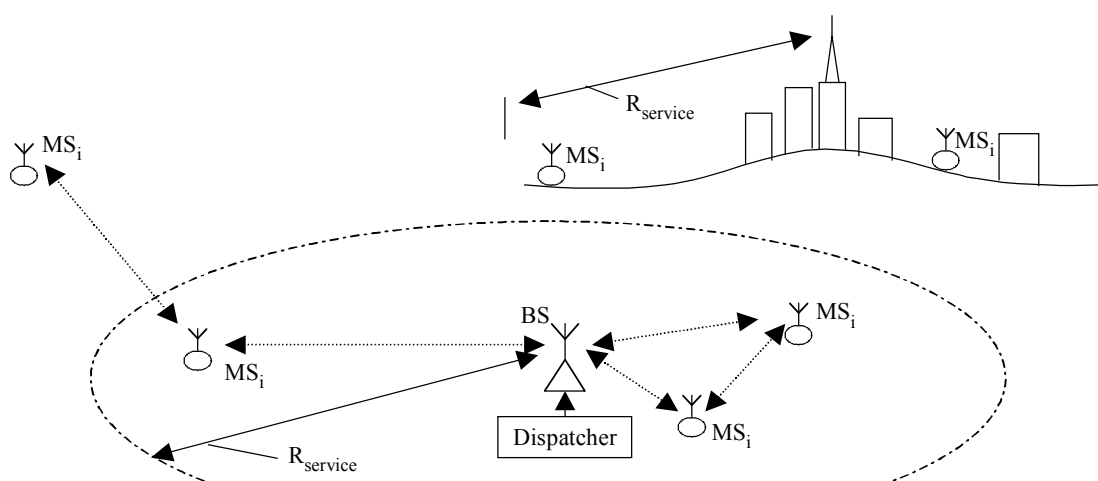
2.2 Private mobile radio (dispatch) systems

Private mobile radio (PMR) systems, also known as private dispatch systems, are the oldest and still most widely used type of land mobile applications. Deployed for the first time in 1929 as the means of communications with police patrol cars, the RF architecture of these systems remains essentially unchanged until today, although trunking has added another dimension.

The major feature of the PMR systems is that they provide instant access to a radio channel (so called push-to-talk principle) and allow communication in a mesh architecture. From the radio planning point of view, PMR systems usually represent one city or a somewhat larger administrative subdivision such as a county, a department, etc. If the area is sufficiently small and unshadowed by topographic obstacles, a single site can be used as shown in Fig. 2.2. When the number of mobile and portable radios increases or when it is necessary to cover larger territories, then additional base stations can be introduced.

Because of their simplicity and comparatively low initial and running cost, such PMR systems are a favourite choice for private mobile communications and today are widely used by emergency services, utility, transportation and taxi companies, and other companies requiring affordable mobile communications. Additionally, their dispatch-oriented operating characteristics frequently match user requirements better than would a “one-to-one” system like a public mobile telephone system.

FIGURE 2.2
PMR system in its basic principal architecture

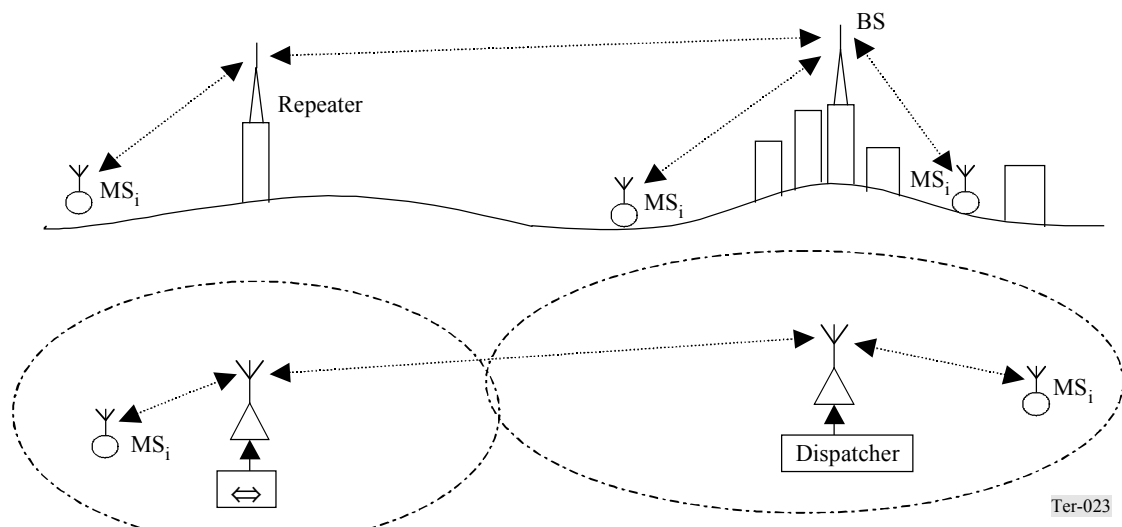


Initially working mostly at VHF frequencies, PMR systems today use many parts of the VHF/UHF frequency range, e.g. around 40 MHz, 160 MHz, 450 MHz and 900 MHz frequency bands. The typical power of base stations is 25-400 W and the power of mobile stations 2-100 W. In areas with flat topography, it is common to install base station antennas in the middle of the service area, usually on the top of high standing buildings in city centres, etc. In cities surrounded by mountains, it is common to install base stations on top of a mountain peak. Most commonly, base stations deploy omnidirectional antennas, although those in surrounding mountain ranges may use directional antennas with wide horizontal beamwidth. With the aforementioned power of transmitters, the expected radius of coverage areas ranges from 25 to 100 km.

Because of their mesh architecture, communications in the PMR systems are very sustainable. Even when a given mobile happens to be in a non-coverage spot, another nearby mobile station may act as a relay to pass a message to the central dispatch office, as shown in Fig. 2.2. Nevertheless, and especially in applications that are sensitive to overall reaction time such as emergency services, the coverage area of PMR systems should be carefully planned with a view to guaranteeing the necessary extent of coverage area and to eliminating any possible shadowed spots.

Since basic PMR systems use a simple protocol for access to a radio channel (which is only one or a few manually selectable channels per network), for extension of coverage areas the option of a repeater station configuration is usually chosen, as shown in Fig. 2.3. However, such repeater stations should be considered in the planning exercise in the same way as the central base station.

FIGURE 2.3
Use of repeater to extend coverage of PMR system



Modern large PMR networks today often use the so-called trunking technologies, which are designed to provide mobile terminals with seamless access to a larger set of available frequency channels, while retaining the essential “push-to-talk” principle of communication. At the same time, this more advanced mode of channel selection introduces the cellular principle of multiple base station deployment over larger territories. However, even in the cellularly-organized trunked PMR networks the individual base stations usually retain the same features as in a single-station network, such as omnidirectional antennas, power and communication range.

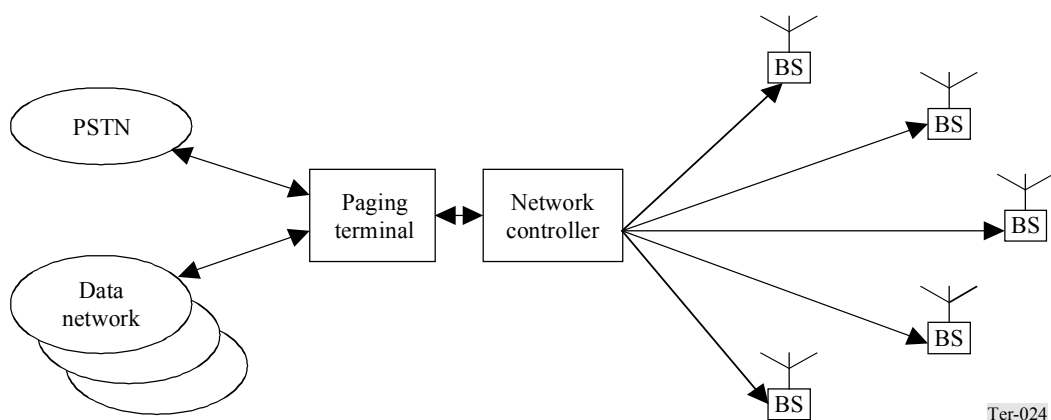
Trunking technologies also allowed the development of such systems as PAMR (public access mobile radio) networks, which are usually the same trunked PMR networks with selective calling, in which available airtime capacity is leased by network operators as virtual PMR to small businesses.

Because PMR systems are mostly used for voice communications, they usually employ narrow frequency channels with channel widths of 33/25 kHz and smaller. This means that the propagation statistics are not frequency selective and are usually considered in terms of field strength variation (fading) characterization over time and over area, that is time and location variability.

2.3 Public radio paging networks

Radio paging networks were the first widely available public mobile networks. They are intended for one-way transmission of alphanumeric messages. The basic structure of a paging network is shown in Fig. 2.4. Pages are initiated either via the public switched telephone network (PSTN) or via a direct connection to a data network or both. The paging terminal handles the page requests and queues and re-formats into a form suitable for transmission. The network controller is the interface to the paging base stations.

FIGURE 2.4
Basic structure of public radio paging network



Since paging networks work essentially in a broadcasting mode of operation, they are planned in a manner that is similar to that of broadcasting networks. Base stations usually operate at VHF or UHF frequencies, usually with one frequency per entire network, with typical power of transmitters 100-400 W and omnidirectional antennas. The expected radius of base station coverage areas for reliable outdoor reception is 50 km or more. Indoor coverage is severely reduced due to building penetration losses. For that reason, quasi-synchronous “simulcast” techniques are frequently employed. To ensure proper reception when moving between neighbouring coverage areas, the base stations in a given network transmit in a quasi-synchronous mode. This also alleviates the need for interference assessment, so network planners need only to ensure proper coverage.

Because of its broadcasting nature, path-general propagation prediction methods are very suitable for planning coverage areas in paging networks, including those methods used with conventional radio and TV broadcasting services. However, care should be taken to make an adjustment for reduced height of receiver antennas (pagers are usually worn on the belt, at approximately 1 m above ground) as well as for associated body loss which is significant for paging receivers. See the discussion on this in Chapter 7 of this Handbook.

2.4 Public cordless telephony systems

The public cordless telephony (CT) systems are derived from the previously mentioned wireless local loop systems. The characteristic feature of CT systems is that they are intended for very short communication distances and are suited for mobile as well as for fixed user terminals. While WLL typically works in a point-to-multipoint mode with the base station installed at the telephone exchange premises and covering a wide service area, the CT systems usually employ radio transmission only in the so called “last mile” of the telephone infrastructure, thus replacing local drop parts of some 0.1-1 km from the street cabinet to the subscriber premises, as shown in Fig. 2.5.

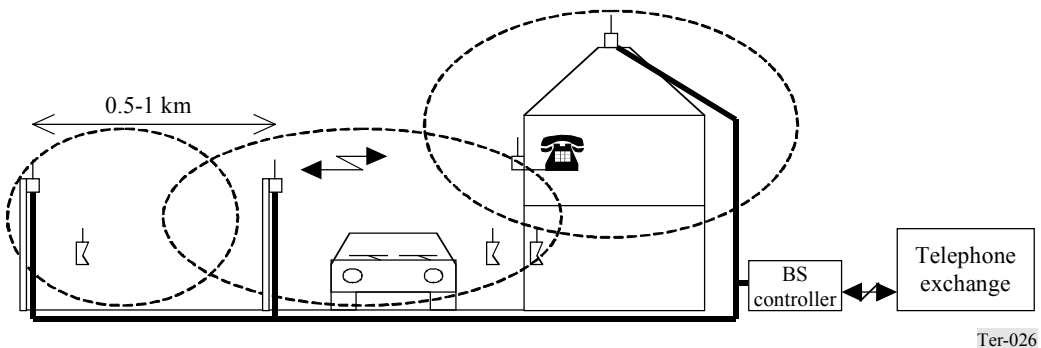
FIGURE 2.5
Wireless local loop system in cordless telephony mode



Such an architecture utilizes base stations with transmitter powers of some 10-100 mW (sometimes up to 0.5 W) and intended communication ranges of not more than 0.5-2 km. Normally some kind of automatic channel selection protocol is used, which allows dynamic assignment of free channels. Therefore CT systems become perfectly suited for network deployment in the highly dense cellular structures with the “lamp-post” principle of base station installations at 0.5-1 m intervals, see Fig. 2.6

FIGURE 2.6

Public CT system installation in urban areas



Public CT networks are intended primarily for installation in urban areas and may cope with traffic loads of up to 10 000 E/km²/floor. Notice that the traffic load is given per floor, because it is assumed that low power base stations create coverage zones only on the same level of multi-storey buildings. The typical power of a user terminal transmitter is around 10 mW in both fixed and mobile versions. Omnidirectional antennas are used on both sides. Due to the small size of the cells and optimization of radio access protocol for toll-quality connections, CT networks usually provide some means of subscriber hand-off between the cells but only for a slow speed of the mobile, e.g. limited to the pedestrians' speed of 4-5 km/h.

Ultimately public CT networks should allow seamless roaming of CT terminals between the privately owned home cordless telephones and their public counterpart network. It is also foreseen that public and private CT networks may form part of the universal international mobile telecommunication systems family, known as IMT-2000.

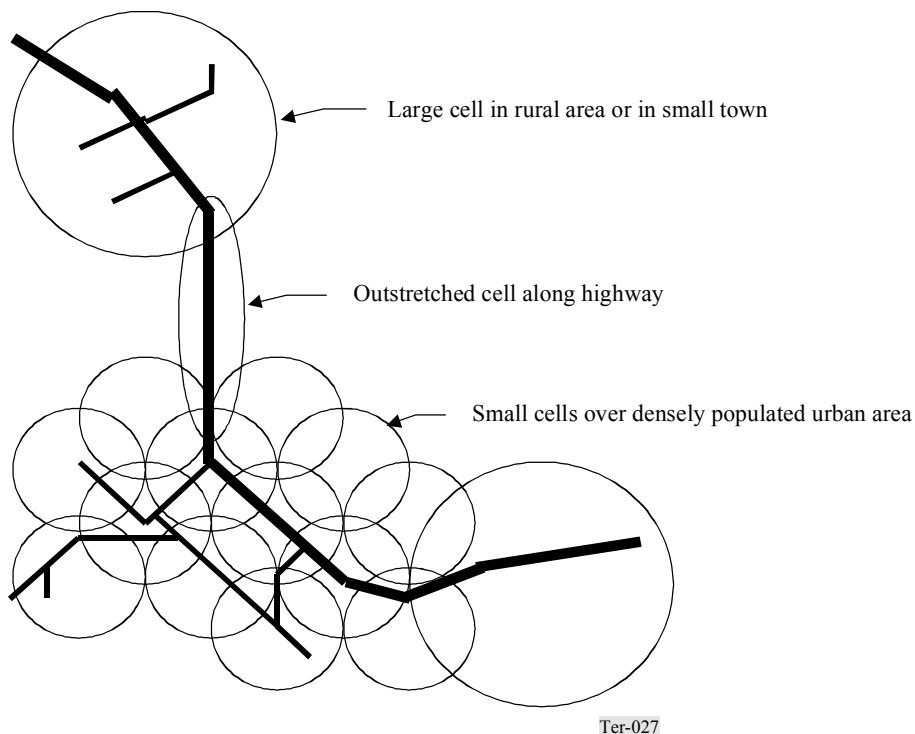
From the radio planning perspective CT networks usually do not require extensive propagation modelling because of the very dense installation of base stations with overlapping coverage areas. Usually it is sufficient to develop some general rules of expected propagation distance, based on operating frequency, typical height of antennas and propagation conditions. These rules may be then used in determining maximum separation distances between base stations and other guidelines for their typical installations.

2.5 Public cellular mobile telephony systems

Mobile telephony systems gradually developed from PMR systems, first providing the possibility for mobile users to connect to the PSTN network by means of manual switching at the dispatcher office, then creating specialized PMR-like mobile telephony systems with the dispatch office being replaced with a manned commutator, and finally with the automatic exchange that was directly connected with the PSTN network.

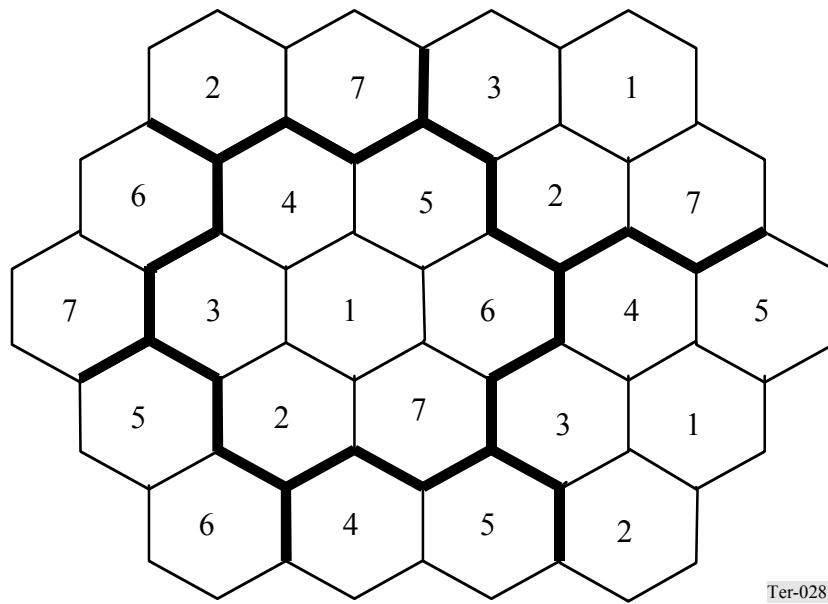
Such public mobile telephony networks featuring automated switching centres and deploying single base stations with radial coverage of metropolitan areas were in operation in many countries from 1960-1980 (and are sometimes still in operation today). However low efficiency of channel utilization and hence very limited traffic capacity in the PMR-type of architecture did not allow wide development of such systems until the concept of cellular deployment was introduced to mobile telephony networks around the 1980s. A basic example of cellular network deployment is shown in Fig. 2.7.

FIGURE 2.7
Example of cellular network architecture



The example in Fig. 2.7 shows how the density and shapes of the cells are adjusted to account for different subscriber density and adapt to the most likely routes of subscriber mobility. Essentially, individual cells in the cellular mobile network are planned as units limited by traffic capacity. This allows enormous flexibility for operators to deploy their networks gradually, first starting with large cells and then splitting them down to smaller and smaller cells as traffic grows. The initial problem of limited spectrum capacity in cellular structures is alleviated by significant frequency reuse, because small coverage areas allow the reuse of the same frequency at small distances, as shown in Fig. 2.8.

FIGURE 2.8
Example of frequency reuse pattern with 7 groups of frequencies in cellular structure



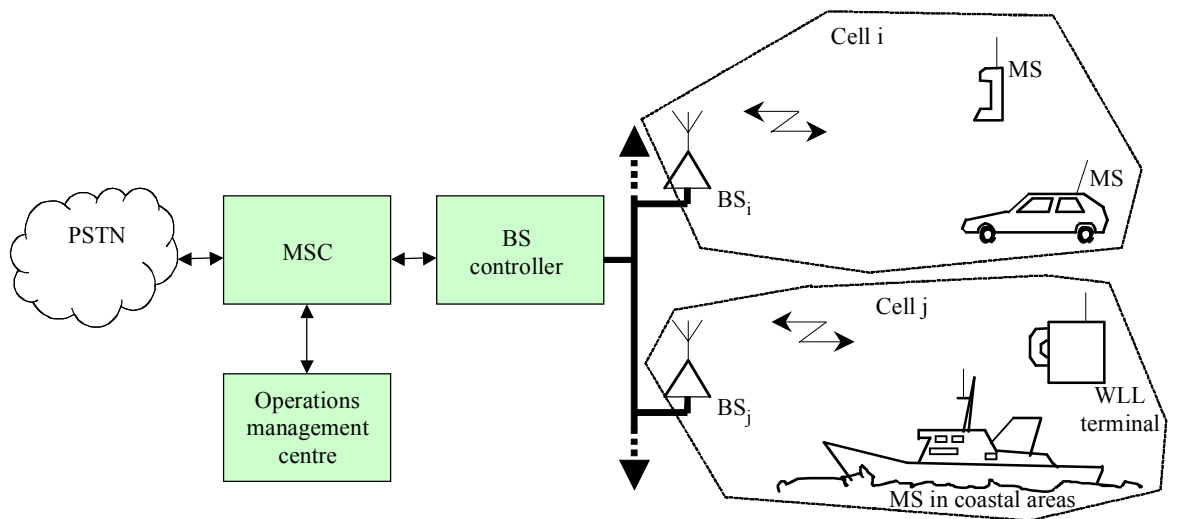
Ter-028

Later, code division multiple access (CDMA) technologies allowed the establishment of networks on a single frequency basis, although the capacity-limited principle of cell formation remained unaffected.

It may be noted that today the three generations of cellular public mobile telephony systems exist: First generation systems are analogue systems, employing some kind of frequency division multiple access (FDMA) protocols with usual narrow-band FM channels. Second generation systems are digital systems, which are largely used today. These employ some kind of digital modulation technology and either time division multiple access (TDMA) in combination with FDMA or CDMA mode of operation. Third generation systems are expected to start commercial operation gradually and are described as a family of various standards, primarily CDMA with frequency division duplex (FDD) or time division duplex (TDD), but also FDMA/TDMA standards. Together they are known under the ITU name of IMT-2000 (International Mobile Telecommunications).

Differences between various systems and different generations lie in the area of the variety of services offered and their quantitative and quality characteristics, different inter-network and inter-system roaming capabilities, etc. However, essentially all cellular telephony networks are similar in so far as the networks themselves and all communications within the networks are managed centrally from the so-called mobile switching centre (MSC), and all interconnections between mobile stations and the network, as well as between mobile stations, are routed through the nearest base station and MSC. A basic network architecture of cellular land mobile telephony systems is shown in Fig. 2.9.

FIGURE 2.9
Basic network architecture of cellular mobile telephony systems



Ter-029

Cellular systems usually employ directive antennas to form the required shape of the cells and also to reduce interference into neighbouring cells in FDMA/TDMA networks. Typical communication distance ranges are 100-300 m for pico-cells in dense urban areas, 0.5-1 km in urban micro-cells, 1-5 km in macro-cells employed in cities with low population densities and suburbs, and 5-25 km in rural areas, along highways, etc. Digital systems often have their maximum communication range tied into the timing structures of communication protocol, e.g. TDMA packet timing in a GSM system provides a maximum communication range of about 35 km. It may also be noted that the communication protocols and channel models in cellular telephony systems should assume a relatively high speed of vehicular mobile stations, in the range of 150-200 km/h.

Cellular mobile systems provide an extremely difficult task for networks planners, and propagation modelling is an important part of it. Because of the need to account for a large number of transmitters and because of high susceptibility to modelling errors, the network and coverage planning of a cellular mobile system usually requires application of dedicated sophisticated software tools that make extensive use of high resolution terrain and clutter databases.

It may be noted that significant differences exist between the planning of cellular networks that employ FDMA/TDMA and CDMA technologies. In the FDMA/TDMA networks, one of the major goals is frequency planning that is based on projected traffic forecasts (which leads to an estimate of cell size and its location) to position base stations and assign them frequencies so that mutual interference within the network is kept to a minimum. At the same time in CDMA networks, where co-frequency operation of neighbouring base stations is normal, the problem of interference is replaced with the problem of power management. This is because in a single frequency operation of a CDMA network a mobile station may distinguish between the different base stations and associate

itself with the nearest only through the estimation of power of received signals. Therefore the task of a CDMA network planner is to ensure that in the service area of a given cell a signal from its base station is dominant over the signals arriving from other cells.

Another characteristic which ought to be addressed is the channel width of the system. First generation systems usually use narrow channels (25/33 kHz) with analogue FM modulation, and they may be modelled as non-frequency selective. Second and third generation systems employ digitally modulated signals in much wider channels, for which delay spread and frequency selectivity aspects need to be considered in the propagation studies.

2.6 Useful references

- [2-1] Handbook on land mobile (Volume 1) – Wireless action local loop, International Telecommunication Union, Geneva, 1997.
- [2-2] Handbook on land mobile (Volume 2) – Principles and approaches on evolution to IMT-2000/FPLMTS, International Telecommunication Union, Geneva, 1997.
- [2-3] Handbook on land mobile (Volume 3) – Radio dispatch systems, International Telecommunication Union, Geneva, (in preparation).
- [2-4] Report ITU-R M.2014 – Spectrum efficient digital land mobile systems for dispatch traffic, International Telecommunication Union, Geneva.

CHAPTER 3

FUNDAMENTAL PROPAGATION PRINCIPLES

3.1 Propagation mechanisms

3.1.1 Free space

If there are no obstacles to propagation, the field strength follows the well-known inverse-square law, i.e. the received power varies as $1/d^2$. In logarithmic terms, the basic transmission loss between isotropic antennas is $L_{bf} = 32.45 + 20 \log f + 20 \log d$, where f is frequency in megahertz and d is distance in kilometres. The dependence on frequency occurs because the physical size and hence the capture area of the receiving antenna decreases with increasing frequency for an antenna of a given design. For the hypothetical isotropic antenna that is used as the basis of this formula, the capture area is $\lambda^2/4\pi$. For other antenna designs, the capture area is also proportional to λ^2 , but the multiplying constant is different. The free-space formula is sometimes used as a very conservative estimate for interference purposes, and also for comparison with total path loss. That is, the difference between the total path loss on a given path and the free-space loss is the attenuation due to blockage by terrain or other obstacles.

3.1.2 Reflections

The Fresnel reflection coefficients for reflection of a plane wave by a plane surface are:

$$R_h = \frac{\sin \psi - \sqrt{n^2 - \cos^2 \psi}}{\sin \psi + \sqrt{n^2 - \cos^2 \psi}} \quad (3-1)$$

for horizontal polarization, and

$$R_v = \frac{n^2 \sin \psi - \sqrt{n^2 - \cos^2 \psi}}{n^2 \sin \psi + \sqrt{n^2 - \cos^2 \psi}} \quad (3-2)$$

for vertical polarization, where ψ is the complement of the angle of incidence and $n^2 = \epsilon - j60\sigma\lambda$, where ϵ and σ are respectively the permittivity and conductivity of the reflecting material. For grazing incidence, i.e. $\psi \ll 1$, the second term in the numerators and denominators dominate, and the reflection coefficient tends toward -1 . This is true for both polarizations, with the result that in most circumstances, the difference in the effect of the ground on the two polarizations is not great. However, for reflections on buildings, the angle of incidence can have any value.

If the ground is curved (convex upward) with radius of curvature a , a factor to multiply R_h or R_v that accounts for the defocusing of the wave is [3-1, p. 224]:

$$D = \left[1 + \frac{2d_1 d_2}{a(d_1 + d_2) \sin \psi} \right]^{-1/2} \quad (3-3)$$

where d_1 and d_2 are the distances from the antennas to the point of reflection. If the ground is concave upward ($a < 0$), this formula accounts for a focusing effect, but such focusing is usually not realized in practice, because the ground does not have the precise shape required.

If the reflecting surface is rough with a Gaussian height distribution, the coherently reflected wave is attenuated by the factor [3-1, p. 246]:

$$\rho_s = e^{-(\Delta\Phi)^2/2} \quad (3-4)$$

where $\Delta\Phi = 4\pi \Delta h \sin \psi/\lambda$, where Δh is the standard deviation of the normal distribution of heights. Equation (3-4) is a quantitative expression of the Rayleigh criterion for specular reflection on a rough surface. The derivation of this formula neglects the shadowing of one peak in the rough surface by the next one, and so is not valid for extremely rough surfaces.

3.1.3 Reflection from ground

Ground reflections are most important on water or smooth Earth. The direct and ground-reflected waves may interfere constructively or destructively, depending on the difference Δr between the lengths of the direct and reflected paths. If the base-station antenna is located at height h_b above flat reflecting ground, and the mobile antenna is at height h_m , the difference between the lengths of the direct and reflected paths is $\Delta r = 2 h_b h_m / d$, where d is the horizontal distance between antennas. This formula is valid if $d \gg h_b$ and $d \gg h_m$, as is usually the case. As d increases, Δr decreases from perhaps several times the wavelength λ to $\Delta r \gg \lambda$. Since reflection from the ground introduces a phase shift corresponding to approximately one-half wavelength (a reflection coefficient of approximately -1), destructive interference occurs for $\Delta r = n\lambda$, where n is an integer. Constructive interference occurs where n is a half-integer. As d increases, the last of these points is at $\Delta r = \lambda/2$, i.e. at $d = 4 h_b h_m / \lambda$, sometimes referred to as a breakpoint [3-2]. For greater distances, the field strength decays as $1/d^4$. For $d \gg 4 h_b h_m / \lambda$, on a plane highly-reflecting Earth, the path loss is given by:

$$L_b = 120 + 40 \log d - 20 \log h_b - 20 \log h_m \quad (3-5)$$

Besides the fourth-power distance dependence, this equation also shows a linear dependence of field amplitude ($20 \log h$) on the height of either antenna. Although this equation is derived from a highly idealized situation, the dependence on distance and height found in non-ideal terrain is roughly similar. Another manifestation of ground reflections is that in mountainous areas, reflections from a steep slope can illuminate a region that would otherwise be in deep shadow, for example along a curved valley with steep sides.

3.1.4 Reflection from buildings

In built-up areas, reflections from buildings are important. Unlike ground reflections, building reflections can occur at all angles of incidence, and it is usually not a good approximation to consider the surface to be perfectly reflecting. The electrical properties of the ground and of building materials are fairly well known. However, the construction of buildings involves different material mixed together or close together (e.g. reinforced concrete), or hollow materials

(e.g. concrete blocks) [3-3]. The surface of buildings can be rough enough to reduce specular reflection and to scatter waves. Since the detailed properties of building walls are usually not known, empirically determined effective values may be used. Results of one study [3-4] suggest that the effective values of relative permittivity of residential building walls range between three and six. Reflection among buildings tends to fill in shadows to some degree.

3.1.5 Diffraction

Diffraction is the mechanism by which waves of any kind propagate around obstacles. On obstructed paths, diffraction is usually the most important propagation mechanism.

Fresnel zones and ellipsoids are often used to visualize diffraction at VHF and UHF. The first Fresnel ellipsoid is the volume for which the excess length of a line from the antennas to any point in the volume is less than $\lambda/2$, where λ is the wavelength. Any cross section of the first Fresnel ellipsoid is a first Fresnel zone. The radius R_1 of a first Fresnel zone perpendicular to the line of sight is given by $R_1 = \sqrt{\lambda d_1 d_2 / (d_1 + d_2)}$. A propagation path is considered obstructed if the first Fresnel ellipsoid is not clear. This is the conventional criterion, although it is a conservative one, since obstacles can penetrate to about 0.6 of the first Fresnel-zone radius without reducing the field strength significantly. The attenuation due to obstacles penetrating the first Fresnel ellipsoid depends on how much of it is blocked and on the shapes of the obstacles. The simplest example is a sharp transverse ridge (modelled as a knife-edge) that blocks exactly half of the first Fresnel zone. In that case, the field amplitude is reduced by half, with a power loss of 6 dB. An obstacle that is broad in the direction of propagation causes greater attenuation than a narrow obstacle. This is an important effect in diffraction over terrain, in which a broad rounded hill or the curvature of the Earth can cause an attenuation that is much greater than a narrow obstacle of the same height. These issues are covered in more detail, for example, in [3-5].

Buildings in a built-up area present something like a very rough surface to a wave propagating over them, but since the buildings certainly shadow each other, it is not a rough surface that can be represented accurately by the rough-surface reflection coefficient of equation (3.4). A single or a few buildings can be represented as solid shapes, but many buildings are reasonably represented as knife-edges. If these are of uniform height and spacing, propagation over them resembles somewhat propagation over ordinary terrain, with a $1/d^4$ dependence on distance [3-6].

In the land-mobile service, waves propagating over buildings must eventually find their way to street level. They do this by diffracting from the nearest rooftops, and reflecting from nearby buildings. If the buildings are arranged in rows without large gaps in the rows, the wave simply diffracts down from the nearest rooftop in the direction of the base station. There may also be a reflection back from the nearest building in the other direction. If the size and placement of

buildings is more complex, several diffractions and reflections may be involved. In urban areas where there are large buildings, the wave is channelled along streets that are oriented along the nominal propagation direction, and the field strength on such streets is usually higher than on perpendicular streets. In suburban areas where there are fewer large buildings, these channelling effects are less important, but absorption by trees becomes important [3-5].

If the base station antenna is located below the nearby roof tops, as is common in microcells, then the predominant propagation is along streets rather than over roof tops, although propagation over roof tops may make some contribution. Propagation along a street is primarily that of a wave over the plane earth, with $1/d^2$ attenuation punctuated with interference fades as far as a break point, and $1/d^4$ attenuation at greater distances. The wave in perpendicular streets is much weaker, but some energy is diffracted into these streets by the corners of buildings.

3.1.6 Refraction

Refractive effects become important only on paths of a few tens of kilometres or more. Therefore, in the land-mobile service, refractive effects are primarily important in estimating interference and frequency reuse rather than in coverage calculations. The usual way of allowing for standard atmospheric refraction is to assume that the radius of the Earth is larger than its real value by a factor $k = 4/3$. This allows for the refractive bending of radio waves toward the Earth. When the Earth's radius is increased by this factor, rays bent due to refraction become straight lines, and calculations can proceed as if there were no atmosphere. A simple way of allowing for the possibility of enhanced signal strength due to non-standard atmospheric conditions is to change the value of k , increasing it to simulate the greater refraction and greater signal strengths to be expected for small percentages of time. However, for very small percentages of time, it is better [3-7] to use statistical empirical methods [3-8] to estimate the increased signal strength.

3.2 Shadowing and rapid fading

3.2.1 Shadowing

The field-strength attenuation in the shadow of large obstacles (hills, mountains) can be estimated deterministically. Below some size, which might be tens or hundreds of metres, and which depends on the resolution of the terrain data and the method used, this cannot be done. The shadowing due to objects smaller than the terrain-data resolution (small terrain features, individual trees and buildings) must be treated statistically. Field-strength values in the shadows of many small obstacles follow a log-normal distribution, once the rapid fading due to multipath propagation has been filtered out. The median of the distribution can be estimated by deterministic methods, while the standard deviation must ordinarily be obtained by large numbers of measurements made in typical situations. Standard deviation values range between 3 and 10 dB [3-5, p. 151]. They tend to increase with frequency, and with the local irregularity of the clutter and terrain. Formulae for estimating the standard deviation are given in [3-9].

3.2.2 Rapid fading

Multipath propagation leads to fading on the scale of a few wavelengths on narrow-band channels, and leads to time dispersion of pulses on wideband signals. These effects can be produced by waves reflected from steep mountainsides, but more often are due to scattering and reflections from buildings and other clutter. Waves arrive at the receiver from different directions, creating an interference pattern that can give rise to rapid fading as a mobile receiver moves through the pattern. The distance Δr between successive fades is given by $\Delta r = \lambda/[2 \sin(\theta/2)]$, where θ is the angle between the propagation directions of the two waves, i.e. varying from one-half wavelength upward. The half-wave spacing results from interference between two oppositely directed waves. If there are many waves of comparable amplitudes coming from all directions, the received amplitude follows a Rayleigh probability distribution. If there is also a single wave (usually the direct wave) with amplitude much greater than that of all the others, the received amplitude follows a Rician distribution. The effects of multipath fading can be mitigated by increasing the transmitted power or by various diversity schemes, or in the case of digital transmission by coding and error correction.

If digital information is to be sent at a high data rate, then the delay spread of a transmitted pulse is of concern. The effect is similar to speaking in a room with a long reverberation time. After speaking each word or syllable, the speaker must wait until the echoes die down before speaking the next one, if the message is to be understood. The radio analogue of the reverberation time is the delay spread, which is a measure of the time during which strong echoes are received. If the delay spread is T , then information bits can be sent no faster than some rate of order $1/T$. This rate cannot be increased by increasing the power, since the power in the echoes also increases. If there is no diversity or coding to correct for the fading, the maximum rate is $1/8T$ [3-10, p. 340]. For a fuller description of this issue, see Section 9.1 of this Handbook.

A number of measurements of delay spreads have been made. Reference [3-10, p. 42] suggests mean delay spreads of $1.3 \mu\text{s}$ in urban areas and $0.5 \mu\text{s}$ in suburban areas. The larger buildings in an urban area are more likely to reflect signals strongly from a distance of a few hundred metres, translating to delays of more than a microsecond to a maximum of about $7 \mu\text{s}$, but smaller values ($< 1 \mu\text{s}$) are observed when the base-station antenna is low, at street-lamp level [3-11]. Much longer delay times can sometimes be found, typically at low amplitude. For example, delays in a mountain valley of up to $30\text{--}40 \mu\text{s}$ have been measured [3-12].

3.3 The statistics of location variability

If the direct line of sight between the two antennas is blocked, and if the signal arrives by way of many reflections of comparable strength, the received power follows a Rayleigh distribution. The

probability density of the instantaneous signal power being $r^2/2$ (i.e., r is proportional to signal amplitude, not in decibels) when the mean power is a^2 , is given by the following function [3-5]:

$$P_r(r) = \frac{r}{a^2} \exp\left(-\frac{r^2}{2a^2}\right) \quad (3-6)$$

This function is not symmetrical about its peak at $r=a$. As a consequence, the mean, median, and root-mean-square are not equal. The median, for example, can be obtained by integrating to obtain the cumulative probability function, and setting that probability to 0.5, to arrive at a median of $\sqrt{\ln 2a} \approx 1.1774a$. The formal standard deviation of the Rayleigh distribution is 5.57 dB, but a more appropriate value to use when combining with log-normal distributions is $\sigma_r = 7.5$ dB [3-13].

If the direct wave, or possibly a strong reflection, is substantially stronger than the other waves, the more general Nakagami-Rice distribution can be used. In this distribution, there is an added free parameter, namely the ratio K of the received power of the direct wave to the mean power of the remaining Rayleigh-distributed wave. This parameter can vary from zero to infinity, depending on whether the signal is pure Rayleigh or pure direct wave. The probability density function is [3-5]:

$$P_r(r) = \frac{r}{a^2} \exp\left[-\frac{r^2 + r_s^2}{2a^2}\right] I_0\left(\frac{rr_s}{a^2}\right) \quad (3-7)$$

where $r_s^2/2$ is the power of the strong steady signal. The function I_0 is the modified Bessel function of the first kind of zero order. The ratio K can be introduced into this equation by substituting $a^2 = r_s^2 / (2 \cdot 10^{K/10})$.

In built-up areas, the distribution is considered to be Rayleigh (or Rice) over a small distance of say 20 m, but the small-distance median value of the signal varies over larger distances because of shadowing by various objects, and is random and log-normal up to perhaps 100 or 200 m. The log-normal distribution is:

$$p(x) = \frac{1}{\sigma\sqrt{2\pi}} \exp\left[-\frac{x^2}{2\sigma^2}\right] \quad (3-8)$$

where x is the signal level in decibels, and σ is the standard deviation (also in decibels) of these levels. Over this larger distance, a combined Rayleigh-log-normal distribution might be used to represent the instantaneous signal, but a simpler alternative [3-13] is to combine standard deviations as if they were both log-normal, and to include other log-normal distributions as well. In this scheme, the overall standard deviation is combined as:

$$\sigma_{total} = \sqrt{\sigma_1^2 + \sigma_2^2 + \dots} \quad (3-9)$$

where the various contributing standard deviations may be, as appropriate, those due to shadowing, prediction error, Rayleigh fading, and any other losses that it might be convenient to consider separately, such as vegetation or vehicles [3-13]. If the objective is to estimate the reliability of predicted coverage, the standard deviation of prediction error should be included. A combined distribution that includes prediction error provides an estimate of coverage over an ensemble of similar areas.

A still simpler alternative for dealing with Raleigh fading [3-14] is to use a log-normal distribution by itself for the median signal and to add a margin of 6 to 10 dB to allow for Rayleigh fading. Since the effect of Rayleigh fading depends on the communications system, it is not always appropriate to include it. Details on various distributions are given in [3-15].

3.4 References

- [3-1] BECKMANN, P. and SPIZZICHINO A. [1987] *The scattering of electromagnetic waves from rough surfaces*. Artech, Norwood, United States of America, p. 503.
- [3-2] Recommendation ITU-R P.1411 – Propagation data and prediction methods for the planning of short range outdoor radiocommunication systems and radio local area networks in the frequency range 300 MHz to 100 GHz, International Telecommunication Union, Geneva.
- [3-3] HOLLOWAY, C. L., PERINI, P. L., DELYSER, R. R. and ALLEN, K. C. [August 1997] Analysis of composite walls and their effects on short-path propagation modeling. *IEEE Trans. Veh. Tech.*, 46(3), p. 730-738.
- [3-4] PIAZZI, L. and BERTONI, H. L. [May 1999] Achievable accuracy of site-specific path-loss predictions in residential environments. *IEEE Trans. Veh. Tech.*, 48(3), p. 922-930.
- [3-5] PARSONS, J. D. [1992] *The mobile radio propagation channel*, Wiley, New York, United States of America.
- [3-6] PIAZZI, L. and BERTONI, H. L. [August 1998] Effect of terrain on path loss in urban environments for wireless applications. *IEEE Trans. Ant. Prop.*, 46(8), p. 1138-1147.
- [3-7] HALL, M. P. M., BARCLAY, L. W. and HEWITT, M. T. [1996] *Propagation of radio waves*, IEE, Stevenage, United Kingdom, p. 446.
- [3-8] Recommendation ITU-R P.1546 – Method for point-to-area predictions for terrestrial services in the frequency range 30 to 3 000 MHz, International Telecommunication Union, Geneva.
- [3-9] Recommendation ITU-R P.1406 – Propagation effects relating to terrestrial land mobile service in the VHF and UHF bands, International Telecommunication Union, Geneva.
- [3-10] LEE, Wm. C. Y. [1982] *Mobile communications engineering*. McGraw-Hill, New York, United States of America, p. 464.
- [3-11] BULTITUDE, R. J. C. and BEDAL G. K. [1987] Propagation characteristics on microcellular urban mobile radio channels at 910 MHz. *IEEE J. Selected Areas Comm.*, 7(1).
- [3-12] MOHR, W. [May 1993] Wideband propagation measurements of mobile radio channels in mountainous areas in the 1 800 MHz frequency range. *43rd IEEE Veh. Tech. Conf. Record*, p. 49-52.
- [3-13] SIWIAK, K. [1998] *Radiowave propagation and antennas for personal communications*. Artech, Boston, United States of America, p. 418.
- [3-14] HAGN, G. H. [1980] VHF radio system performance model for predicting communications operational ranges in irregular terrain. *IEEE Trans. Comm.*, 28(9), p. 1637-1644.
- [3-15] Recommendation ITU-R P.1057 – Probability distributions relevant to radiowave propagation modelling, International Telecommunication Union, Geneva.

CHAPTER 4

MODELLING TECHNIQUES FOR PROPAGATION PREDICTION

Chapter 4 describes several techniques and actual models that are used to predict propagation of radiowaves. The first section (4.1) addresses the use of generalized empirical “point-to-area” models, sometimes also correctly referred to as “site-general” models. These models require only general information about the area (such as terrain roughness) in which the radiowaves propagate and do not consider characteristics of specific propagation paths. The method to extend the scope of application of empirical model by means of tuning (optimal parameter selection) is also presented.

Section 4.2 describes the use of terrain specific empirical models, which are also known as “point-to-point” or “site-specific” models. These models differ from the generalized models described in the first section in that they use detailed information about the particular propagation path involved. This information may be either a simple 2-dimensional path profile or very detailed terrain and ground cover (buildings, vegetation, etc.) database. If the path data are sufficiently accurate, the more exact point-to-point methods will usually produce more accurate results than the less accurate point-to-area methods, at the penalty of greatly increased computation time and complexity. It should be noted, however, that greater accuracy is not always necessary in the land mobile services, where typically the received signals suffer from significant fading fluctuations.

Section 4.3 gives a brief overview of various ray tracing techniques and other more rigorous techniques, that attempt to predict the field strength in a nearly deterministic manner by means of accounting all possible paths that radiowaves travel in a multipath mobile environment. Such techniques are suitable for the conditions usually met when transmitting antennas are installed below rooftop levels in cities or within buildings, when the number of ray paths to be considered is reduced by natural surrounding obstacles.

Section 4.4 describes diffraction modelling, which allows calculation of a loss in signal strength when radiowaves travel around obstacles. These obstacles are often approximated as simple knife-edges, cylinders or spheres.

Finally, Section 4.5 presents some useful guidance to potential users as to how to select the model which would be most appropriate in commonly encountered engineering practices, such as network planning, interference assessments, frequency assignment or re-use. Also, guidance is given on model selection to evaluate measurement campaigns for assessment of system performance.

4.1 Generalized point-to-area models

Generalized empirical models, such as those described in Recommendation ITU-R P.1546 [4-1], which has superseded Recommendations ITU-R P.370 [4-2] and ITU-R P.529 [4-3], provide engineers with very convenient tools for field strength prediction in the coverage areas of radio

stations. In their basic form, such models do not involve sophisticated calculations and do not require detailed knowledge about particular propagation paths, therefore they may be used without high-resolution terrain databases or advanced computational facilities.

The essence of most of the empirical propagation prediction models may be represented by a basic expression:

$$E_R = -\gamma \cdot \log(R) + K(P_{BS}, f, h_{BS}, h_{MS}, \dots) \quad (4-1)$$

Equation (4-1) means that the received field strength E_R is presented in empirical models as a logarithmic function of distance R with slope parameter γ , plus an offset parameter K , which in itself is a function of some initial network design parameters: power of transmitter (P_{BS}), operating frequency (f), heights of antennae at base and mobile stations (h_{BS} and h_{MS}), etc. The differences between various empirical models arise mostly in establishing and treating those empirical parameters γ and K .

Recommendation ITU-R P.1546 [4-1] provides electric field strengths in dB(μ V/m), referenced to 1 kW e.r.p., as functions of path distance ranging from 1 to 1 000 km, in both graphical (i.e., curves) and tabular (i.e., fixed precision numeric values) formats. The graphical results are presented at three discrete frequencies: 100, 600 and 2 000 MHz. Furthermore, the graphical and tabular presentations include eight transmitter/base antenna heights above the surrounding clutter, ranging from 10 to 1 200 m, for three different time percentages (50%, 10% and 1%) and for land, warm sea and cold sea paths, all for 50% of locations. Values of the maximum expected field strengths, as functions of distance, frequency, time percentage and path type, are also provided.

For general planning not requiring high predictive accuracy, Recommendation ITU-R P.1546 provides graphical curves of field strength for the frequency ranges 30-300 MHz, 300-1 000 MHz and 1 000-3 000 MHz, respectively. However, for users requiring increased predictive accuracy, Recommendation ITU-R P.1546 contains a step-by-step procedure for the proper sequential application of interpolation and/or extrapolation in distance, frequency, antenna height and time percentage, and also including location percentages other than 50% and the recommended nexus for the calculation of the associated basic transmission loss. A method for mixed-path (i.e., a combined land-sea path) field strength computation is also given within the context of the step-by-step procedure. Details of the various antenna height corrections, the interpolations, the extrapolations, the mixed-path field strength computation and the basic transmission loss are also provided in Recommendation ITU-R P.1546.

Some empirical models are presented graphically as a set of curves statistically derived from large sets of measurements. Recommendation ITU-R P.1546 [4-1] is the ITU-R recommended model for terrestrial mobile propagation at VHF/UHF and has been developed from the Recommendation ITU-R P.370 [4-2] model and the Okumura model [4-4].

4.1.1 Okumura and Hata models

The Okumura model is commonly used in planning of the land mobile services. It is the culmination of a careful analysis of a large set of signal strength measurement data gathered in a wide variety of terrain and vegetation and urban clutter environments at several different frequencies in the VHF and UHF bands. The model includes signal strength prediction graphs for bands centred at

150, 450, 900, and 1 500 MHz, based on propagation conditions found to be typical of areas in and around Tokyo, Japan during the early 1960s. Values are provided for several environments, such as dense urban, suburban and open. Additional corrections to the basic Okumura curves are provided for different types of terrain, degrees of terrain ruggedness, slope of the land, over land vs. over-water paths and so on, to such an extent that practical computer implementation of the model becomes difficult.

Hata later published a set of equations [4-5] based on a greatly simplified version of the Okumura model. The Hata model (referred to as the Okumura-Hata model) provides mathematical formulae that approximate the original Okumura curves. It also introduces limitations on the acceptable frequency range (100 to 1 500 MHz), distance from the transmitter site (1-20 km) and transmitter antenna heights (30-200 m above the surrounding terrain). The distance limitation, in particular, reduces the Hata equations' applicability to the design of terrestrial land mobile systems other than cellular systems. The height limitation also reduces the applicability of this model for the mountain top sites.

The Okumura-Hata and other generalized empirical models provide reasonably accurate predictions of coverage in land-mobile radio systems, when they are applied in an environment similar to that where the model was originally developed. The scope of application of general empirical models may be further extended by the means of fine tuning of the model to some specific environmental conditions. This technique is described in detail in the following section. Because the Okumura and Okumura-Hata models are “point-to-area” prediction models, they should not be used for point-to-point predictions. Other models, such as Longley-Rice (see Section 4.2), are better suited to the task of predicting radio system performance for specific paths.

The Okumura-Hata model does have the advantage of simplicity – the ability to predict system performance based on a very limited set of input data. Its simple, straightforward formulation lends itself to easy application on small computers or spreadsheets. The model’s principal determinants of signal strength are the frequency, the effective radiated power, the transmit and receiver antenna heights, and the path length. It has become the “default” model for many types of planning tools.

Recommendation ITU-R P.529 [4-3] extended the applicability of the Hata equations to Okumura’s original 100 km distance. It also included VHF propagation curves adapted to land mobile applications based on the methods described in Recommendation ITU-R P.370. This has now evolved into Recommendation ITU-R P.1546 which has extended the frequency, antenna height and distance ranges.

Possibly the most important advance contained in the original Okumura model [4-4] is the quantification of the effects of different types of urban and vegetation clutter. The differences between urban area and open area paths can be impressive. For example, at 200 MHz, the increase in signal strength for an open area path as compared with an urban area path is of the order of 20 dB. The model also attempts to account for the difference in signal attenuation as a function of the downward angle from source into the surface clutter.

One thing that can be lost by using a “simple” model is accuracy. A fundamental assumption of the Okumura-Hata model is that the transmitting antenna has an “effective height” above the surrounding terrain. The model also assumes a flat or smooth Earth between the terrain at the transmitter and the receiver. The model’s Rolling Hilly Factor attempts to account for terrain

undulation in a statistical manner, but it should not be applied in a point-to-point situation. Okumura's Isolated Ridge factor can provide reasonably accurate results, provided that the path geometry closely matches the model's assumptions. However, this last assumption excludes most practical paths. More recent attempts [4-8] have been made to apply more conventional diffraction loss models to Okumura's curves with limited success.

As has been discussed, Okumura developed the model specifically to include the effects of surface clutter. The Hata version of the model follows suit by incorporating Recommendations (see Recommendation ITU-R P.529-3 [4-3]) regarding excess path losses which can be used in planning of systems.

In summary, the Okumura-Hata model is a widely used planning tool for land mobile radio systems. But careful consideration should be given to the differences that may exist between the situations and environments considered by the model's authors and those that exist for any particular system design case. The approach shown in the following sections describes a way of overcoming some of the problems in the application of empirical models.

However, there might be cases when application of empirical models is not appropriate in principle, e.g. in mountainous areas or other areas with highly irregular terrain.

4.1.2 Testing and tuning of generalized empirical point-to-area models

4.1.2.1 Necessity for tuning of empirical models

As the name implies, empirical models are developed from the results of practical field measurements and therefore become adjusted to the environment in which these original measurements were made. If then such models are applied blindly in environmental conditions notably differing from those of the original, the prediction errors may increase significantly. For example, the precision of a properly tuned empirical model in predicting median field strength may be expected to be in the order of ± 5 dB. Such precision is adequate for many practical cases, especially when dealing with the land mobile services where it is comparable with normal signal variations due to fading and shadowing. If the same general model were applied blindly in the unspecified environment, its precision may sometimes drop down to some $\pm(15\dots20)$ dB, which is clearly not acceptable.

Therefore, the practical value and scope of application of general empirical models may be significantly increased by means of their testing and adapting to particular propagation conditions or to conditions in specific country or region. The following section describes how this testing may be performed in its simplest form and how the necessary changes may be introduced into a selected empirical model such as the Okumura-Hata model from Recommendation ITU-R P.529 [4-3].

4.1.2.2 Minimum set up for model testing

Before applying a general empirical model in the particular region of "unknown" properties, it is a good practice to test the performance of a selected model or to compare performances of several models. The testing is described below. It can make use of existing radio stations (e.g. base stations of land mobile systems: cellular, paging, etc.) as reference transmitters. On the measurement side, it is possible to use widely available calibrated handheld RF field monitors or, in restrictive

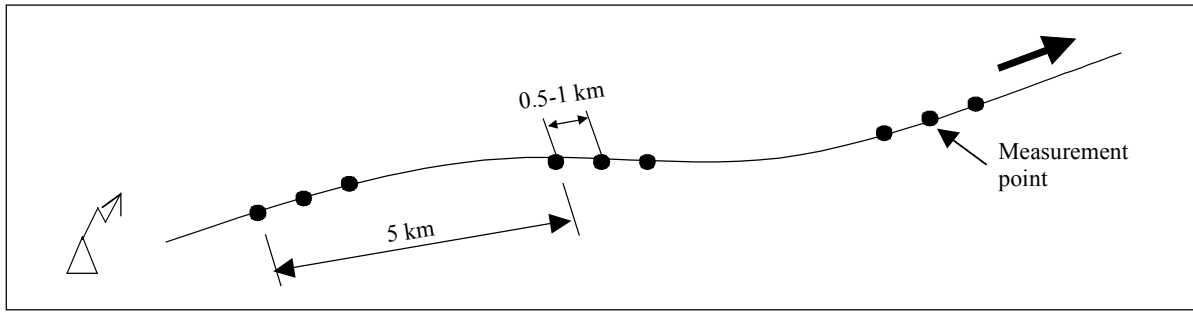
circumstances, even subscriber units of those land mobile systems-under-test with field monitoring functions. These arrangements mean that such measurements may be done fairly quickly and with very limited human and financial resources. For more formal and detailed description of the field measurements please refer to the ITU Spectrum Monitoring Handbook [4-16].

Although the more measurements the better the result, for a rough testing of the empirical model it may be sufficient to carry out static measurements in coverage areas of at least two or three existing radio transmitters. However it is important to ensure that these coverage areas are selected for testing so that they represent the most typical propagation conditions of that region (urban/suburban, vegetation density, irregularity of terrain, etc.). In each of the selected coverage areas it is advisable to take field measurements within at least 15-20 different distances from transmitter. For each of these distances the measurement sample should include at least 5-10 measurements, preferably taken at different directions from the transmitter, to ensure proper evaluation of the median field strength. If tested transmitters employ directional antennas, then care should be taken that the measurement points should all be within the main beam of the transmitter antenna. The antenna of the test receiver should be placed at an appropriate height, that is 1.5-2 m for the land mobile services.

It is most convenient to perform such measurements along the available radial route (such as a road) within the coverage area and at the points with certain given distances between them, say each 1 km. One of the possible setups for clustering such measurement points is shown in Fig. 4.1.

FIGURE 4.1

Example of clustering measurement points along the radial route from reference transmitter



Ter-041

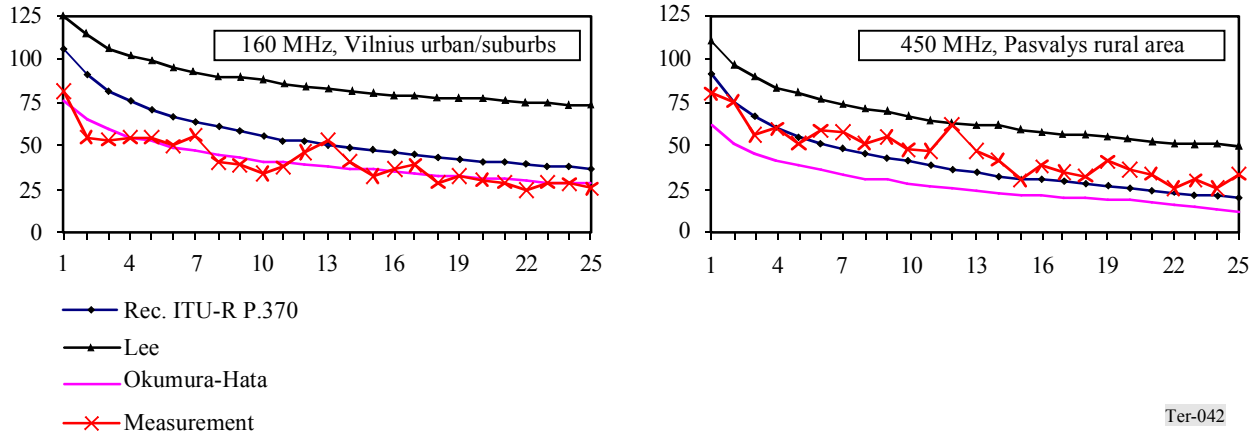
At each of the measurement points the median field strength should be recorded against the distance from the transmitter. Since the number of measurements is very limited in this case, they may be carried out without automation but with manual recording of measured field strength. The distances from the transmitter may be determined by any available means: a GPS receiver with differential distance measurement capabilities, the odometer of a car on a strictly radial route, or a map of a suitable scale.

As a result of such measurements, a set of measured field strength values for given distances will be obtained. These measurements may be then compared with the results of modelling, taking care to adjust model parameters (antenna height, radiated power, etc.) for each of the measurement routes, because they may differ, e.g. antenna gain and hence radiated power may be different in different

directions. If the model will be used in different frequency bands, then it is also advisable to perform testing in all those frequency bands concerned. Fig. 4.2 shows an example of comparing measurement and modelling results.

FIGURE 4.2

**Examples of comparing measurement results with several empirical models,
averaged field strength dB(μ V/m) vs. distance from transmitting station, km**



Ter-042

It is advisable to compare measurements with results obtained using several models, as shown in Fig. 4.2, where models from Recommendation ITU-R P.370 [4-2], Lee [4-7] and Okumura-Hata [4-3] were used. Then even subjective analyses of such comparisons can be used to decide which of the tested models performs best and whether it performs well enough.

For example, for that particular region where examples in Fig. 4.2 were derived, one may conclude that Okumura-Hata model is the best and sufficient model for modelling field strength in the 160 MHz VHF band in urban/suburban conditions. However, from the same example it may be seen that the Okumura-Hata model should be corrected before applying it for the propagation prediction in the 450 MHz band in rural areas.

However, it is dangerous to make such conclusions based on measurements at only one frequency band/coverage area. At least two or three coverage areas (transmitters) should be examined in each of the frequency bands and conclusions may be drawn only when they are similarly confirmed in all cases.

Performance of the models may be more formally evaluated and models may be compared among themselves by means of applying statistical analysis and measures, such as the least squares criterion. According to this criterion, a model best fitting some experimentally obtained results would give a minimum in the following expression [4-14]:

$$\sum_{i=1}^n [y'_i - \varphi(x_i, a, b, c, \dots)]^2 = \min \quad (4-2)$$

where:

y'_i : experimental result for the point x_i ;

n : number of measurements in a set

$\varphi(x_i, a, b, c, \dots)$: model result for point x_i and transmitter parameters a, b, c, \dots

It is then clear, that by substituting the $\phi(x_i, a, b, c, \dots)$ with various tested models in turn and computing results of equation (4-2) for these models for all sets of experimental measurements, one can evaluate the unbiased performance of each of the tested models in all cases. By combining all of these comparisons, the most suitable model may be selected as that providing the best fit with experimental results.

4.1.2.3 Model tuning

When testing shows that the precision of the selected empirical model is not sufficient, the model requires tuning. This may be done through a fine adjustment of the empirical parameters of the model. In preparing the selected model for tuning, its formula should be transformed to the basic form (4-1), so that the two basic empirical parameters: slope γ and initial offset K appear. The process of tuning the model is then a matter of modification of those two parameters.

The practical example below shows how the process may be applied to the Okumura-Hata model given in Recommendation ITU-R P.529 [4-3]. The Okumura-Hata model in this Recommendation provides the following expression for received field strength E_R dB(μ V/m):

$$E_R = 39.82 + P_{BS} - 6.16 \log f + 13.82 \log h_{BS} + a(h_{MS}) - (44.9 - 6.55 \log h_{BS})(\log R)^b \quad (4-3)$$

where:

P_{BS} : radiated power of the transmitter (dBW)

f : operating frequency (MHz)

h_{BS} : effective height of the transmitter antenna (m) above average terrain within 3-15 km

h_{MS} : height of receiver antenna (m)

$$a(h_{MS}) = (1.1 * \log f - 0.7) * h_{MS} - (1.56 * \log f - 0.8)$$

R : distance from the transmitter (km)

$b = 1$ for $R \leq 20$ km

$b = 1 + (0.14 + 1.87 * 10^{-4} * f + 1.07 * 10^{-3} * h_{BS}) * (\log(R/20))^{0.8}$ for $20 \leq R \leq 100$ km

From equation (4-3) it may be seen that the offset parameter is expressed in the Okumura-Hata model as:

$$K = 39.82 + P_{BS} - 6.16 \log f + 13.82 \log h_{BS} + a(h_{MS}) \quad (4-4)$$

The necessary tuning may be introduced into the offset parameter (4-4) by adjusting the initially constant parameter $E_0 = 39.82$ dB(μ V/m).

At the same time, the overall slope parameter in the Okumura-Hata model (4-3) may be represented as follows:

$$\gamma_{SYS} = -\gamma \cdot (44.9 - 6.55 \log h_{BS}) \quad (4-5)$$

Equation (4-5) introduces the initial slope parameter γ , which initially equals one and which may be adjusted.

Thus the correction of the Okumura-Hata model (4-3) may be achieved by tuning of parameters E_0 and γ of the model. The most appropriate tool for such tuning may be the statistical method of least squares.

It may be shown [4-15] that using this method the following solution may be obtained for statistical estimates of parameters K and γ_{SYS} :

$$\begin{aligned}\tilde{K} &= \frac{\sum x_i^2 \cdot \sum y_i - \sum x_i \cdot \sum x_i y_i}{n \cdot \sum x_i^2 - (\sum x_i)^2} \\ \tilde{\gamma}_{SYS} &= \frac{n \cdot \sum x_i y_i - \sum x_i \cdot \sum y_i}{n \cdot \sum x_i^2 - (\sum x_i)^2}\end{aligned}\quad (4-6)$$

Equation (4-6) allows for very simple and formal calculation of parameters E_0 and γ of the Okumura-Hata model (4-3) from a given set of static experimental measurements $\{(x_i = \log R_i; y_i)\} i = 1 \dots n$.

This means, that the particular offset and slope parameters in the original Okumura-Hata model may be calculated from equations (4-6), (4-4) and (4-5):

$$\begin{aligned}\tilde{E}_0 &= \tilde{K} - P_{BS} + 6.16 \log f - 13.82 \log h_{BS} - a(h_{MS}) \\ \tilde{\gamma} &= -\frac{\tilde{\gamma}_{SYS}}{44.9 - 6.55 \cdot \log h_{BS}}\end{aligned}\quad (4-7)$$

For example, analysis performed using equations (4-6) and (4-7) with the measurement sets obtained during a measurement campaign in Lithuania [4-15], gave a number of E_0 and γ values for various coverage areas and different frequency bands for that particular Eastern European region. By grouping those results according to their urban or rural origin and frequency band, the resulting average values for the empirical model parameters were derived (see Table 4.1).

TABLE 4.1

Example of calculated modified empirical parameters of the Okumura-Hata model (4-3) for various area types and various frequency bands

	160 MHz		450 MHz		900 MHz	
	Urban	Rural	Urban	Rural	Urban	Rural
E_0	40	40	40	50	35	60
γ	1.25	1.20	1.30	1.20	1.00	1.25

The values in Table 4.1 allow accurate prediction of the field strength using the Okumura-Hata model in that region with the accordingly modified empirical parameters. This example demonstrates how the practical calculation of modified model parameters may be summarized into a single reference table, convenient for further use.

4.2 Methods using terrain and ground cover information

One of the most widely used propagation prediction models that take account of the terrain irregularity is the Longley-Rice model [4-10]. It takes its origins in the electromagnetic theory and signal loss variability expressions derived from extensive sets of measurements as given by ‘National Bureau of Standards Technical Note 101’ [4-9] (“Tech Note 101”). Tech Note 101 develops an extensive compilation of mathematical formulae that can be applied to the task of predicting the performance of radiocommunications systems over a wide range of terrain and climatic conditions, but the manual application of those formulae is onerous, if not impossible, even for a single point-to-point propagation path.

However, two of the authors of Tech Note 101 developed a computer program, the Irregular Terrain Model (ITM) [4-10], which became popularly known as the “Longley-Rice Model”. This computer model applies versions of the computational procedures developed in Tech Note 101, and is useful in the frequency range of 20 MHz to 20 GHz, in areas with varied terrain and climatic conditions, over a distance range from one to 2000 km.

The ITM computer model actually consists of two different modules (or algorithms) which are to be used under different circumstances. The first of these is the “area prediction” model [4-11], which is meant to be used when only moderate information about the propagation paths is known. It is particularly useful in mobile and broadcast situations, in the design of generalized systems, and in discussing general problems of interference between types of systems. It is less accurate at short ranges, particularly when high antennas are involved, for it will predict lower signal levels (higher losses) than would typically be measured. For medium and long ranges it should give good results. The area prediction will ask for a terrain roughness factor (ΔH), surface refractivity (N_s), and average terrain heights depending upon the options chosen.

The second module in the ITM program is the “point-to-point prediction” model, which is designed to be used on a fixed path where certain gross features of the intervening terrain profile are known. This model is particularly good for evaluation of specific communication links and for solving special interference problems. It is not at all valid on the standard microwave line-of-sight links and should generally not be used for that situation. (The treatment of such links is normally quite different from the ITM approach. Median signal levels are usually at or near free space values, and variability around the median follows a different set of laws.)

While the Longley-Rice Model Version 1.2.2 does include an area prediction mode, the model is most often used in repetitive point-to-point predictions where a terrain database is available. Only the use of the model in its point-to-point mode will be discussed here.

In operation, the model examines the geometry of a radio path along a given profile of terrain data to determine several important parameters; the most important of which are the distances to the radio horizons from the path end-points and the total path length. Based on these data, a determination is made as to whether the path is line-of-sight (i.e. the end points are mutually

visible) or obstructed. If the path length is greater than the sum of the transmitter and receiver horizon distances, then a combination of knife-edge theory and smooth-Earth diffraction loss is used. Finally, for distances well beyond the “smooth Earth” radio horizon, scatter theory is applied.

Certain facets of the 1.2.2 Version of the Longley-Rice model are approximate. For example, even though it is assumed that a complete and accurate terrain profile is at hand for the path under consideration, the model does not determine a ground-reflection point through direct examination of the path. Rather, it performs a least-squares fit to the terrain data in the central 80% of the path and assumes a spectral reflection from that theoretical surface. Also, there are additional restrictions on the range of applicability for formulae used in the model. Additionally, there can be certain discontinuities in predicted path loss when the model switches between algorithms, particularly from the line-of-sight mode to the obstructed-path mode. Practical implementations of the model must allow for these conditions to occur and be addressed properly.

Also the model fails to explicitly address the effects of vegetation and buildings. It would appear that the model does make some allowance for such “clutter”, but only to the extent that the data, against which the model’s performance was confirmed, were themselves influenced by clutter. This issue was addressed in a paper [4-12] that developed empirical graphs to show the differences between Longley-Rice Model predictions and signal strength data gathered by Okumura, *et al.* [4-4]. The paper presents specific recommendations for additional modules that could be written to adjust the results of the Longley-Rice Model for different clutter environments. However, it does not directly compare Longley-Rice predictions with observed signal strength data. Rather, the comparisons were made against a graphical presentation of an area prediction model (the “Okumura Model”) [4-4]. The Okumura model, in turn had been adjusted to portray the observed effects of vegetation and building clutter of a specific geographic region (the Tokyo urban area) and conditions far removed from those that exist elsewhere. Therefore the restrictions on the Okumura model carry over to this case as well. In sum, the point-to-point predictions of one model were compared with the predictions of another model whose purpose is to provide general estimates of signal performance over an area. A comprehensive discussion of the Longley-Rice model, as compared with one other known terrain based model TIREM, was published in Volume 37 of the IEEE Transactions on Vehicular Technology (February 1988) [4-13]. Discussion of some other path-specific propagation prediction methods may be found in [4-29] and [4-30].

To summarize, the Longley-Rice model is a widely recognized radiowave propagation prediction model that is available in the public domain. The above remarks are intended only to identify specific aspects of the model’s performance that could and should be improved.

Currently the ITM model descriptions, algorithms, FORTRAN source codes and samples are available for access from the U.S. Administration at <http://elbert.its.bldrdoc.gov/itm.html>. The models require terrain elevation databases to extract terrain path profiles. One source of a worldwide terrain data base (GLOBE) is publicly available from the U.S. Administration at <http://www.ngdc.noaa.gov/seg/topo/globe.shtml> and the files needed to extract the terrain data are available from <http://elbert.its.bldrdoc.gov/globe.html>.

4.3 Ray tracing, GTD-UTD, parabolic and integral equation methods

The following material discusses Ray tracing, the geometric and uniform geometric theories of diffraction, and the parabolic and integral equation methods. For more practical information on these topics, see Recommendation ITU-R P.526 as well as Parsons [4-35] and Cátedra [4-36].

4.3.1 Ray tracing and geometric theory of diffraction (GTD) – uniform theory of diffraction (UTD) methods

These methods are applicable to electromagnetic propagation and scattering problems which can be said to be high-frequency. In this context, high-frequency means that the properties of the background medium and the scatterers' characteristic dimensions vary negligibly over intervals of the order of a wavelength of the electromagnetic wave. It is also typical that these methods are applied to problems where the background medium's material properties are isotropic, homogeneous and lossless, although these restrictions are not required by the theory. With these restrictions, however, it is possible to characterize the propagation of electromagnetic waves excited by certain sources as ray-like, i.e. in straight lines, from the source to an observation point. Furthermore, on each ray, the electromagnetic wave's propagation vector, electric field vector and magnetic field vector are mutually orthogonal. The direction of the propagation vector is parallel to the straight line from the source point to the observation point and the surfaces of constant amplitude and phase for the fields lie in planes orthogonal to this direction. The electromagnetic wave can thus be said to be locally planar, thereby allowing simplifications, akin to geometric optics, in the treatment of the problem.

In ray tracing's simplest form, as the name implies, one simplifies the electromagnetic problem to that of the geometric accessibility of rays emanating from the source point to (arbitrary) observation points. It follows that the problem then reduces to the locations of shadow boundaries. Shadow boundaries are the loci of points separating regions of space where rays from the source to an observation point are accessible and those regions where the rays are not (i.e. inaccessible). This particular instance of a shadow boundary is usually referred to as an incident shadow boundary. It is also possible for rays, incident from the source, to undergo one or more specular reflections from the surfaces of scatterers, when these are present. The loci of points separating regions of space where these rays are accessible from those regions of space where these rays are not referred to as reflection shadow boundaries. Observation points located in regions of space where only direct rays from the source to the observation point are accessible (i.e. lit regions) have a field strength calculable from the amplitude and phase of the source excitation and, where appropriate, the distance between the source and observation point. Observation points located in regions of space where specularly reflected rays are also present (accessible) have field strengths which are the sum of the direct wave and a reflected wave, suitably spread or focused, if the radius of curvature of the reflecting surface is finite. Observation points located in regions of space accessible to neither direct nor reflected rays have zero field strength.

The problem with all this, apart from the assumptions that the scatterers are all quite opaque and very large electrically, is that it neglects diffraction. This neglect is addressed by the geometric theory of diffraction (GTD) and its extension, the uniform (Geometric) theory of diffraction (UTD). GTD postulates that diffracted rays exist. These diffracted rays are produced when rays illuminate the edges, corners and vertices of scatterers that give rise to the shadow boundaries discussed

above. Scalar diffraction coefficients have been derived by asymptotic expansion of Sommerfeld's exact solution for wedge diffraction. However, these diffraction coefficients have the unhappy property of becoming singular on the incident and reflection shadow boundaries, which can contain observation points of interest. In order to remedy this shortcoming, UTD was developed. In UTD, the GTD scalar diffraction coefficients are multiplied by a transition function. The transition function vanishes at the same rate that the diffraction coefficient becomes unbounded at the shadow boundary. The product is bounded and uniform across the shadow boundary, allowing reliable computation of the diffracted field everywhere in space, when the other assumptions are valid. Recommendation ITU-R P.526 gives an example of UTD applied to a finitely conducting wedge obstacle. There have been numerous extensions to UTD.

4.3.2 Parabolic equation (PE) methods

The parabolic equation (PE) is an approximation of Maxwell's equations, the derivation of which is based on the notions that backscattered waves may be neglected, that vertical angles are always small and that variation in the coordinate transverse to the vertical plane containing the propagation direction can be taken care of by other means. One can then describe a functional variation of the field as:

$$\Phi = u(x, z) \cdot e^{ikx} \quad (4-8)$$

where $u(x, z)$ is slowly varying in x . Given these assumptions, it can be shown that, applying the two-dimensional Helmholtz equation that Φ must satisfy and upon neglect of the second derivatives of u with respect to x (the principal direction of propagation), one obtains a parabolic differential equation for u . Solutions are obtained by applying appropriate boundary conditions at the source point and the upper and lower boundaries in z . One consequence of the neglect of the backscattered wave in the PE is, once the fields are known along a vertical plane at a given x location, the fields at all greater x locations are determined.

Solutions to the PE are generally obtained numerically for propagation problems involving actual terrain and/or variability of the refractive index lapse rate in x and/or z . Examples of the numerical solutions are implicit finite difference methods and split step spatial fast Fourier transform approximation methods. Because of the numerical approximations used to solve the PE, there are Nyquist-like criteria related to spatial discretization and the wavelength of the electromagnetic wave propagation being modelled, and these relate to numerical stability and accuracy considerations. Consequently, PE solutions are far more computationally intensive than GTD or UTD solutions.

4.3.3 Integral equation (IE) methods

Closely related to the parabolic equation method, the integral equation (IE) method starts from Green's theorem equating the volume and surface integrals of functions continuous throughout the volume, along with their Laplacian and normal derivative operators. After some manipulation, the volume integral reduces to the 4π times the free space field, that being the contribution to the field in the absence of the Earth, while the surface integral has three contributions: an integral over the surface of the Earth, an integral over an infinitesimal hemispherical surface surrounding the

singularity of the Green's function and a surface closing above the Earth at infinity. The integral over the infinitesimal closed surface yields 2π times the scalar function we seek. The integral over the surface at infinity vanishes. Finally, by appeal to the method of stationary phases, the contributions in the direction transverse to the propagation path are integrated out leaving only a line integral to evaluate. The method can be shown to give good results for the analytically accessible cases of a flat and smooth spherical Earth.

Solutions to the IE are found numerically. The integral equation is in the form of a linear Volterra integral equation of the second kind, using a method attributed to Wagner [4-34]. Practically speaking, it is calculated only for frequencies less than a few tens of MHz, due to the complications of solving the IE.

4.4 Diffraction modelling

4.4.1 Summary of earlier methods, spherical Earth, knife-edge, and cylinder models

Diffraction occurs when the direct path between the two terminals is blocked by one or more opaque obstacles. In such a situation, although the field-strength at the receiving terminal will be lower than it would be in the absence of the obstacles, some signal will still be received by means of the process of diffraction. In addition, obstacles that approach the line of sight but do not actually block it may still have a significant effect upon the received field strength.

Generally the obstacles to be considered will be land terrain features or the surface of the sea. Terrain features will often be quite irregular in shape. Thus, traditionally they have been approximated to various stylised shapes in order to make practical calculations of the expected loss due to diffraction. Such shapes include knife-edges, wedges, cylinders and spheres.

4.4.1.1 Knife-edge diffraction modelling

The simplest shape used for modelling terrain is the simple knife-edge. With this approach the terrain is approximated to a series of such edges. The method of Fresnel can then be conveniently used to calculate the diffraction loss of such a knife-edge. This involves constructing an imaginary surface known as a Huygens surface above the edge as shown in Fig. 4.3. Huygens' Principle then states that each point on this surface acts as a secondary radiator. Calculation of the diffracted field then involves integrating contributions from points on the surface from the top of the knife-edge to infinity. This integration is shown graphically by the Cornu Spiral shown in Fig. 4.4. The spiral is normalized in terms of a parameter v , where:

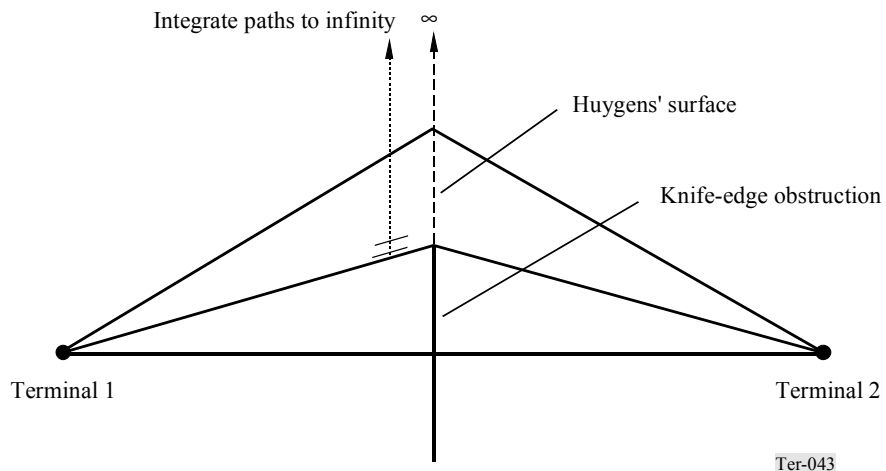
$$v = 2\sqrt{(\Delta d/\lambda)}$$

where:

Δd : the difference in length between the direct path between the terminals and that which just passes over the knife-edge.

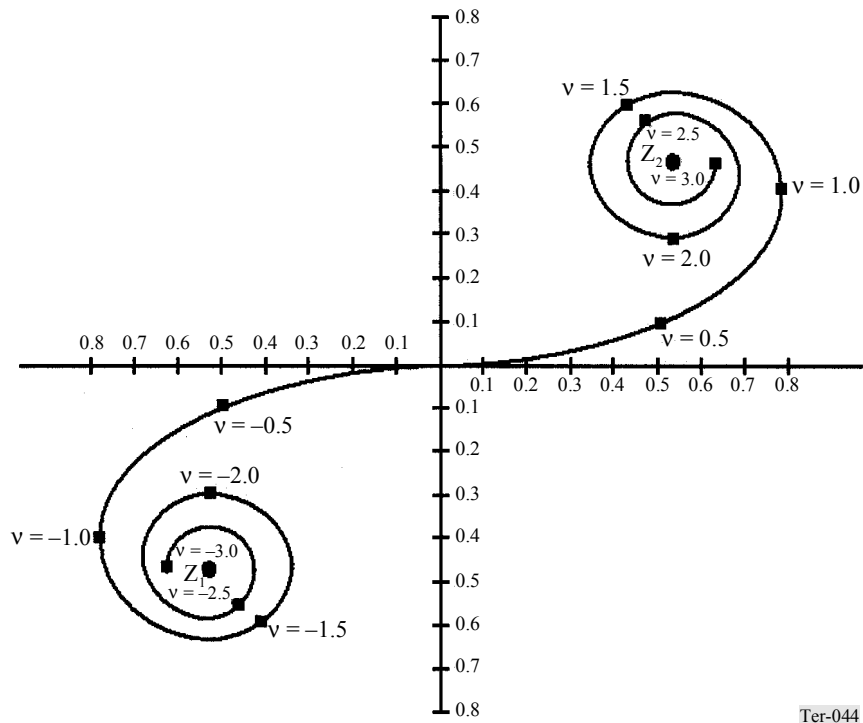
The free space field strength is represented by the distance between the two asymptotic points, Z_1 and Z_2 . When part of the wavefront is obstructed by the knife-edge, the value of the field strength is represented by the distance between the point on the spiral corresponding to the peak of the knife-edge and the appropriate asymptotic point (Z_1 or Z_2).

FIGURE 4.3
Knife-edge diffraction



Often a propagation path will contain several obstacles so that multiple knife-edges will be needed to model it completely. As described in the following Sections, there are a number of techniques that have been proposed for dealing with multiple knife-edges.

FIGURE 4.4
The Cornu Spiral representation of knife-edge diffraction



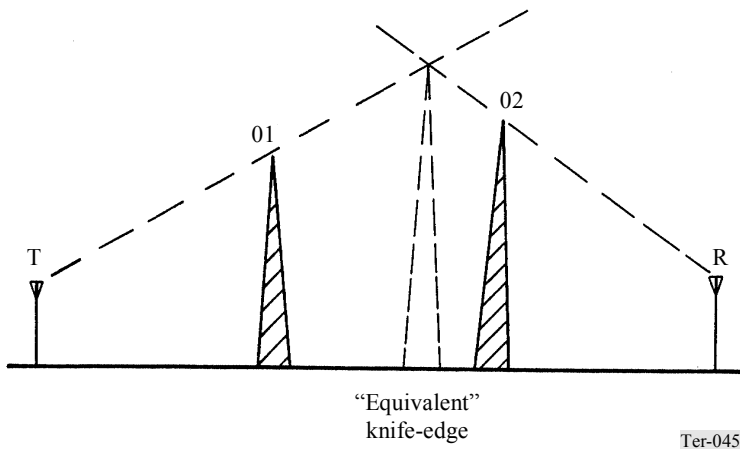
4.4.1.2 The Millington method

The Millington method [4-17] may be used to calculate diffraction by two knife-edge obstacles. It is rigorous and involves integration over both Fresnel surfaces. Thus it requires a double integral. In principle the technique could be extended to calculate any number of edges. However, each additional edge would require an additional integral. Such nested integrals are likely to be impractical for more than about 3-4 edges.

4.4.1.3 The Bullington method

The Bullington method [4-18] is also intended to deal with two knife-edges. However, the two edges are combined to form a single virtual edge. Thus only a single integration is needed. This simplification is at the expense of some accuracy. If the diffraction losses are small, such as at VHF, the errors can be less than 3 dB. However, as frequency increases and diffraction losses become greater, errors may increase to as much as 10 dB. The method underestimates the losses.

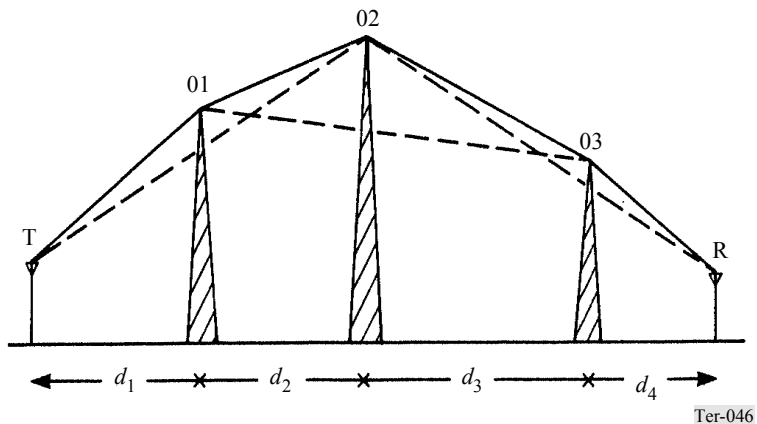
FIGURE 4.5
Bullington construction for multiple knife-edge diffraction calculation



4.4.1.4 The Epstein-Peterson method

The Epstein-Peterson [4-19] method can easily be used for any number of knife-edges. The loss for each edge is calculated in turn, based on imaginary terminals placed at the top of the adjacent edges (or one of the real terminals for the first and last edge). The individual losses (dB) are then added to derive the overall loss. Millington showed that this method is subject to errors of up to 3 dB high or low. For two diffracting edges when the second edge and second terminal are deep in the shadow of the first edge, the loss is underestimated. Millington proposed a correction factor given in reference [4.17], which can be used with such paths to improve the accuracy. Millington's correction does not, however, apply to paths with three or more knife-edges.

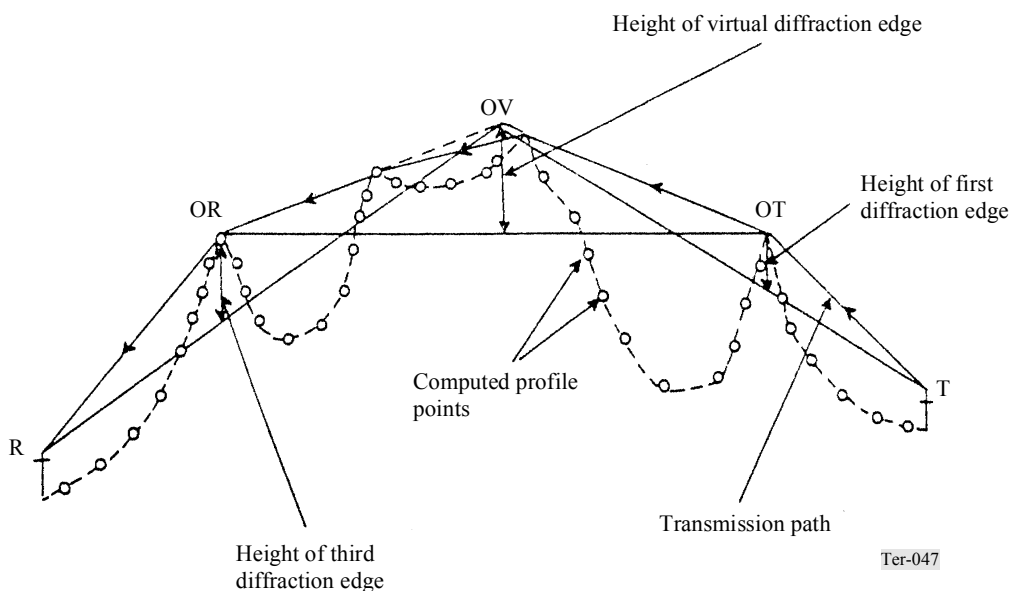
FIGURE 4.6
Epstein-Peterson construction for multiple knife-edge diffraction calculation



4.4.1.5 The Edwards-Durkin method

The Edwards-Durkin method [4-20] might be termed a hybrid between the Bullington method and the Epstein-Peterson method. For paths with up to three obstacles, it follows the Epstein-Peterson method. For paths with four or more obstacles, it identifies the two “outermost” obstacles; i.e. the two obstacles nearest the transmitting and receiving sites, respectively. We shall call them OT and OR, respectively. It then sets up a construction similar to the Bullington construction to create a “virtual obstacle” between. We shall call that obstacle OV. The diffraction calculation is then done for the path from T to OT to OV to OR to R, see Fig. 4.7.

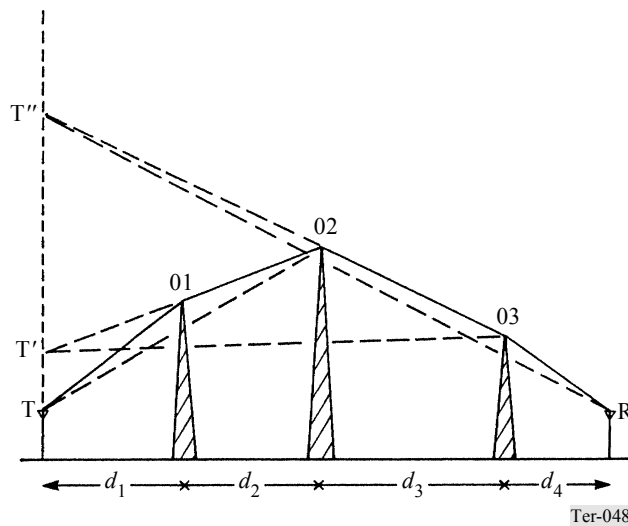
FIGURE 4.7
Edwards-Durkin construction for multiple knife-edge diffraction calculation



4.4.1.6 The Shibuya method

The Shibuya method [4-21] is similar to the Epstein Peterson method, except that in calculating the diffraction losses, the transmitting terminal is taken to be at a virtual point above the actual location, chosen so that the two terminals and the edge lie on a straight line (see Fig. 4.8). Generally, provided the losses at the individual edges are greater than 12 dB, this method is equivalent to the Epstein-Peterson method with the Millington correction.

FIGURE 4.8
Shibuya construction for multiple knife-edge diffraction calculation



4.4.1.7 The Deygout method

The Deygout method [4-22] involves calculating the loss for each edge in the absence of all other edges. The edge giving the highest loss is identified as the main edge and this loss value is taken to be the value for this edge. The main edge is then taken to be a terminal and the sub-paths each side are treated in the same way. The path is thus subdivided until all edges have been considered and the overall path loss is then taken to be the sum (dB) of all the losses of the individual edges. The Deygout method always overestimates the losses of a multiple knife-edge path. Correction factors are therefore possible. Causebrook [4-31] has proposed a method of correction that gives very good results with the Deygout method when restricted to a maximum of three knife-edges. López [4-23] has proposed a similar construction that overcomes the pessimism of the Deygout construction.

4.4.1.8 The López method

The López method [4-23] is very similar to that of Deygout. It overcomes the pessimism inherent in the Deygout method by changing the geometry of the calculation such that the diffraction angle of the main edge is based upon the actual path geometry rather than upon the assumption that the main edge is free standing. As seen in Fig. 4.9, the Deygout construction, the diffraction angle for the main obstacle is associated with T-O2-R. In Fig. 4-10, the López construction, the angle measurement includes the effect of the intervening obstacles.

FIGURE 4.9
Deygout construction for multiple knife-edge diffraction calculation

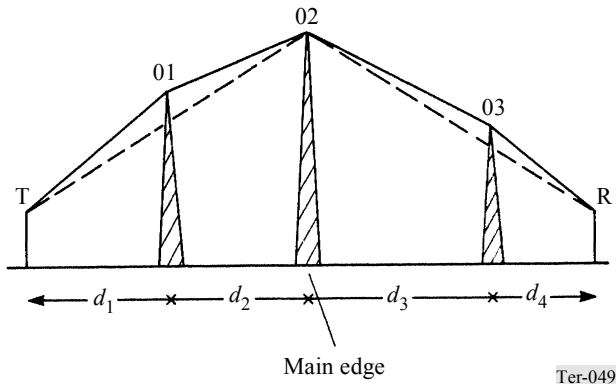
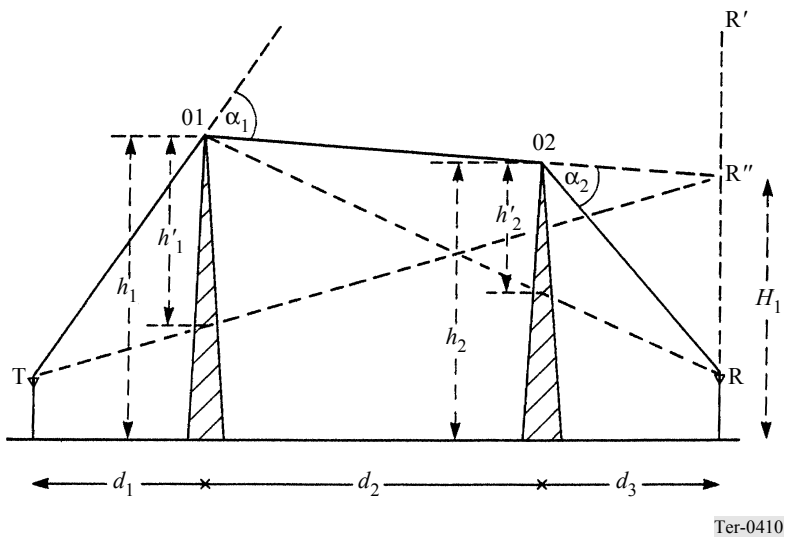


FIGURE 4.10
López construction for multiple knife-edge diffraction calculation



4.4.1.9 Spherical Earth and cylinder models

Although diffraction due to knife-edges can be accurately modelled and techniques such as that of Deygout can be used where there may be many such edges, real terrain does not closely resemble a series of such edges. In general since the knife-edges are placed at the high points of the terrain between the two terminals, no account is taken of the terrain between these points. This normally results in an underestimation of the resulting diffraction loss, giving a field-strength prediction higher than the measured value.

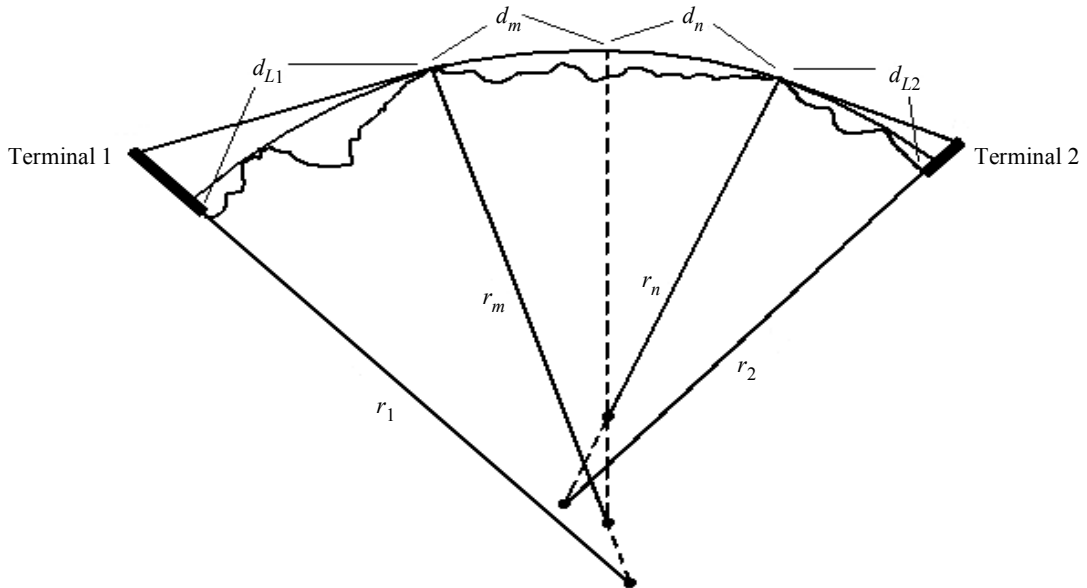
At the opposite extreme, obstacles can be approximated to a sphere or cylinder. The obvious application of this technique is when the obstacle is the surface of the sea. In order to calculate the diffraction loss over such a spherical surface we must solve Maxwell's equations in its presence. In

the late 19th century many scientists were working on such a solution, starting with Rayleigh in 1871. However, the first practical solution was provided by Van der Pol and Bremmer in 1937 [4-24]. This solution expressed the result in the form of a residue series. To reduce computation time it is normal to use a simplified form developed by Vogler which used only the first term of the residue series [4-25].

Curved surfaces, or cylinders, can also be used to approximate terrain features. Rounded hills may be approximated by means of individual cylinders. Where there are multiple rounded hills, techniques similar to those already described for multiple knife-edges may be adopted. However, it is known that this approach can give significant errors, particularly where the terrain is irregular.

Another method for using cylinders was proposed by Rice *et al.* [4-9] and is often used. With this approach the terrain is approximated to a series of four cascaded cylinders. Figure 4.11 shows how a typical propagation path can be modelled in such a way. The first cylinder, radius r_1 is chosen such that the horizon line from one terminal is a tangent and it just contains the terrain between this tangent point and the terminal. Similarly the final cylinder is chosen from the horizon of the other terminal and the terrain. The radii, r_m and r_n of the middle two cylinders and the distances d_m and d_n are chosen such that there are no slope discontinuities at the junctions between the spheres. From the various parameters shown in Fig. 4.10, are calculated overall effective values of the parameters r_1 , r_2 , r_m , r_n , d_n , d_{L1} and d_{L2} . These are then used with the same Vogler approximation to the residue series to calculate the path loss.

FIGURE 4.11
Cascaded cylinder approach



- r_1, r_2, r_m, r_n : radii of cylinders
- d_n : total path distance
- d_{L1} : horizon distance from one terminal
- d_{L2} : horizon distance from other terminal

This then represents an alternative diffraction method to the various multiple knife-edge approaches outlined above. However, whereas the multiple knife-edge approach tends to underestimate the diffraction loss, the cascaded cylinder approach tends to overestimate. This has led to methods using both the multiple knife-edge and cascaded cylinder methods. A linear interpolation between the two results is then taken to be the true value. The weighting factor between the two methods is determined empirically using a set of profiles for which measured field-strength values are available. There is little scientific basis for this approach, but it does appear to give improved predictions in some situations.

While spherical Earth solutions are more accurate than cylindrical solutions, they are significantly more complex from an analytic standpoint. For realistic Earth radii and paths, the difference between the spherical Earth and cylindrical solutions is negligible.

4.4.1.10 Other models

Other types of stylized obstacle have been used in prediction methods. In particular, single obstacles have been modelled as wedge shapes [4-33]. Diffraction calculation over such a surface is essentially similar to that of a knife-edge, with a Huygens surface above the obstacle. A reflected wave from the surface of the wedge is, however, allowed on both sides. This gives rise to a four ray method by which the overall diffraction loss is calculated.

4.4.2 Recommendation ITU-R P.526

This ITU-R Recommendation deals with the problem of radiowave propagation over diffraction paths. Since, for practical applications, it is quite difficult to establish a general solution covering all types of terrain, prediction methods are provided for the diffraction over a smooth spherical Earth and the diffraction over terrain obstacles

In the case of a spherical Earth, Recommendation ITU-R P.526 presents two methods numerical and graphical, based on the same approximation, i.e., the dominance of the first term of the residue series [4-26]. In both methods, the attenuation relative to free-space is given by three separated terms, one containing the distance dependence and the two others corresponding to the antenna height-gain functions. The numerical method, which can be easily coded in a pocket calculator, is adequate for applications where repeated use is necessary, while the graphical method is better for a quick estimation of a given situation. The accuracy of these methods is acceptable even if the path profile is not exactly a smooth spherical Earth. However, the terrain irregularities must be small when compared to the first Fresnel zone radius in the middle path. A practical example is given in [4-27].

Regarding the diffraction over an irregular terrain, depending of the type of obstacle, different prediction methods are provided. The simplest one is the single knife-edge obstacle. This idealized model is relevant only in cases where the radius of curvature of the obstacle can be neglected. An approximate expression is given for the calculation in the diffraction region ($v > -0.7$) (see Section 4.4.1.1), avoiding the use of a more complicated formula associated with the Cornu Spiral shown in Fig. 4.4. Based also on the knife-edge model, Recommendation ITU-R P.526 describes a simplified solution for estimating the shielding effect of a finite-width screen such as a mountain range or a building.

A better approximation to the problem of the diffraction over an isolated obstacle should take into account its dimension along the longitudinal direction. The solution adopted in Recommendation ITU-R P.526 is to add an additional attenuation due to the curvature of the obstacle to the knife-edge loss. The accuracy of this method depends mainly on the procedure used to obtain the radius of curvature at the obstacle top.

Recommendation ITU-R P.526 also describes a method for predicting the diffraction loss due to a finitely conducting wedge. This may be applied to diffraction around the corner of a building or over the ridge of a roof, or where terrain may be characterized by a wedge-shaped hill.

The problem of multiple diffraction is much more complicated. For the diffraction over two knife-edges, two methods are given in Recommendation ITU-R P.526. The simplest one is due to Epstein and Peterson [4-19] with a correction based on Millington *et al.* [4-17]. However, if one edge is predominant, the Deygout method [4-22] should be used. Both methods may be applied to the case of rounded obstacles.

No rigorous method exists for the prediction of radiowave attenuation due to the diffraction over several rounded obstacles. However, Assis [4-32] proposed a simplified model that attempts to do so. Recommendation ITU-R P.526 adopts a model based on Deygout method, limited to a maximum of three knife-edges, plus an empirical correction derived from measurements carried out on a large number of paths in United Kingdom.

Recommendation ITU-R P.526 does not cover the case of irregular terrain that has no pronounced features (rolling terrain), where neither the smooth Earth nor the multiple diffraction methods are applicable.

4.5 Propagation model considerations

The propagation prediction model and its parameters should be selected very carefully, so as to obtain the meaningful results from a modelling exercise. To select the most appropriate model, this section describes a few general rules and considerations on this subject.

Generally, a selected propagation model may range from the basic free-space loss formula to the sophisticated path-specific calculation engine. So the principal aim of a selection should be to choose the simplest and most readily available model that would be just sufficient to provide the necessary precision and meaning of the results in the prescribed propagation conditions. If the sophisticated path-specific models are not available, then one should first try to consider possibilities provided by the generalized point-to-area empirical models described at the beginning of Chapter 4.

Radiocommunication Study Group 3 has developed a set of models, which may be used in different conditions under the various circumstances. All these models are summarized in Recommendation ITU-R P.1144 [4-28]. This Recommendation provides a general guidance on selection of a suitable ITU-R propagation prediction model, based on the principal user requirements, such as the system to which a model is to be applied, frequency range, modelling distance and propagation data available. Table 4.2 provides a convenient recapitulation of Recommendation ITU-R P.1144, as regards the land mobile propagation at the VHF/UHF frequency ranges.

TABLE 4.2

Guide to the selection of ITU-R radiowave propagation prediction model for the land mobile applications at VHF/UHF frequencies
 (extracted from Rec. ITU-R P.1144)

Method	Application	Type	Output	Frequency	Distance	% time	% location	Terminal height	Input data
Rec. ITU-R P.1546	Terrestrial services	Point-to-area	Field strength	30 to 3 000 MHz	1 to 1 000 km	1 to 50	1 to 99	Tx/base: effective height from less than 0 m to 3 000 m Rx/mobile: ≥ 1 m	Terrain heights and ground cover (optional) Path classification Distance Tx antenna height Frequency Percentage time Rx antenna height Terrain clearance angle Percentage locations
Rec. ITU-R P.534	Fixed Mobile Broadcasting	Point-to-point via sporadic E	Field strength	30 to 100 MHz	0 to 4 000 km	0 to 50	Not applicable	Not applicable	Distance Frequency
Rec. ITU-R P.843	Fixed Mobile Broadcasting	Point-to-point via meteor-burst	Received power Burst rate	30 to 100 MHz	100 to 1 000 km	0 to 5	Not applicable	Not applicable	Frequency Distance Tx power Antenna gains

4.5.1 System planning

Propagation prediction is one of the most important elements in the planning of radio-communication systems. Usually the task of a land mobile radio network planner is to cover the largest service area (or the entire prescribed service area) with the minimum necessary number of base stations. At the same time, the necessary minimum field strength and the signal-to-interference ratio, hence the communication quality, must be ensured over the entire projected service area.

For predicting the field strength of the wanted signal in system planning exercises it is, therefore, generally advisable to use a model that provides “worst-case” predictions of predicted field strength. This approach ensures that the model predicts “guaranteed” field strength of a signal, hence the system designers are assured of the proper coverage of service area.

To ensure a “worst-case prediction”, a model and its parameters should be selected according to the following rules:

- model should be selected for the prescribed conditions of the use: frequency band, range, height of receiving antenna;
- if model is supplied with some correction factors, these should be tuned so as to account for the most severe constraints, e.g. lowest receiving antenna, depolarization effects, attenuation in vegetation, etc.;
- if model accounts for time and location variability statistics, the higher values of these should be used – at least 50% of time 50% of locations to obtain averaged results or higher (e.g. up to 90% or even 99% of locations) to obtain the most pessimistic results.

It should be also noted that radio signals are subject to severe fading in most typical conditions of land mobile service propagation. Therefore, it is usually a good practice to account also for the predicted depth of fading signal variations. The statistical models for fading are described in Section 3.3 of this Handbook. Using obtained estimates of fading (for given percentage of reliability), the fading may be conveniently taken into account by means of degrading the effective sensitivity of the mobile receiver and then estimating the edge of coverage area for this reduced value of threshold sensitivity. For example, if the sensitivity of a receiver is -105 dBm and it is estimated that the depth of fading for 99% does not exceed 15 dB, then, when calculating the projected coverage area, threshold sensitivity should be reduced to -105 dBm + 15 dB = -90 dBm.

4.5.2 Interference assessment and spectrum management

Unlike system planning, when propagation prediction models are used to assess unwanted interference and other similar spectrum management activities, they are usually used so as to provide “best case” results. This is because in such tasks it is important to take into account the strongest levels of possible interference, which naturally correspond to the most favourable propagation conditions of the unwanted (interfering) signal.

Therefore, for interference assessment, the propagation prediction model and its parameters are usually selected with the following criteria:

- model should be selected for conditions which are the most favourable to propagation of the unwanted signal; e.g. when considering interference at comparatively short ranges or with high antenna elevations, even the free-space loss formula may be used, which is otherwise considered to be unsuitable for land mobile applications;
- correction factors, if any, should be tuned towards the most favourable propagation conditions, e.g. highest receiving antenna height, line-of-sight allowances, etc.;
- if the model accounts for time and location variability statistics, the lower values of these should be used – typically 10% of time at 50% of locations or lower (e.g. down to 1% of time).

It should be noted that interference assessment often forms the part of international administrative spectrum management duties under the terms of the ITU Radio Regulations and related legal documents. Therefore the national radiocommunication administrations often use certain mutually agreed propagation models for interference assessment and international frequency coordination.

4.5.3 Comparison of measurements and predictions

Quite often system designers are required to verify the projected coverage areas with the actual measurements once the system is installed. If the base station is equipped with an omnidirectional antenna, then such verification is usually done by means of taking the field-strength measurements along 3-5 radial routes. If the base station antenna is directional or if the coverage zone contains certain specifically targeted service areas (e.g. highway, business centre, etc.), then the measurements are taken within those targeted areas.

In such verification measurement campaigns the test receiver is usually moved outwards from the base station and the received field strength is monitored and compared with the predicted values and with the prescribed value of receiver sensitivity threshold.

Sometimes it is also necessary to make a check of projected levels of interference. In such case measurements are usually carried out along some interference protection perimeter, e.g. along political boundaries.

4.6 References

- [4-1] Recommendation ITU-R P.1546 – Method for point-to-area predictions for terrestrial services in the frequency range 30 to 3 000 MHz, International Telecommunication Union, Geneva.
- [4-2] Recommendation ITU-R P.370 – VHF and UHF propagation curves for the frequency range from 30 MHz to 1 000 MHz, International Telecommunication Union, Geneva.
- [4-3] Recommendation ITU-R P.529 – Prediction methods for the terrestrial land mobile service in the VHF and UHF bands, International Telecommunication Union, Geneva.
- [4-4] OKUMURA, Y. *et al.* [1968] Field strength and its variability in VHF and UHF land mobile radio service. *Rev. Elec. Comm. Lab.* 16(9-10), p. 825-873.
- [4-5] HATA, M. [1980] Empirical formula for propagation loss in land mobile services. *IEEE Trans. Veh. Tech.*, 29(3), p. 317-325.

- [4-6] LEE, W. C. Y. [1982] *Mobile communications engineering*. McGraw-Hill, New York, United States of America, p. 464.
- [4-7] LEE, W. C. Y. [1995] *Mobile communications design fundamentals*. 2nd Edition. McGraw Hill.
- [4-8] BADSBERG, M., ANDERSEN, J. B. and MOGENSEN, P. [January 1995] Exploitation of the terrain profile in the Hata model. COST 231 TD(95)009.
- [4-9] RICE, P. L. *et al.* [May 1965] Transmission loss predictions for tropospheric communications circuits. NBS Technical Note 101; two volumes.
- [4-10] LONGLEY, A. G. and RICE, P. L. [1968] Prediction of tropospheric radio transmission loss over irregular terrain – A computer method. ESSA Tech. Report ERL 79-ITS 67.
- [4-11] HUFFORD, G. A, LONGLEY A. G. and KISSICK, W. A. [April 1982] A guide to the use of the ITS irregular terrain model in the area prediction mode. NTIA Rep. 82-100.
- [4-12] LONGLEY, A. G. [April 1978] Radio propagation in urban areas. OT Rep. 78-144.
- [4-13] IEEE Vehicular Technology Society Committee on Radio Propagation [February 1988] Coverage prediction for mobile radio systems operating in the 800/900 MHz frequency range. *IEEE Trans. Veh. Tech.* 37(1).
- [4-14] MEDEISIS, A. and KAJACKAS, A. [April 2000] Adaptation of the universal propagation prediction models to address the specific propagation conditions and the needs of spectrum managers. Millenium Conf. on Antennas and Propagation (AP 2000), Davos.
- [4-15] MEDEISIS, A. and KAJACKAS, A. [May 2000] On the use of the universal Okumura-Hata propagation prediction model in rural areas. IEEE Veh. Tech. Conf. (VTC 2000 Spring) Conf. Record, Tokyo.
- [4-16] ITU Handbook on Radio Spectrum Monitoring, 1995.
- [4-17] MILLINGTON, G., HEWITT, R. and IMMIRZI, F. S. [1962] Double knife-edge diffraction in field strength predictions. *Proc. Inst. Elec. Eng.*, 109C, 16, p. 419-429.
- [4-18] BULLINGTON, K. [1947] Radio propagation at frequencies above 30 megacycles. *Proc. Inst. Radio Eng.*, 35, 10, p. 1122-1136.
- [4-19] EPSTEIN, J. and PETERSON, D. W. [1953] An experimental study of wave propagation at 850 Mc/s. *Proc. Inst. Radio Eng.*, 41, 5, p. 595-611.
- [4-20] EDWARDS, R. and DURKIN, J. [September 1969] Computer prediction of service areas for V.H.F. mobile radio networks. *Proc. IEE*, 116(9), p. 1493-1500.
- [4-21] SHIBUYA, S. [1987] *A basic atlas of radio-wave propagation*. Wiley, New York, United States of America, p. 263.
- [4-22] DEYGOUT, J. [1966] Multiple knife-edge diffraction of microwaves. *IEEE Trans. Ant. Prop.*, 14(4), p. 480-489.
- [4-23] LÓPEZ GIOVANELLI, C. [March 1984] An analysis of simplified solutions for multiple knife-edge diffraction. *IEEE Trans. Ant. Prop.*, 32(3), p. 297-301.
- [4-24] VAN DER POL, B. and BREMMER, H. [1937] The diffraction of electromagnetic waves from an electrical point source round a finitely conducting sphere, with application to radiotelegraphy and the theory of the rainbow. *Phil. Mag.*, XXIV, p. 141-176 (Part 1) and p. 825-862 (Part 2).
- [4-25] VOGLER, L. E. [1964] Calculation of groundwave attenuation in the far diffraction region. *Radio Sci.*, 68D, 7, p. 819-826.
- [4-26] Recommendation ITU-R P.368 – Ground-wave propagation curves for frequencies between 10 kHz and 30 MHz, International Telecommunication Union, Geneva.

- [4-27] Handbook on radiowave propagation information for predictions for terrestrial path communications, International Telecommunication Union, Geneva, in preparation.
- [4-28] Recommendation ITU-R P.1144 – Guide to the application of the propagation methods of Radiocommunication Study Group 3, International Telecommunication Union, Geneva.
- [4-29] COST 207 [1989] Digital land mobile radio communications. Final Report, Office Official Publ. Eur. Comm., ISBN 92-825-9946-9.
- [4-30] COST 231 [1999] Digital mobile radio towards future generation systems. Final Report, Office Official Publ. Eur. Commission., EUR 18957, ISBN 92-828-5416-7.
- [4-31] CAUSEBROOK, J. H. and DAVIES, B. [1971] Tropospheric radiowave propagation over irregular terrain: the computation of field strength for UHF broadcasting. BBC Research Report No. 43.
- [4-32] SOARES DE ASSIS, M. [March 1971] A simplified solution to the problem of multiple diffraction over rounded obstacles. *IEEE Trans. Ant. Prop.*, 19(3), p. 292-5.
- [4-33] LUEBBERS, R. J. [September 1984] Propagation prediction for hilly terrain using GTD wedge diffraction. *IEEE Trans. Ant. Prop.*, 32(9), p. 951-5.
- [4-34] WAGNER, C. [1953] On the numerical solution of Volterra integral equations. *J. Math. Phys.*, 32, p. 289-401.
- [4-35] PARSONS, J. D. [2000] *Mobile radio propagation channel*. 2nd Ed., Wiley, New York, United States of America.
- [4-36] CÁTEDRA, M. F. and PÉREZ-ARRIAGA, J. [1999] *Cell planning for wireless communications*. Artech House.

CHAPTER 5

TERRAIN DATABASES (AVAILABILITY AND USE)

Many propagation prediction algorithms for the VHF and UHF ranges of Radiocommunication Study Group 3 are terrain-based. That is, they rely on terrain data as one of the bases of their calculations. Generally speaking, there are two kinds of terrain data applicable to radio propagation calculations: hypsographic and morphologic. Hypsographic data describes the elevation characteristics of the terrain being described; i.e. terrain height. Morphologic data describes the ground cover characteristics.

Digital databases established for the purpose of propagation predictions need to contain information which is related to the type of prediction being undertaken. For frequencies above about 30 MHz, information about the terrain height and ground cover is currently needed. For detailed propagation predictions for frequencies above about 1 000 MHz, especially in urban areas, information about the location, size and orientation of individual buildings is currently needed in addition to terrain height information.

Statistically-based propagation prediction algorithms, such as those in Recommendation ITU-R P.1546 [5-1], do not require detailed hypsographic data because they are generally based upon an effective antenna height rather than on actual path geometry. More detailed prediction algorithms, such as those in Recommendation ITU-R P.526 [5-2], require somewhat more detailed data to perform adequately. Horizontal spacings of 200 m between data points and r.m.s. vertical accuracies of ± 15 m have proven adequate for this sort of method. The accuracy of both statistical and path-geometry-based algorithms is improved if the morphologic characteristics of the area are taken into account.

It is to be expected that increasingly sophisticated prediction models will be developed which will permit more detailed propagation predictions but which will also demand more detailed information and, potentially, a reduced horizontal spacing for the data samples. Consult Recommendation ITU-R P.1058 [5-3] for further information.

5.1 Terrain height

A number of administrations, as well as private organizations, have made available hypsographic data of varying quality.

The horizontal spacing between data-points, which should be used in a topographic database, depends upon the use to which the data will be put. It is not practicable to recommend a particular value. In practice horizontal spacings in the approximate range 20 m to 1 km, or the equivalent in latitude-longitude, are typical. Various propagation-prediction models not only have different

requirements for horizontal resolution, but differing sensitivity to changes in horizontal resolution. It should not be assumed that improving horizontal resolution with a given propagation method always improves prediction accuracy.

The accuracy of propagation prediction models can be strongly affected by the accuracy of terrain height data in a topographic database. The accuracy of terrain heights is typically expressed as a root-mean-square (r.m.s.) error value. Horizontal resolution, vertical accuracy, and the propagation method in use, will all affect the calculated result. In general, the more detailed deterministic propagation methods require greater resolution and accuracy in topographic data, but details will vary in individual cases. An r.m.s. error of 15 m in terrain height data has been found acceptable for many purposes.

Most current topographic databases used for propagation prediction and radio planning have 2-dimensional arrays of data at equal intervals in the chosen coordinate system, referred to as “gridded data”. This has the advantage that horizontal coordinates need only be provided for reference points, with most data consisting of self-indexing arrays of height values. For rectangular projections the horizontal data spacing will typically be the same throughout a complete database. For latitude-longitude coordinates the longitude spacing is sometimes increased in steps as latitude increases in order to keep the longitude scale-factor approximately constant.

When drawing a profile between two arbitrary locations, few or none of the data points in a grid-based database will coincide exactly with the profile. Various methods are available for extracting terrain height data in such cases. The following are recommended according to circumstances:

- when the height data are in some way representative of a square area of land, data should be placed in the profile for each square through which it passes. Each profile point may be placed on the normal from the profile line to the corresponding data point, although this will not in general produce equally-spaced profile points. If the propagation method requires equally-spaced points, it is acceptable to move profile points to accomplish this;
- when the height data represent only the height at each exact point, the preferred extraction method is to pre-determine equally spaced profile points and obtain the terrain height for each by bi-linear interpolation from the immediately-surrounding gridded-data values.

During the process of profile construction, the curvature of the Earth can be taken into account by increasing the interpolated terrain height values by a correction factor that is dependent on the effective Earth radius and on the position of the point along the profile. For a discussion of effective Earth radius, see Recommendation ITU-R P.452, § 4.3 [5-7].

The Global Land One-kilometre Base Elevation (GLOBE) digital elevation model (DEM) is a worldwide, multi-source-derived, open, digital elevation dataset in raster format. GLOBE 1.0 [5-4] has a horizontal resolution of $30'' \times 30''$ in latitude and longitude, referenced to the World Geodetic System 84 (WGS 84). These range from 90° N latitude to 90° S latitude and from 180° W longitude to 180° E longitude, respectively. The resulting rasterised complete dataset can be thought of as having 21 600 rows and 43 200 columns.

The “vertical” units are elevations in metres above mean sea level. On the land, these range from values of –407 to 8 752 m. On the sea, elevations are marked as no-data and assigned a value of –500. There is an associated file containing source information for the elevation data. The mask for sea elevations in the source/lineage file is 0. The user can then distinguish elevation values of 0 for land from sea values by resetting the sea values from –500 to 0, when using the source/lineage mask. This is particularly useful when considering mixed (land-sea) paths.

As mentioned above, GLOBE 1.0 elevation data are derived from a variety of sources [5-5]. In some cases, e.g., North America, they are derived from high resolution DTED’s and can thus be assumed to have accuracies comparable to these datasets. In some other parts of the world, the sources of data may have coarser resolution. Users should consult [5-3] for a comprehensive discussion of the elevation accuracies. In the 2001–2002 timeframe, it is expected that data from the Space Shuttle’s Imaging Radar Mission will be incorporated into GLOBE, providing $3'' \times 3''$ resolution data from 60° N latitude to 60° S latitude.

Software for terrain profile elevation extraction from the GLOBE 1.0 DEM is available. The Fortran source code for this software can be obtained from the World Wide Web: <http://elbert.its.bldrdoc.gov/globe.html>.

The software extracts the profile along the great circle between a transmitter and receiver. The terrain height of a profile point on the great circle, PP, is calculated by bilinear interpolation on the GLOBE DEM, taking the elevations of the four terrain points, P1-P4, containing the latitude and longitude of the profile point.

5.2 Ground cover

The range of possible ground categories is very large and the full range is unlikely to be relevant to any individual geographic area. Table 5.1 (from Recommendation ITU-R P.1058 [5-3]) gives descriptive titles and a two-level coding scheme for a set of ground cover categories. A category describes the type of ground cover in a specified area (e.g. a 100 m square). Where more than one type of cover exists in the area under consideration the dominant category should be described. Categories in upper case may be used when a more detailed classification is not required, or more detailed information does not exist.

A category may be indicated by a two-digit code as indicated in the first column of Table 5.1. When available, up to three optional parameters may be supplied to add precision to the description implied by a category name:

- *Height H_c* : This should represent the characteristic height of ground cover in metres above ground, ignoring isolated objects of greater height. In mathematical terms this will most often be best approximated by the modal cover height, but the intention is to provide the most characteristic height of the ground-cover skyline above ground level.
- *Density D_c* : The percentage of the terrain in the area under consideration which is covered by any ground cover having a height equal to or greater than H_c .
- *Gap-width G_c* : This should represent the typical width (m) of gaps in the ground cover.

TABLE 5.1

Categories to be listed in a macroscopic ground cover database

00		Unknown
10	RURAL OPEN	
	11	Pastures, grassland
	12	Low crop fields
	13	High crop fields (e.g. vines, hops)
	19	Park land
20	TREE COVERED	
	21	Irregularly spaced sparse trees
	22	Orchard (regularly spaced)
	23	Deciduous trees (irregularly spaced)
	24	Deciduous trees (regularly spaced)
	25	Coniferous trees (irregularly spaced)
	26	Coniferous trees (regularly spaced)
	27	Mixed tree forest
	28	Tropical rain forest
30	BUILT-UP AREA	
	31	Sparse houses
	32	Village centre
	33	Suburban
	34	Dense suburban
	35	Urban
	36	Dense urban
	37	Industrial zone
40	DRY GROUND	
	42	Sand dunes
	43	Desert
50	WET TERRAIN (no trees)	
	52	Marshlands
	54	Mud flats
60	FRESH WATER	
70	SEA WATER	
80	CRYOSPHERE	
	82	Sea ice
	83	Freshwater ice
	84	Glacier
	86	Dry snow
	88	Wet snow
90	OTHER	(Specify)

Note that H_c must be supplied if D_c is supplied, and that D_c must be supplied if G_c is supplied.

In view of the wide variability of ground cover it will often only be possible to obtain estimates for the parameters H_c , D_c and G_c . Nevertheless they can be valuable in adding precision to the generic categories. This may be done for a complete data set as a whole, or may be supplied individually for each point of a data set, such as for a path profile.

These considerations may be extended to any special situations where detailed propagation predictions are required. Table 5.2 provides some examples of categories of ground cover together with a possible mechanism for recording their characteristics; this is basically an extension of the first approach.

TABLE 5.2

Additional categories and parameters for database of special structures

Ground cover category	Parameters
Row of buildings (A well defined row of buildings in isolation, typically a row of terraced houses along a road)	<ul style="list-style-type: none"> – Mean building height – Coordinates at end points of row
Isolated building (Isolated building within a square)	<ul style="list-style-type: none"> – Building height – Coordinates of building centre – Area covered by the building
Line of trees (Typically a tree-lined road)	<ul style="list-style-type: none"> – Mean tree height – Coordinates at ends of tree line
Towers (Electricity pylons, wind turbines, etc.)	<ul style="list-style-type: none"> – Height of feature – Coordinates at centre of feature

5.3 Use of databases in available modelling and planning methods

Radiocommunication Study Group 3 has several Recommendations that describe modelling and planning methods that are useful in planning terrestrial land mobile radio systems. See Recommendation ITU-R P.1144 [5-6]. Some of the algorithms described in those Recommendations (e.g. Recommendation ITU-R P.1546) are of a general (“point-to-area”) nature, whereas others (e.g. Recommendation ITU-R P.452 [5-7]), the so-called “point-to-point” models, are based upon the geometry of the specific path under consideration. Propagation predictions made with algorithms falling into the former category, being independent of path geometry, do not require hypsographic data. With “point-to-point” predictions, on the other hand, hypsographic data are essential. It should be emphasized here that the term “point-to-point” as used here refers to predictions that are dependent upon path geometry and does not refer to fixed paths, such as those frequently encountered in microwave systems.

5.3.1 Area metaphor

A point-to-point prediction is begun by laying-out the required coverage area using some metaphor corresponding to the geometry of the area. Commonly used metaphors include “radial”, “stepped radial”, “grid mapped from radial data”, and “tiled”. These are described below:

- In the “radial” method, data are taken along radials at equal angular spacings. Each point along the radial represents an annular segment of area. This method has the advantages of simplicity and speed, but the disadvantages of (a) diverging so that calculations made at a long distance from the base station site are made at larger tangential distances between calculations, and (b) they are unsuitable for calculations where the overlay of data from multiple sites is required, such as interference or simulcast predictions.
- The “stepped radial” method is similar to the radial method, but it incorporates an increase in the number of radials as the distance from the site increases. For example, one program starts at 8 radials out to 2 km, increases to 16 radials from 2 to 4 km, increases to 32 radials from 4 to 8 km, etc. This overcomes disadvantage (a) discussed above for the “radial” method, but it does not overcome disadvantage (b).
- In the “grid mapped from radial data” method, the program sets up a grid of tiles, data are taken at equal angular spacings as in the “radial” method, then the program finds the radial that passes nearest the centre of each grid, using these data to represent the grid. This overcomes disadvantage (b) of the “radial” method and it allows re-use of radial data, but it makes for uneven radial spacing.
- The “tiled” method truly takes radials to the centres of all tiles in the area. This gives the most accurate representation of the available data and overcomes both disadvantages (a) and (b) of the “radial” method, above. However, it generally requires more radials because one radial is required to the centre of each and every tile. This results in longer run times.

5.3.2 Profile considerations

Regardless of which area metaphor is used, a point-to-point prediction over an area will require that numerous terrain profiles be extracted from the database. Each profile represents the profile of the terrain between the base station and a potential mobile station location. Profile data are typically extracted following either of two methods: (a) the interpolation method, and (b) the “nearest data point” method.

In the interpolation method, the program seeks to extract data points at equal intervals; for example, 200 m. In this example, profile data values would be determined for distances 200, 400, ... m from the base site. Since the vast majority of radials will not run in the cardinal directions where data

already exist, some form of interpolation is used to find values corresponding to those distances. Studies have shown that complex forms of interpolation do not yield significantly more accurate results than does simple bi-linear interpolation (see Recommendation ITU-R P.1144).

In the “nearest data point” method, all points within a given tolerance (usually about half of the horizontal resolution of the database) of the radial line are extracted. Their database elevation values are used, rather than interpolated values. The position of each extracted value along the radial line is calculated based upon the position that a perpendicular drawn through the data point to the radial would lie on. This results in uneven spacings of elevation data points along the radial.

Neither method of profile consideration has an advantage over the other. However, some program implementations require even spacings. As to data resolution it should be borne in mind that taking data at a finer resolution than that available from the database will not result in greater accuracy; however, it will result in additional processing time.

5.4 References

- [5-1] Recommendation ITU-R P.1546 – Method for point-to-area predictions for terrestrial services in the frequency range 30 to 3 000 MHz. International Telecommunication Union, Geneva, 2001.
- [5-2] Recommendation ITU-R P.526 – Propagation by diffraction. International Telecommunication Union, Geneva.
- [5-3] Recommendation ITU-R P.1058 – Digital topographic databases for propagation studies. International Telecommunication Union, Geneva.
- [5-4] GLOBE Task Team and others (Hastings, David A., Paula K. Dunbar, Gerald M. Elphingstone, Mark Bootz, Hiroshi Murakami, Hiroshi Maruyama, Hiroshi Masaharu, Peter Holland, John Payne, Nevin A. Bryant, Thomas L. Logan, J.-P. Muller Gunter Schrier and John S. MacDonald), eds., 1999. The global land one-kilometer base elevation (GLOBE) digital elevation model, Version 1.0. National Oceanic and Atmospheric Administration, National Geophysical Data Center, 325 Broadway, Boulder, Colorado, 80305, United States of America. Digital database on the World Wide Web (<http://www.ngdc.noaa.gov/seg/topo/globe.shtml>) and CD-ROMs.
- [5-5] HASTINGS, D. A. and DUNBAR, P. K. [1999] Global land one-kilometer base elevation (GLOBE) digital elevation model. Documentation Volume 1.0. “Key to Geophysical Records Documentation (KGRD) 34”. National Oceanic and Atmospheric Administration, National Geophysical Data Center, 325 Broadway, Boulder, Colorado, 80305, United States of America.
- [5-6] Recommendation ITU-R P.1144 – Guide to the application of the propagation methods of Radiocommunication Study Group 3. International Telecommunication Union, Geneva.
- [5-7] Recommendation ITU-R P.452 – Prediction procedure for the evaluation of microwave interference between stations on the surface of the Earth at frequencies above about 0.7 GHz. International Telecommunication Union, Geneva.

CHAPTER 6

PROPAGATION WITHIN AND INTO BUILDINGS AND UNDERGROUND

The indoor wireless propagation problem is broadly distinguished from the outdoor wireless propagation problem by much shorter path lengths and the ubiquity and importance of multipath in almost all cases of interest. The mixed problems, outdoor-indoor and indoor-outdoor wireless propagation, which combine aspects of each, will be deferred to the last part of this section. For the indoor-indoor wireless propagation problem, two solution approaches are available, depending on the level of detailed knowledge of the propagation situation. As in the outdoor propagation problem, these subdivide neatly into site-specific and site-general approaches. In what follows, both are discussed.

6.1 Site-specific approaches

Confining our attention, for now, to the simple cases where both the transmitter and the receiver are indoors, within the same building and in the same room, then the indoor propagation problem reduces to the solution for a resonant cavity (perhaps loaded) with lossy (i.e., imperfectly electrically conducting) walls. The solutions of Maxwell's equations can then be obtained for an empty, regularly shaped resonant cavity (i.e., boundary conditions which are separable in a useful, three dimensional, coordinate system), with perfectly conducting walls.

When one departs from the fairly simple, regularly shaped indoor propagation situations of the previous paragraph, which are amenable to analytical techniques, it is usually necessary to appeal to fully three-dimensional numerical solutions of Maxwell's equations. Each is computationally intensive and each requires discretization of space down to fractions of a free-space wavelength at the highest frequency of interest, for accurate solutions to the problem in question.

However, having acknowledged the existence of rigorous, analytical/numerical solutions to ideal and quasi-ideal cases, it is also important to note that, for many practical situations of interest, either the frequency of operation is too high, the geometrical complexity and/or cavity size is too great and/or there is not enough detailed information or predictability to warrant such an approach. In these cases, one may use simpler concepts, while recognizing the limitations inherent in this approach. If one falls back to concepts such as free space path loss coupled with diffraction, reflection and/or transmission losses, which is the common practice in ray tracing solutions based on geometrical optics, it is important to recognize that this may lead to both underestimates and overestimates of the losses that can occur in the indoor propagation environment.

Clearly, adoption of any site-specific solution approaches is contingent upon specific siting information, detailed building layout information and, at least moderate information about the dielectric and magnetic material properties of walls, etc. It is worth noting, with regard to the last point, that these material properties may be, in general, frequency dependent, even for homogeneous materials. The frequency dependency of material properties can be expected to be considerably more complex in cases where the building materials involve hybrids, such as steel

reinforced concrete, or other kinds of multi-layer slab configurations. Detailed building structural information is required for accurate simulation results. Some general guidance on the effects of building materials is referenced in Recommendation ITU-R P.1238. Furthermore, it is also important to know the locations, sizes and detailed compositions of important apertures, such as windows and doors, if these are present.

6.2 Site-general approaches

In contrast to the more detailed site-specific approaches described above, Recommendation ITU-R P.1238 provides for a site-general model of the indoor propagation loss. The model accounts for indoor propagation loss as a function of the frequency (MHz), the separation distance (m) between the base station (i.e., transmitter) and the mobile/portable (i.e., receiver) and the number of building floors between the base station and the mobile/portable. The formula for the indoor propagation loss, L_{total} , is:

$$L_{total} = 20 \log f + N \log d + L_f(n) - 28 \quad \text{dB} \quad (6-1)$$

where:

- f : frequency (MHz)
- N : path loss coefficient
- d : separation distance between the base station and the portable (m) ($d > 1$ m)
- L_f : floor penetration loss (dB)
- n : number of building floors between the base station and the portable ($n \geq 1$).

Note, however, that both the path loss coefficient, N , and the floor penetration loss, L_f , are functions of the frequency and the building type, as one might expect, given the previous discussion of site-specific approaches. Note, also, that the floor penetration loss, L_f , is neglected when the base station and the portable are on the same building floor. Typical values for N and L_f are reproduced in Tables 6.1 and 6.2, respectively.

TABLE 6.1
Power loss coefficients, N , for indoor transmission loss calculation

Frequency	Residential	Office	Commercial
900 MHz	—	33	20
1.2-1.3 GHz	—	32	22
1.8-2.0 GHz	28	30	22
4 GHz	—	28	22
5.2 GHz	—	31	—
60 GHz ⁽¹⁾	—	22	17

(1) 60 GHz values assume propagation within a single room or space, and do not include any allowance for transmission through walls. Gaseous absorption around 60 GHz is also significant for distances greater than about 100 m which may influence frequency re-use distances. (See Recommendation ITU-R P.676.)

TABLE 6.2

Floor penetration loss factors, L_f (dB) with n being the number of floors penetrated, for indoor transmission loss calculation ($n \geq 1$)

Frequency	Residential	Office	Commercial
900 MHz	–	9 (1 floor) 19 (2 floors) 24 (3 floors)	–
1.8-2.0 GHz	$4 n$	$15 + 4(n - 1)$	$6 + 3(n - 1)$
5.2 GHz	–	16 (1 floor)	–

The following general remarks pertain to the site-general model of Recommendation ITU-R P.1238, particularly for the 900-2 000 MHz band:

- i) Paths dominated by a pure line-of-sight (LoS) component have a path loss coefficient of 20 (approximately). However, it is also necessary that the building walls, ceiling and floor be suitably distant for this condition to occur.
- ii) For long unobstructed paths, the first Fresnel zone breakpoint may occur, particularly for lower frequencies, giving rise to sub-path diffraction. In these cases, the path loss coefficient will increase rapidly from a value of 20 to a value of roughly 40, in the vicinity of the breakpoint.
- iii) For paths in long, narrow corridors or hallways on a single floor, the path loss coefficient may be less than 20. This is a result of the fact that the corridor behaves (roughly) as a resonant cavity. This is likewise true for paths in single rooms with moderately reflective walls and suitable dimensions.
- iv) For paths in buildings in which the rooms are separated by full, floor-to-ceiling walls (e.g., closed plan office buildings), the path loss coefficient for room-to-room paths is typically found to be near in value to 40.
- v) For paths traversing multiple floors, it is expected that the floor penetration loss will be limited by paths through multi-floor atria, stairwells or other lower loss mechanisms than direct transmission through the building's floors.

The alert reader will note an apparent change of tone in the discussions of site-general approaches to the indoor propagation problem vis-à-vis site-specific approaches. In particular, the terminology has reverted to references more familiar in the discussion of outdoor propagation problems. It is, however, wholly consistent with the approximate solution to the site-specific indoor problem using ray tracing combined with the Geometric and Uniform Theory of Diffraction (GTD-UTD), which has been discussed in Section 4.3.1.

To bring a modicum of closure to the discussion of site-general approaches to the indoor propagation problem, note that the site-specific approaches discussed above allow for the computation of the channel impulse response, $h(t)$, at least in principle, as well as the indoor propagation loss, L_{total} . (It is important to emphasize that, for the indoor propagation problem, the channel is really many different channels.) The channel impulse response is vital for link simulation studies in which one evaluates the choice of modulation and, in digital systems, symbol rates, encoding schemes, etc., on the overall (i.e., end-to-end) system performance. Such studies might yield, for example, predicted BER as a function of S/N or $S/(I + N)$. Clearly, then, a site-general model is needed for the (indoor) channel impulse response.

While many physical phenomena can influence the channel impulse response, for the indoor propagation problem the principal phenomenon of interest is the distribution and strength of the various multipath components arising from scattering by the relevant surfaces, etc., that populate the indoor problem. Using an analogy to resonant cavity theory, the “multipath” decay rate is characterized by equation (6-2).

$$h(t) = \exp(-t/T) \quad (6-2)$$

where:

t : time (s)

T : cavity characteristic decay time (s).

Recalling results from classical resonant cavity theory, the characteristic decay time, T , will be related to the cavity dimensions, the electrical and magnetic material properties of the cavity’s walls, floor and ceiling and the cavity mode.

One interesting feature of the exponentially decaying model of the channel impulse response, $h(t)$, when suitably normalized, is that the square root of its second central moment on the time interval $[0, \infty]$ is T , the cavity’s characteristic decay time. If one then simply measures the r.m.s. delay spreads for indoor channels of certain types (e.g., residential, office and commercial), then these delay spreads are easily related to the exponentially decaying channel impulse response model through this single parameter. This is precisely what is recommended in Recommendation ITU-R P.1238 if it is appropriate to use the exponentially decaying channel impulse response model. From the foregoing discussion, it would seem that the exponentially decaying channel impulse response models are appropriate for r.m.s. delay spreads corresponding to speed-of-light travel times of, perhaps, two to three characteristic dimensions of the indoor “cavity”, or more.

Another, frequently invoked, channel impulse response model is the wide sense stationary uncorrelated scattering (WSSUS) model. The basic concept here idealizes the (indoor) channel impulse response as a multivariate function, $g(t, \tau)$, of time, t , and the multipath delay, τ . The

(possibly complex) received response, $w(t)$, due to a (possibly complex) transmitted signal, $z(t)$, modulating a time harmonic transmission at carrier frequency, f_c , which then propagates through the channel, is obtained by convolution over the continuum of multipath delays, viz.:

$$w(t) = \int z(t-\tau)g(t,\tau) d\tau \quad (6-3)$$

For each multipath delay, τ , the time variation of the channel impulse response is assumed to be a random process, the statistics of which are (wide sense) stationary. Furthermore, different multipath delays are associated with rays having different paths from “different” scattering centres. Hence, for different delays, this scattering is assumed to be uncorrelated. It is further assumed that the probability distribution function (in delay) of the scattering amplitudes is that of a normally distributed random variable. Stationarity of the statistics of the time variation along with the uncorrelated nature of the scattering delays imply that the autocorrelation function of the channel impulse response, $R_g(t,s;\tau,\xi)$, obeys:

$$R_g(t,s;\tau,\xi) = P_g(\Delta t; \xi) \delta(\xi - \tau) \quad (6-4)$$

where:

t, s : time variables

ξ, τ : delay variables

$\Delta t = s - t$

P_g : power density.

When the fading is slow no variations occur in the impulse response of the channel as a function of time and the autocorrelation function reduces to:

$$R_g(t,s;\tau,\xi) = P_g(\xi) \delta(\xi - \tau) \quad (6-5)$$

where $P_g(\xi)$ is the power delay profile which gives the power density as a function of time delay and its Fourier transform gives the coherent bandwidth of the channel. When there is a dominant mode, i.e. some 10-12 dB above other mode amplitudes, the normal distribution assumption is no longer valid, and the channel statistics become Rician giving rise to a wider coherent bandwidth than can be estimated from the Fourier transform of the power delay profile. In this case the spaced frequency correlation function should be used.

Since the statistics of the channel impulse response constitute the only observables that need to be matched, it is possible to develop so-called “N-channel” models obeying the required auto-correlation function from measurement of the power delay spectrum, etc. An example of this appears in Recommendation ITU-R P.1238.

6.3 Combined (indoor-outdoor and outdoor-indoor) propagation

In situations involving propagation over combined paths, either indoor-to-outdoor or vice versa, it is usually appropriate to concentrate on the points-of-entry (or exit) that allow for the transmission of electromagnetic radiation between the two environments. Points-of-entry can be apertures such as windows, skylights and doors, ventilation intake and exhaust penetrations, other structural openings and, if the electromagnetic shielding provided by the building materials is low, even the exterior skin of the building itself. If the distributions of the electromagnetic fields across the points-of-entry are known or, alternatively, can be inferred, then these points-of-entry can replace the actual

sources of radiation (either indoor or outdoor) as equivalent radiation sources (i.e., either outwardly or inwardly, respectively). The total field at the desired observation point will then be the result of superposition of the fields at the observation point due to each of the equivalent sources, taken individually. If it happens that a single point-of-entry is expected, on physical grounds, to dominate the response at the observation point, then it is often sufficient to concentrate on obtaining the desired electromagnetic fields' distributions for this single point-of-entry, excluding the others. For additional detail on this subject, see Bethe [6-3].

An alternate, empirically based, approach is to use empirical data for building entry loss (defined in Recommendation ITU-R P.1411) and then account for the transmission effects of interior walls and panels, ignoring diffraction and reflection. Davidson [6-4] consolidated the results of several building entry loss measurement programmes and found that, for medium-sized office buildings, the building entry loss can be calculated from formula (6-6):

$$L_{be} = 37 - 7.9 \log f_{\text{MHz}} \quad (6-6)$$

At 914 MHz, Seidel [6-5] found attenuation factors for soft partitions and interior walls to be approximately 1.4 and 2.4 dB, respectively. LaFortune [6-6] found the value for soft partitions to be 1.5 dB at 917 MHz. Galeitner [6-7] found the value for interior walls at 1800 MHz to range between 5.8 and 6.7 dB, depending upon the composition of the interior walls. Interior attenuation factors are summarized in Table 6.3.

TABLE 6.3

Interior attenuation factors (dB)

Frequency (MHz)	~900	1800
Soft partitions	1.4-1.5	
Interior walls	2.4	5.8-6.7

6.4 References

- [6-1] Recommendation ITU-R P.1411 – Propagation data and prediction methods for the planning of short range outdoor radiocommunication systems and radio local area networks in the frequency range 300 MHz to 100 GHz. International Telecommunication Union, Geneva.
- [6-2] Recommendation ITU-R P.1238 – Propagation data and prediction models for the planning of indoor radiocommunication systems and radio local area networks in the frequency range 900 MHz to 100 GHz. International Telecommunication Union, Geneva.

- [6-3] BETHE, H. A. [1944] Theory of diffraction by small holes. *Phys. Rev.*, Vol. 66, p. 163-182.
- [6-4] DAVIDSON, A. L. *et al.* [February 1997] Measurement of building penetration into medium buildings at 900 and 1500 MHz. *IEEE Trans. Veh. Tech.*, 46(1), p. 161-168.
- [6-5] SEIDEL, S. Y. and RAPPAPORT T. S. [February 1992] 914 MHz path loss prediction models for indoor wireless communications in multifloored buildings. *IEEE Trans. Ant. Prop.*, 40(2), p. 207-217.
- [6-6] LAFORTUNE, J.-F. and LECOURS M. [May 1990] Measurement and modelling of propagation losses in a building at 900 MHz. *IEEE Trans. Veh. Tech.*, 39(2), p. 101-108.
- [6-7] GALEITNER, R. and BONEK E. [1994] Radio wave penetration into urban buildings in small cells and microcells. 44th IEEE Veh. Tech. Conference Record, p. 887-891.

CHAPTER 7

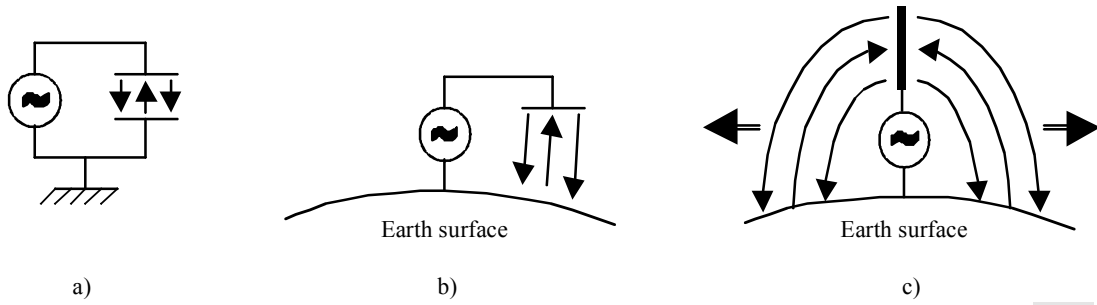
ANTENNA CONSIDERATIONS

7.1 Emission of radiowaves

Antennas are a primary factor to consider in any study of propagation of radiowaves, because the antenna is that element of a radio system that emits electromagnetic radiowaves into the ether. At the receiving end, an antenna picks up the radiowaves from the ether and converts them back into the electric signals. Thus, the choice of the antennas as well as their installation will greatly affect the way the radiowaves will propagate and the overall quality of radiocommunication link.

The principle of antenna operation may be easily understood through the simple analogy with a conventional capacitor, where an alternating electric field is created between the plates by an external signal generator, as illustrated in Fig. 7.1a). If one now considers that the surface of the Earth is used as one capacitor plate and the other plate is gradually removed from that surface, see Fig. 7.1b), and then converted into a single standing wire, this releases the alternating field causing it to propagate in all directions from the antenna along the surface of the Earth, see Fig. 7.1c). This exactly explains the operation of the dipole antenna (also known as Hertzian antenna), which is a basic antenna in land mobile applications.

FIGURE 7.1
Principle of operation of the dipole antenna

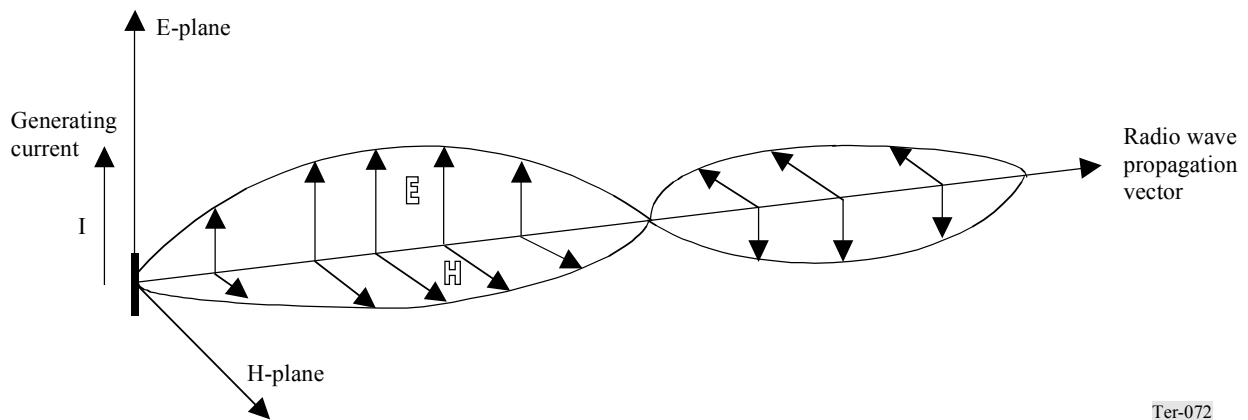


Ter-071

Radiowaves are essentially the combinations of two alternating fields – electric and magnetic, with their respective vectors being always normal to each other. Their multiplication produces the resulting propagation vector (power vector, called Pointing vector), which is normal to the wavefront and describes the direction of radio wave propagation, (see Fig. 7.2).

One important characteristic of electromagnetic waves is their polarization, which describes the orientation of electric and magnetic field vectors in relation to the ground plane. The orientation of the electric field vector is the reference used when describing the polarization of a radio wave. This means that whenever it is said that the radio wave is vertically or horizontally polarized, that implies that the electric field vector is oriented vertically or horizontally respectively to the ground plane (Earth surface). For example, the wave shown on Fig. 7.2 is vertically polarized.

FIGURE 7.2
Structure of electromagnetic (radio) wave



Ter-072

The polarization of a radiowave is normally determined by the orientation of the transmitting antenna and its structure. For example, a vertically installed singular dipole antenna, as illustrated on Fig. 7.1c), would emit vertically polarized radiowaves, of the type shown on Fig. 7.2.

The polarization property of radiowaves is important in two major aspects. First of all, it is a cardinal rule that the transmitting and receiving antennas should have the same polarization in order to guarantee maximum received signal strength. Similar logic suggests that the transmitting and receiving antennas should be of opposite polarization to achieve the best possible de-coupling, for example when protecting a receiver from a possible interfering transmitter of known polarization. However, in the land mobile services the polarization of radiowaves is often affected by numerous reflections and diffractions over the non-line-of-sight propagation path. The impact of this phenomenon is addressed in more detail later in this section.

Another major aspect of polarization is that it may directly affect the propagation of radiowaves. When a radiowave is travelling along the surface of the Earth (which possesses certain conductivity), currents are generated in the surface which cause absorption of power from the passing radiowave. Horizontally polarized waves are more severely affected by this absorption. Generally, surface absorption is less over water paths and also less profound at higher frequencies.

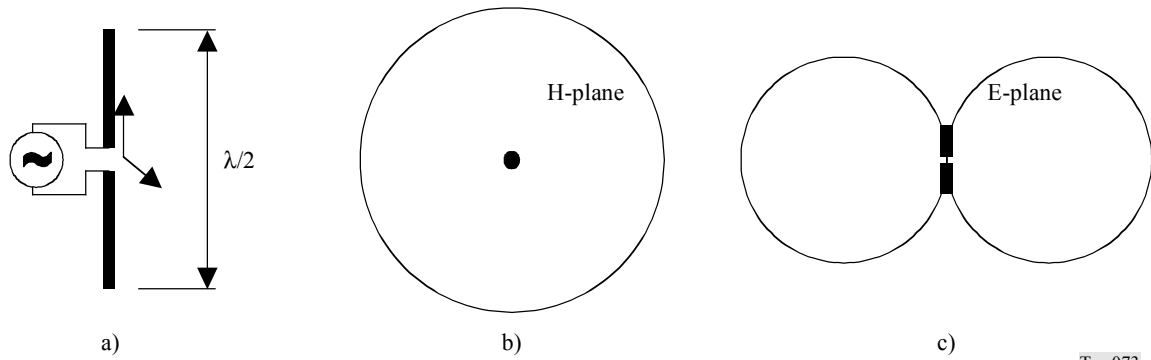
Other fundamental propagation effects are described in detail in Chapter 3 of this Handbook.

7.2 Reference isotropic radiator and dipole antenna

A hypothetical ideal radiator, called an isotropic radiator, is used in describing real antennas. It may be considered as an imaginary point, radiating equally in all directions through the sphere around it. Such a unity-gain (zero-gain on logarithmic scale, see details in Appendix B) elementary antenna provides a useful reference base for the uniform description of directivity of real antennas.

The simplest real antenna, which most closely resembles the isotropic radiator, is a half-wavelength dipole antenna, see Fig. 7.3a). It radiates equally in all directions in the horizontal plane (omnidirectional) (Fig. 7.3b)), but has non-uniform directivity in the vertical plane (Fig. 7.3c)).

FIGURE 7.3
Half-wavelength ($\lambda/2$) dipole antenna and its radiation patterns in two planes



Ter-073

Irregularity of the radiation pattern in the vertical plane means that the dipole antenna concentrates radiated energy in the direction normal to its central point, that is in the horizontal plane. Thus, the dipole antenna provides directional gain, which equals 1.64 times or 2.15 dB, relative to an isotropic radiator.

Formally, the power gain of an antenna is defined [7-1] as the ratio, usually expressed in decibels, of the power required at the input of a loss-free reference antenna (usually an ideal isotropic radiator) to the power supplied to the input of the given antenna to produce, in a given direction, the same field strength or the same power flux-density at the same distance. When not specified otherwise, the gain refers to the direction of maximum radiation. The gain may be considered for a specified polarization.

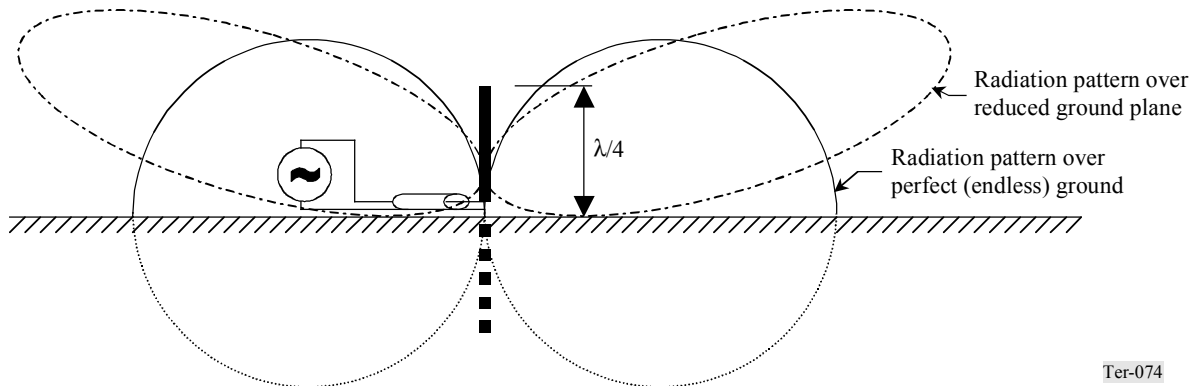
Because of its simplicity and constructional convenience, dipole antennas are widely used in the land mobile services. The gains of some other (composite) antennas in land mobile applications are often expressed in relation to the standard half-wavelength dipole, to show the comparative improvement over a basic dipole antenna. In decibel units such gain is denoted as “dBd”, where “d” stands for “dipole”. To transform this into the gain relative to an isotropic radiator, add 2.15 dB to the dipole related gain.

Some dipole antennas used in practice behave like a half-wavelength dipole but are in fact a quarter-wavelength ($\lambda/4$) in length. In such dipoles the second radiating leg is replaced with its virtual mirror over the perfectly conducting plane, which may be the Earth’s surface or a vehicle’s roof. Operation of the $\lambda/4$ -dipole is illustrated in Fig. 7-4.

The radiation pattern of a $\lambda/4$ -dipole in the E-plane resembles that of the reference $\lambda/2$ -dipole when the ground plane is “perfect”, that is its conductivity and dimensions are sufficient. However, this is difficult to achieve in practice because usually the antenna is mounted high above the ground and it is difficult to achieve proper ground in mobile applications. One means of partially overcoming this problem is to mount fixed antennas or vehicular antennas over “virtual ground” elements, which may be a set of three to five conducting rods radially placed at the base of the dipole or it may be the surface of the vehicle body for vehicle mounted antennas. However, such virtual ground may not fully replace the perfect reflecting plane, therefore it is referred to as the “reduced ground”. In

such cases the radiation pattern of the $\lambda/4$ -dipole rises slightly upwards in the E-plane, as shown in Fig. 7.4. In the H-plane the radiation pattern of the $\lambda/4$ -dipole remains omnidirectional. The gain of the $\lambda/4$ -dipole over a *perfect* ground is 5.2 dBi or 3.05 dBd. In reduced ground situations, gains of -1 dBd are typical at the horizon.

FIGURE 7.4
Quarter-wavelength ($\lambda/4$) dipole antenna and its radiation pattern in E-plane



Ter-074

7.3 Antenna characteristics

Some of the major antenna characteristics used in propagation studies in the land mobile services are briefly described below.

Directivity (power gain)

This parameter describes the ability of an antenna to concentrate radiated energy in the given direction. The formal description of the gain is given in Section 7.2.

Directivity of the antenna is usually described by polar plots, showing the comparison of power radiated over the 360° arc. Two diagrams are usually used, describing antenna directivity in the vertical and horizontal planes, which are marked as E- or H-plane

Polarization

The emitted radiowaves are considered to be polarized in the plane of the length of the conducting antenna elements, which is the plane of electric E-field.

Circular polarization may be used sometimes by employing crossed dipoles or helical-wound antennas to reduce the multipath propagation losses. See discussion on effects of cross-polarization in Section 7.6.

Design frequency and bandwidth

Since the physical dimensions of an antenna are related to its operating wavelength, the design is optimized to a particular frequency, called the design frequency. The design frequency is often considered as a centre frequency of the band of operating frequencies.

Acceptable limits of deviation of the operating frequency (frequency channel width) from the design frequency are defined by the bandwidth of an antenna. This bandwidth is normally given as a percentage of the design frequency and describes the band of frequencies over which antenna performance will not degrade to an unacceptable level. Otherwise, the operating frequency range of the antenna is stated.

These parameters are seldom used in the propagation modelling on the assumption that the antenna is tuned to the operating frequency, but it is important to observe them especially in practical field applications, such as test measurements or coverage verification measurements.

Beamwidth

The beamwidth parameter is closely linked to the directivity of an antenna and is usually used in a description of directional antennas. The beamwidth (also referred to as the half-power beamwidth) is specified as the total width, in degrees, of the main radiation lobe, limited by the angles at which the radiated power has decreased by half (-3 dB on logarithmic scale) from that of the main radiation direction. Directional antennas are very often used in base station installations, therefore their horizontal beamwidth should be taken into account when modelling the coverage areas of such base stations. Although directional antennas are seldom used on the mobile side in land mobile systems, this may occur, for example, when calibrated directional antennas are used for propagation measurements. In such cases the beamwidth of an antenna should be sufficiently wide to pick up most of the highly scattered multipath signal. On the other hand, directional antennas may be used at the remote terminal for the opposite reason, that is to limit the number of multipath rays.

7.4 Base station antennas

In most typical land mobile applications in the VHF/UHF ranges, such as PMR (private dispatch), paging and other similar systems with radial coverage, the base stations usually employ dipole antennas or collinear arrays of dipole antennas. Mounted vertically, such antennas produce omnidirectional vertically polarized fields. Ideally, a radiating dipole should be placed on top of a mast or other support to avoid affecting directivity because of reflections from metal surroundings. Placing the antenna more than one wavelength from metallic structures will reduce this effect.

Directional antennas are used in the PMR kind of land mobile systems only when it is necessary to avoid interference with other systems or when it is impractical to locate the base station close to a centre of the service area.

In public cellular systems, highly directional antennas (with beamwidths ranging in average from 60° to 120°) are used at the base stations commonly to form the necessary pattern of service cells and at the same time to reduce co-channel interference into neighbouring cells. In such systems, omnidirectional antennas are used only occasionally in remote rural installations with low subscriber density, often with local repeater stations.

In propagation studies the direction from the base station to the remote terminals is of primary concern, and the actual directivity of the antenna is an important element of the studies. Another important characteristic of base station antenna installation is the height of the antenna above the ground or effective height of the base station antenna. The latter is used to describe the height of the antenna over the average terrain height in the areas with irregular terrain. The precise definition of the effective height varies slightly from model to model, however in the ITU-R models it is usually the height of the antenna over the average height of terrain in the distance from 3 to 15 km from the transmitter in the direction of the receiver.

7.5 Mobile station antennas

The most common type of antenna used for the mobile stations, is the “whip” antenna, a metal rod, forming a quarter-wavelength dipole. The efficiency of such antennas is low because of the practical difficulties in establishing a proper reflecting ground plane at the mobile stations, especially for hand-held terminals. This situation is slightly better for vehicle mounted antennas when they are mounted over the centre of a metallic rooftop.

Although the actual height of a mobile station antenna is difficult to define, for propagation studies of land mobile applications 1.5 m antenna height is commonly used as a reference. However, in certain systems the actual height of a mobile station antenna may be considerably higher, e.g. when antennas are installed on top of large business-type vehicles, such as buses, railway cars, etc. For broadcasting or for point-to-point applications, the height of a receiving (remote) terminal antenna is considered to be 10 m above ground.

It is, therefore, important to ensure that the chosen propagation prediction model assumes the proper height of the mobile station antenna or that an appropriate antenna height correction factor is used. Such factors are supplied with most of the widely used models.

If the mobile station employs a directional antenna, care should be taken to account for its effects on the reception of arriving signals.

Where vehicular mobile antennas have a higher gain in the horizontal plane than the standard dipole antenna, the appropriate value of antenna gain should be used in modelling.

7.6 Impact of the land mobile environment

The following sub-sections describe in greater detail the impact that a typical land mobile environment may have to a general consideration of antennas and their characteristics. This text is largely based on the material in Recommendation ITU-R P.1406 [7-3].

7.6.1 Depolarization phenomena in the land mobile environment

In the land mobile environment some or all of the transmitted energy may be scattered out of the original polarization due to diffraction and reflection of the radiowave. It is convenient to take this depolarization effect into consideration by using a cross-polarization discrimination (XPD) factor, as defined in Recommendation ITU-R P.310.

It is reported, that XPD measurements at 900 MHz show that:

- XPD depends little on distance;
- the average XPD in urban and residential areas ranges from 5 dB to 8 dB;
- the average XPD in open areas is over 10 dB;
- the average correlation between vertical and horizontal polarization is 0.

It is also known, that XPD increases with decreasing frequency, to about 18 dB at 35 MHz.

The comparatively low values of XPD noted above are due to the considerable amount of scattering in typical conditions of land mobile services, especially in urban and residential areas. This phenomenon may, however, be turned into a useful technique for improving reception through polarization diversity. In this case, the most basic option would be to use two orthogonal linear polarizations at the base station.

As an alternative to diversity, circular polarization at the base station and linear polarization at the mobile terminal, while resulting in a 3 dB polarization mismatch, can take advantage of the depolarization due to scattering and provide a more constant received signal level in the mobile environment.

7.6.2 Antenna height gain: base and mobile

Height gain refers to a change in received signal strength with change of antenna height. Although usually increasing with height (positive height gain), it can also decrease with height (negative height gain) in certain point-to-point communication cases. For example, this may happen if, in the absence of local clutter, the direct signal can interact with a ground-reflected ray from the same transmitter. The resulting field strength variation, in a vertical direction, is a series of maxima and minima as the path geometry causes the two signals to go in and out of phase.

In practice, however, particularly in land mobile systems, clutter and other reflected signals tend to minimize this two-ray effect and it can be neglected in most situations at frequencies above 200 MHz. Instead, it is usually found that raising the antenna simply reduces the effective clutter loss causing the received signal to increase with height. Since antenna height is related to clutter loss in this way, this form of height gain can be categorized in terms of reference receiver antenna heights for the type of ground cover (dense urban, urban, suburban) as in Recommendation ITU-R P.1546 [7-4]. In other prediction methods, especially those that use a terrain data base, antenna height is frequently linked directly to the calculation of clutter loss.

For base stations, operating at frequencies below 200 MHz and located in open areas, 2-ray effects can sometimes be found so that re-positioning of the antenna may be required to avoid negative height gain. Such an effect is difficult to predict precisely, since a detailed knowledge of the terrain profile at the reflection point is required. Above 200 MHz, due to the smaller wavelength, this particular problem tends to diminish and at UHF and above it can be ignored.

7.6.3 Correlation/space diversity

Space diversity is practical for antennas having cross-correlations up to about 0.7. In general, this makes portable and mobile diversity reception nearly impractical. For the base station case, however, a number of techniques are possible for reducing the cross-correlation between antennas. The two most practical are vertical and horizontal separation.

To reduce the cross-correlation to 0.7 or less, vertically spaced antennas must be separated by approximately 17 wavelengths or more. Horizontal separation can be more effective, depending upon the relative orientations of the plane of the antennas versus the direction of motion of the mobile. If the vertical plane through the antennas is perpendicular to the direction of motion of the mobiles, the cross-correlation will be approximately the same as that for the vertical separation case. With optimum orientation, horizontal antennas can be separated by as little as 8 wavelengths. It should be borne in mind that nearly optimal orientations can be maintained only in special cases, such as systems using sectored antennas.

7.6.4 Realizable antenna gain of the vehicular mobile station

Since vehicular mobile stations usually operate in a multipath environment, it is not surprising that mobile antenna gain will not, in most cases, match that measured on the test range. Additionally, even in line-of-sight non-multipath conditions, the vertical angle of arrival is not necessarily horizontal. In fact, practical cases exist where the vertical angle of arrival can exceed 10°. In the latter case, the vertical angle of arrival could easily be on a null or a minor lobe, rather than the main lobe of the mobile antenna's vertical pattern.

For example, some test measurements with the mobile antennas rated at 3 dB and 5 dB gain relative to a $\lambda/4$ vertical monopole in practical situations have shown that their practical gain values rarely meet the values measured on an antenna range. In multipath situations or in clear situations with high angles of arrival ($>2^\circ$), the practical gain of either antenna is approximately 1.5 dBd (that is relative to a $\lambda/4$ vertical monopole) over a distance range of up to at least 55 km. In clear situations with low elevation angles, full gain may be realizable.

7.6.5 Body loss

The presence of the human body in the field surrounding a portable transceiver, cellular phone, or paging receiver can degrade significantly the effective antenna performance – the closer the antenna to the body the greater the degradation. This effect is also frequency dependent, as the results of detailed studies on portable transceivers at four commonly used frequencies reveal. These results are given in Table 7.1, as derived from Recommendation ITU-R P.1406. A related study [7-5] showed similar, but not identical, results. Values of body loss for frequencies other than those shown in Table 7.1 may be estimated through a simple extrapolation.

TABLE 7.1

Typical body loss as related to the antenna efficiency of a portable transceiver

(based on Recommendation ITU-R P.1406)

Frequency (MHz)	Body loss at waist level (dB)	Body loss at head level (dB)
160	19.0	10.0
450	13.0	4.5
800	14.5	8.5
900	15.5	10.0

When an antenna of the mobile station is made as an integral part of an entire unit (as often is the case with hand-held stations in public systems: mobile phones, pagers), then its gain is not usually specified and it is not possible to correct it with the body loss factor. In such cases the body loss is accounted as a reduction of receiver sensitivity or radiated power of the transmitter. Alternatively, body loss may be introduced into the calculation of the overall signal loss in the power budget calculations.

7.7 References

- [7-1] Recommendation ITU-R P.341 – The concept of transmission loss for radio links. International Telecommunication Union, Geneva.
- [7-2] DAVIES, J. [1994] *Newnes Radio Engineer's Pocket Book*. Butterworth-Heinemann.
- [7-3] Recommendation ITU-R P.1406 – Propagation effects relating to terrestrial land mobile service in the VHF and UHF bands. International Telecommunication Union, Geneva.
- [7-4] Recommendation ITU-R P.1546 – Method for point-to-area predictions for terrestrial services in the frequency range 30 to 3 000 MHz. International Telecommunication Union, Geneva, 2001.
- [7-5] HILL, T. and KNIESEL, T. [November 1991] Portable radio antenna performance in the 150, 450, 800, and 900 MHz bands “outside” and in-vehicle. *IEEE Trans. Veh. Tech.*, 40(4), p. 750-6.

CHAPTER 8

ENVIRONMENTAL NOISE

8.1 Radio system performance factors

There are many factors that contribute to the performance of radio systems. They include the following:

- selection of bandwidth, modulation, signal and channel coding;
- quality of the input signal as degraded by channel impairments, such as multipath;
- amount and types of interference signals that are present along with the desired signal; and
- level and characteristics of noise that are present with the desired signal at the receiver's detector, demodulator, or decoding circuits.

This section deals with the last factor, noise, and the ways to estimate the noise levels that may be present in a land mobile radio system. The section provides background on noise terms and noise power expressions, gives the sources of information on noise (relative to land mobile radio applications) that are contained in Recommendation ITU-R P.372, and suggests where new measurements indicate changes in historical noise levels.

8.2 Noise terms and background

8.2.1 Noise components

Radio system noise can be attributed to two types of source:

- receiver noise or internal noise due to the radio system itself, and
- environmental noise or external noise from sources outside the radio system.

Depending upon such factors as the receiver design, where in the radio spectrum the system operates, and the location where the system is used, either the receiver noise can dominate or the environmental noise can be the dominant source of noise.

8.2.2 Noise power and noise temperature

The random motion of free electrons in a resistive conductor creates a noise voltage across the conductor. The resistive circuit is shown in Fig. 8.1. The noise power, n , which would be measured in a resistor at an absolute temperature, t , in units of K (Kelvin), and within a bandwidth, b , (Hz), is called the thermal noise power. The mean thermal noise power, n (W), available in a resistor is:

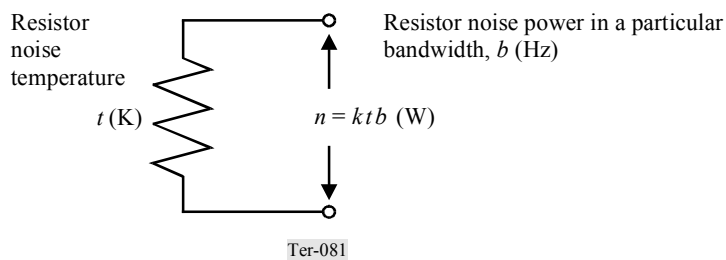
$$n = k t b \quad (8-1)$$

where $k = 1.38 \times 10^{-23}$ (W/(K · Hz)) is Boltzmann's constant. If a standard room temperature ($\sim 17^\circ$ C) of $t_0 = 290$ K is used as a reference temperature for the resistor, then the reference noise power, n_{ref} , in a 1 Hz bandwidth becomes

$$\begin{aligned} n_{ref} &= k t_0 b \\ &= (1.38 \times 10^{-23} \text{ (W/(K · Hz)} \times (290 \text{ K}) \times (1 \text{ Hz}) \\ &= 4 \times 10^{-21} \text{ W} \end{aligned}$$

In decibel form, the reference noise power, N_{ref} , equals -204 dBW (in a 1 Hz bandwidth).

FIGURE 8.1
Noise power from a resistive conductor at a specified temperature
and within a given bandwidth



8.2.3 Noise factor

Consider an amplifier having a gain, g_{amp} , and bandwidth, b , in Hz. The amplifier circuit is shown in Fig. 8.2. Assume an input signal power, s_{in} , and an input noise power, n_{in} , due to a resistive load, are measured at the amplifier's input terminals. Assume an output signal power, s_{out} , and output noise power, n_{out} , are available at the amplifier's output terminals.

A term called noise factor, f , originally was defined [8-1] as the ratio of the input signal-to-noise ratio to the output signal-to-noise ratio.

$$f = \frac{\left(\frac{s_i}{n_i} \right)}{\left(\frac{s_o}{n_o} \right)} \quad (8-2)$$

An alternate term, noise figure, is denoted by capital F and is defined as the decibel expression of the noise factor; i.e. $F = 10 \log_{10} f$.

The output signal power is related to the input signal power by the amplifier gain:

$$s_{out} = g_{amp} s_{in} \quad (8-3)$$

and the input noise power is related to the noise temperature of the input termination, t_{in} :

$$n_{in} = k t_{in} b \quad (8-4)$$

When the input termination is at the reference temperature, t_0 , the input noise power is:

$$n_{in} = k t_0 b \quad (8-5)$$

The output signal-to-noise power ratio can be written as:

$$\frac{s_{out}}{n_{out}} = \frac{\frac{s_{in}}{k t_0 b}}{f} \quad (8-6)$$

and the output noise factor can be related to the noise factor of the amplifier by:

$$n_{out} = f g_{amp} k t_0 b \quad (8-7)$$

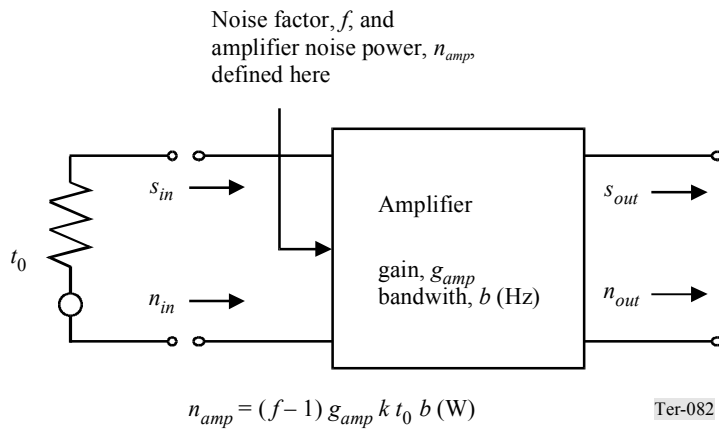
Consider the case when the amplifier is noiseless. The noise at the output of the amplifier would be the noise at the input, $k t_0 b$, multiplied by the amplifier's gain:

$$n_{noiseless\ amp} = g_{amp} k t_0 b \quad (8-8)$$

Now to find the noise at the output due only to the amplifier itself, subtract the noiseless amplifier noise power from the total noise power:

$$\begin{aligned} n_{amp} &= n_{out} - n_{noiseless\ amp} \\ &= f g_{amp} k t_0 b - g_{amp} k t_0 b \\ &= (f - 1) g_{amp} k t_0 b \end{aligned} \quad (8-9)$$

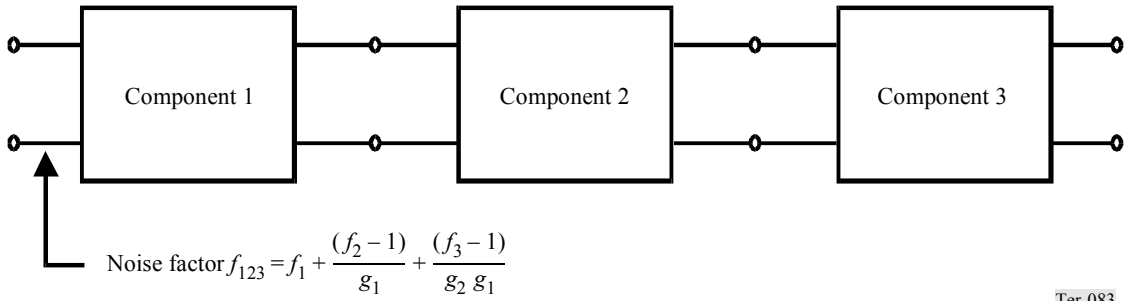
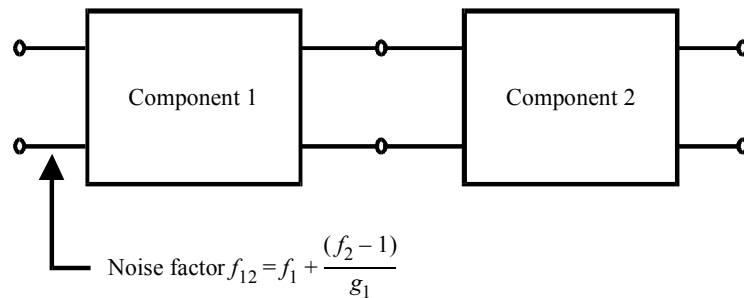
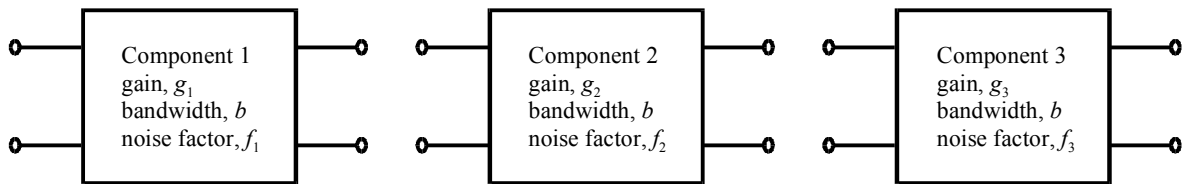
FIGURE 8.2
Noise factor for a single device



8.2.4 Noise factor for cascaded components

Consider the overall noise figure of two and three components cascaded together as in Fig. 8.3. Let the noise factors and gains of the three devices be defined as f_1, f_2, f_3, g_1, g_2 , and g_3 , respectively.

FIGURE 8.3
Noise factors for cascaded devices



Ter-083

Following the pattern set by the single component above, the total output noise power of the two-component circuit would be:

$$n_{out} = f_{12}g_1g_2k t_0 b \quad (8-10)$$

but this is just the output noise of the first component multiplied by the gain of the second device with the additional noise created by the second component by itself:

$$n_{out} = n_1g_2 + n_2 \quad (8-11)$$

Using the equations above, this becomes:

$$f_{12}g_1g_2k t_0 b = f_1g_1k t_0 b g_2 + (f_2 - 1)g_2k t_0 b \quad (8-12)$$

Thus, the overall noise factor, f_{12} , of the two-component network is:

$$f_{12} = f_1 + \frac{(f_2 - 1)}{g_1} \quad (8-13)$$

and the overall noise factor, f_{123} , of the three component network is:

$$f_{123} = f_1 + \frac{f_2 - 1}{g_1} + \frac{f_3 - 1}{g_1 g_2} \quad (8-14)$$

If the first two devices are passive with attenuation (l) rather than gain, then:

$$g_1 = \frac{1}{l_1} \quad (8-15)$$

$$g_2 = \frac{1}{l_2} \quad (8-16)$$

and

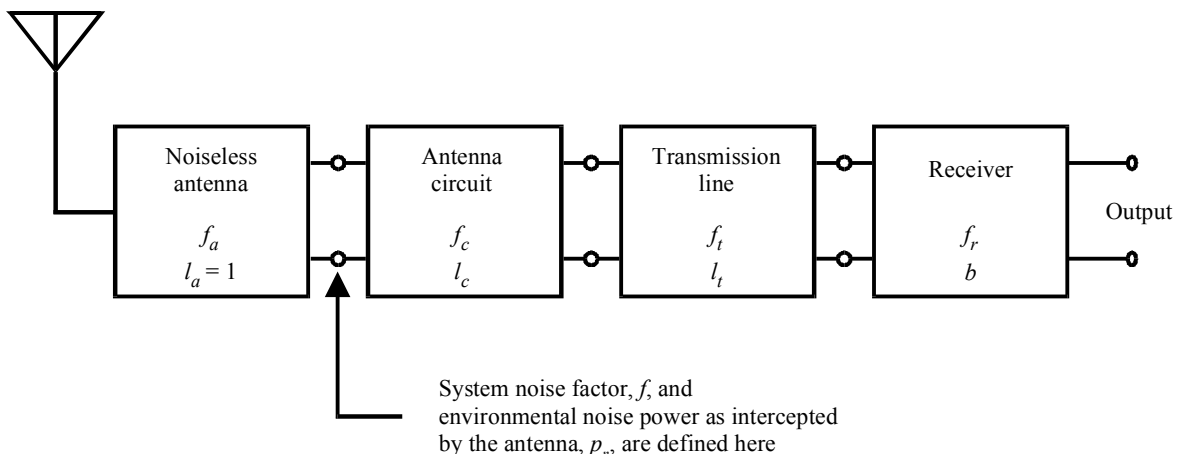
$$f_{12} = f_1 + l_1(f_2 - 1) \quad (8-17)$$

$$f_{123} = f_1 + l_1(f_2 - 1) + l_1 l_2(f_3 - 1) \quad (8-18)$$

8.2.5 Noise factor for receiving systems

Recommendation ITU-R P.372 defines the components of a receiving system and the parameters needed to specify the noise factor, f , of a receiving system. The block diagram of the receiving system and its parameters are shown in Fig. 8.4. While several references (e.g [8-9], [8-10], [8-11]), describe receiving system noise figure and antenna noise figure, the following development along with Fig. 8.4 apply to the information found in Recommendation ITU-R P.372.

FIGURE 8.4
Antenna noise factor and receiving system noise factor



$$f = f_a + (f_c - 1) + l_c(f_t - 1) + l_c l_t(f_r - 1)$$

The following definitions apply to the parameters used in the Recommendation:

- p_n : available environmental noise power from an equivalent lossless antenna (W)
- f_a : noise factor at the antenna associated with environmental noise as intercepted by the antenna
- l_a : antenna loss (assumed to be lossless, $l_a = 1$)
- k : Boltzmann's constant, 1.38×10^{-23} (W/(K · Hz))
- t_0 : reference temperature, assumed to be room temperature 290 K
- b : noise power bandwidth of the receiving system (Hz)
- f_c : noise factor associated with the antenna circuit losses
- l_c : antenna circuit loss (available input power/available output power)
- f_t : noise factor associated with the transmission line losses
- l_t : transmission line loss (available input power/available output power)
- f_r : noise factor of the receiver.

Referring to Fig. 8.4, while the output of the antenna circuit is a location that can be used to measure signal-to-noise power ratios, it is not the desired location to reference the system performance. Instead, the output of the antenna is where it is desired to specify the system signal-to-noise power ratio, the antenna noise factor, f_a , and the system noise factor, f . Based upon the above equations, the system noise factor can be written

$$f = f_a + l_a(f_c - 1) + l_a l_c (f_t - 1) + l_a l_c l_t (f_r - 1) \quad (8-19)$$

With the assumption that the antenna itself is lossless ($l_a = 1$), the system noise factor becomes as equation (1) in Recommendation ITU-R P.372:

$$f = f_a + (f_c - 1) + l_c (f_t - 1) + l_c l_t (f_r - 1) \quad (8-20)$$

All parameters in the equation are dependent on the receiving system, except for the antenna noise factor, f_a , which indicates the amount of environmental noise that would be intercepted by an antenna in a particular environment and specified bandwidth.

The antenna noise figure, F_a , represents the antenna noise factor in decibels:

$$F_a = 10 \log_{10} (f_a) \quad (8-21)$$

The environmental noise power, P_n , is the decibel form of p_n :

$$\begin{aligned} P_n &= 10 \log_{10} (p_n) && \text{dBW} \\ &= F_a - 204 + B \end{aligned} \quad (8-22)$$

where the noise bandwidth, B , is the decibel form of b :

$$B = 10 \log_{10} (b) \quad \text{dB(Hz)} \quad (8-23)$$

The noise bandwidth is often close in value to the receiver's 3 dB signal bandwidth.

Values for the antenna noise figure are contained in Recommendation ITU-R P.372.

8.3 Antenna noise figure information in Recommendation ITU-R P.372

Recommendation ITU-R P.372 provides antenna noise figure information for systems operating from 0.1 Hz to 100 GHz. Three types of environmental noise can be present at the receiving antenna: atmospheric noise, galactic noise, and man-made noise. Atmospheric noise levels vary diurnally with night time presenting the highest values. Man-made noise, as indicated in the Recommendation, is greatest in urban environments and least in quiet rural environments. (It is noted that the source of man-made noise estimates given in the Recommendation came from references [8-2, 8-3] whose measurement data were collected over 25 years ago.) Typically, the galactic noise is about 5 to 10 dB greater than quiet rural noise.

Most land mobile radio systems operate in the frequency range from about 30 MHz to 3 GHz; in this frequency range, atmospheric noise can be ignored. Figure 10 of the Recommendation presents the antenna noise figure, F_a , and the median antenna noise figure, F_{am} , values in this range where man-made and galactic noise sources dominate.

The Recommendation provides an estimate of the median noise figure within business areas using the expression for systems in the frequency range $200 \text{ MHz} < f_{MHz} < 900 \text{ MHz}$:

$$F_{am} = 44.3 - 12.3 \log_{10} f_{MHz} \quad (8-24)$$

Table 8.1 compares the results of the overall system noise figure for two systems operating at 200 and 900 MHz by using the equation above to estimate F_{am} at the two operating frequencies. Typical values are selected for the noise figure of the receiver and the losses of the antenna circuit and the transmission line.

TABLE 8.1

Comparison of system noise figures for LMR systems at 200 and 900 MHz

		200 MHz system	900 MHz system
Antenna	F_{am}	16 dB	8 dB
	f_{am}	39.81	6.26
Antenna circuit	L_c	1 dB	1 dB
	l_c	1.26	1.26
Transmission line	L_t	1 dB	1 dB
	l_t	1.26	1.26
Receiver	F_r	9 dB	9 dB
	f_r	7.94	7.94
	b	6 kHz	6 kHz
System	F	17.1 dB	12.5 dB
	f	51.42	17.86
	P_n	-149.1 dBW	-153.7 dBW

For these two particular situations, the system noise figure and the system noise power are dominated by environmental noise for the 200 MHz system and by the receiver noise for the 900 MHz system.

The median noise figure, F_{am} , represents the value expected for 50% of the time and 50% of the locations, in a particular environment. To estimate man-made noise at other periods of time, Recommendation ITU-R P.372 provides decile values relative to median. The man-made noise level that would be available for at least 90% of the time (taking account of “within the hour” variability) at a given location is found by subtracting the lower decile value, D_l , from the median, F_{am} . Similarly, the noise level for no more than 10% of the time is estimated by adding the upper decile value, D_u , to the median. Table 2 of the Recommendation suggests different upper decile values for the different environments of business, residential, and rural and only for operating frequencies up to 250 MHz. A revisit by researchers [8-4] of the original data indicated that the decile values should be modified to $D_u = 9.7$ dB and $D_l = 7$ dB, regardless of man-made environment and of frequency.

Within a given environment, the noise figure will change from location to location. The standard deviation of the median noise figure due to location variability, σ_L , is given [8-2] in Table 8.2, for one operating frequency, 250 MHz, that is within the land mobile radio spectrum under consideration.

TABLE 8.2

Standard deviation of location variability at 250 MHz

Environment	Business	Residential	Rural
σ_L	3.8 dB	2.9 dB	2.3 dB

An observation in [8-5] based on noise measurements made more recently than those of Recommendation ITU-R P.372 notes that man-made noise demonstrates a diurnal character, depending upon human activity. However, the measurements did not show the within-the-hour time variability as presented in Recommendation ITU-R P.372. Some indications were given that automotive noise is not the large contributor of man-made noise as it reportedly was when measurements were made for the man-made noise expressions found in the Recommendation. Unfortunately, there have been an insufficient number of noise measurements to demonstrate whether this conclusion has any basis.

Other contributors of broadband noise, for example, such as digital devices and switched mode power supplies may have become more significant. These sources have different characteristics, especially with respect to peak-to-mean levels and discrete spectral components at clock frequencies and harmonics.

8.4 Noise measurements for specific applications

For some land mobile radio applications, the signal levels may be near the system noise level. For those situations, noise measurements in the environments that the radios are to be used would provide better estimates of the noise levels than those estimates based upon historical data, such as from Recommendation ITU-R P.372.

An RF noise measurement methodology is given in [8-6] which identifies the trade-offs between using a communications receiver (designed for the land mobile service application) and a laboratory-grade measurement receiver. Another recent report [8-7] provides information and gives details on the noise measurement process used to collect noise measurement characteristics in the 136-138 MHz band. Mobile noise measurements were recently made and reported [8-8] that relate noise levels to a number of land use – land cover (LULC) categories. The same reference describes the process used to make the mobile measurements.

8.5 References

- [8-1] FRIIS, H. T. [July 1944] Noise figures of radio receivers. *Proc. IRE*, 32(7), p. 419-422.
- [8-2] SPAULDING, A. D. and DISNEY, R. T. [June 1974] Man-made radio noise Part 1: Estimates for business, residential, and rural areas. U.S. Department of Commerce, OT Report 74-38.
- [8-3] DISNEY, R. T. [1972] Estimates of man-made noise levels based on the Office of Telecommunications ITS data base. Proc. of the IEEE International Conference on Communications, Order No. 72CH0622-1-COM, 20-13/20-19.
- [8-4] SPAULDING, A. D. and STEWART, F. G. [January 1987] An updated noise model for use in IONCAP. U.S. Department of Commerce, NTIA Report 87-212.
- [8-5] WEBSTER, J. G. [1999] Editor (Roger Dalke, Section Author), “Radio Noise”, IN: Wiley *Encyclopedia of Electrical and Electronics Engineering*, John Wiley & Sons, Inc., New York, United States of America, p. 128-140.
- [8-6] Telecommunications Industry Association [1999] Wireless communications systems performance in noise- and interference-limited situations recommended methods for technology-independent modeling, simulation, and verification. TIA document TSB-88A.
- [8-7] ACHATZ, R. et al. [September 1998] Man-made noise in the 136-138 MHz VHF meteorological satellite band. NTIA Report 98-355, U.S. Department of Commerce, Boulder CO, United States of America.
- [8-8] RUBINSTEIN, T. N. [September 1998] Clutter losses and environmental noise characteristics associated with various LULC categories. *IEEE Trans. on Broadcasting*, 44(3), p. 286-293.
- [8-9] HESS, G. C. [1998] *Handbook of land mobile radio system coverage*. Artech House, Boston, United States of America, p. 201-02.
- [8-10] SIWIAK, K. [1995] *Radio propagation and antennas for personal communication*. Artech House, Boston, United States of America, p. 80-81.
- [8-11] SKOMAL, E. N. and SMITH Jr., A. [1985] *Measuring the radio frequency environment*. Van Nostrand Reinhold, New York, United States of America, p. 2-7.

CHAPTER 9

CHANNEL CHARACTERISTICS FOR DIGITAL MODULATION SCHEMES

In a radio link, a part of the energy radiated by the transmitting antenna reaches the receiving station through different paths. Along these paths, interaction may occur between the electromagnetic field and various objects. Possible interactions are specular reflection on long plane surfaces, diffuse scattering from surfaces exhibiting small irregularities or from objects of small size, transmission through dense material, shadowing by obstacles, etc. At the position of the receiving antenna, the resulting electric field is spread both in time delay and direction. In radio systems using digital modulation schemes the properties of the time-varying, frequency-dispersive radio channel are important to know. In such radio environments not only the narrow-band signal is relevant but also the time delays and angles-of-arrival of the individual multipath components are important. Multipath signals are not seen as interferers only; in some systems their energy is used to improve the signal level.

The dispersive nature of the propagation channel is described by the angle-resolved location-variant impulse response $h(\vec{x}, \tau, \varphi)$ of the electric field:

$$h(\vec{x}, \tau, \varphi) = \sum_{i=1}^n h_i(\vec{x}, \tau, \varphi) \quad (9-1)$$

where:

- \vec{x} : denotes the MS position
- τ : time delay
- φ : angle-of-arrival
- n : number of multipath signals.

Each of these components embodies a specular and a diffuse part.

9.1 Characterization in time domain

By considering the propagation channel between the transmit antenna and the antenna of a stationary receiver the field strength-delay spectrum (FDS) describes the complex impulse response $g(t)$ of the terrain in a narrow frequency band around f_0 :

$$\underline{g}(t) = \sum_{i=1}^n g_i e^{j\psi_i} \delta_0(t - \tau_i) \quad (9-2)$$

where:

- g_i : amplitude of the i -th signal
- ψ_i : phase of the i -th signal
- τ_i : time delay of the i -th signal.

Since the bandwidth of a receiver is limited, the signals arriving within a certain time period cannot be resolved. This is accounted for by the convolution of $g(t)$ with the receiver impulse response function $w(t)$, which is matched to the transmit signal:

$$\underline{h}(t) = \underline{g}_a(t) * \underline{w}(t) \quad (9-3)$$

$\underline{g}_a(t)$ is the FDS, where each multipath signal is weighted with the antenna diagrams of the transmitter and receiver. The expected received power, $P_m(t)$, can then be derived:

$$P_m(t) = cE[\underline{h}(t)\underline{h}^*(t)] \quad (9-4)$$

c is a constant converting field strength into received power. Based on $P_m(t)$ the delay spread S [9-1] can be derived for the characterization of the propagation channel in the time-domain:

$$S = \sqrt{\frac{\int_{-\infty}^{+\infty} t^2 P_m(t) dt}{\int_{-\infty}^{+\infty} t P_m(t) dt - t_m^2}} \quad (9-5)$$

where:

$$t_m = \sqrt{\frac{\int_{-\infty}^{+\infty} t P_m(t) dt}{\int_{-\infty}^{+\infty} P_m(t) dt}} \quad (9-6)$$

S is a rough criterion to assess the performance of a digital system. As long as S is small compared to the duration T of the digital symbol the channel can be assumed to be resistant to inter-symbol interference.

9.2 Characterization in frequency domain

For many applications like frequency hopping or spread spectrum techniques, it is necessary to characterize the propagation channel in the frequency domain. The relation between the complex impulse response $g_a(t)$ and the complex transfer function is given by the Fourier transform:

$$\underline{G}_a(f) = \sum_{i=1}^n g_{a,i} e^{-j(2\pi f \tau_i - \Psi_{a,i})} \quad (9-7)$$

where:

$g_{a,i}$: amplitude of the i -th signal weighted with the antenna diagrams

$\Psi_{a,i}$: phase of the i -th signal weighted with the antenna diagrams.

As the amplitudes and phases of the scattered multipath components vary statistically $G_a(f)$ is also a variable of a stochastic process. Such a weak stationary process is described by its autocorrelation function [9-2]. The autocorrelation function describing the random process in the frequency domain is the frequency correlation function (FCF):

$$l_{\underline{H}\underline{H}}(\Delta f) = \int_{-\infty}^{+\infty} \underline{H}(f) \underline{H}^*(f + \Delta f) df \quad (9-8)$$

where:

$$\underline{H}(f) = G_a(f) \underline{W}(f) \quad (9-9)$$

and $\underline{W}(f)$ is the Fourier transform of $w(t)$. A more comprehensive description of correlation functions of the mobile radio channel can be found in [9-2]. $l_{\underline{H}\underline{H}}$ is a measure to quantify frequency selective fading effects. Parameters such as correlation or coherence bandwidth [9-1] of the radio channel are derived from $l_{\underline{H}\underline{H}}$.

9.3 Characterization in angular domain and Doppler spectra

The Doppler frequency $f_{d,i}$ of each multipath signal depends on the velocity of the vehicle, the wavelength and the angle-of-arrival:

$$f_{d,i}(\alpha_i) = \frac{v}{c_0} f_0 \cos \alpha_i = f_{d,max} \cos \alpha_i \quad (9-10)$$

where:

- v : vehicle velocity
- c_0 : speed of light
- α_i : incidence angle in azimuth
- $f_{d,max}$: maximum Doppler shift.

The maximum Doppler shifts occur at alpha $i = 0^\circ$ and 180° . As each multipath signal has a different angle-of-arrival and amplitude a wide Doppler spectrum exists. This phenomenon is well known in the literature [9-2, 9-3]. For planning purposes, usually the simplified case of the so-called Jakes Spectrum [9-3] is applied, where it is assumed that all incoming signals have the same magnitude and equally distributed angles-of-arrival. This assumption characterizes the worst case.

The application of multiple directive antennas, i.e. directional diversity, may lead to significant capacity improvements in cellular mobile radio. However, in such antenna concepts the angles-of-arrival are important. Therefore directional channel models have been developed [9-4, 9-5].

9.4 WSSUS channels

One of the most popular assumptions for a physically reasonable simplification of signal description in mobile radio channels is the wide-sense stationary uncorrelated scatterer (WSSUS) assumption. The wide-sense stationary (WSS) case means:

- the mean value of the signal in the time domain is constant;
- the time correlation function of the signal in the time domain depends only on the time difference Δt and not on the absolute time itself.

In practical situations WSS conditions occur during short time spans corresponding to small regions when the MS (mobile station) is moving. The stationary regions extend typically over several wavelengths λ to several tens of wavelengths λ .

The uncorrelated scatterer (US) assumption is dual to the WSS assumption, in that it assumes that contributions with different delays τ are statistically uncorrelated. This condition means that interference processes, which cause statistical fluctuations of amplitude, are independent for the different scatterer clusters, i.e. groups of scatterers that cannot be resolved in direction. The WSSUS assumption is typically fulfilled in macro-cellular environments. However, investigations in [9-6] have shown that the assumption US is sometimes violated in small cells, especially in indoor environments.

9.5 Modelling the wideband channel

In order to forecast the characteristics of the wideband radio channel both site-specific and site-general models have been developed. The site-specific methods are used to predict channel characteristics for a specific area whereas the site-general models are used for system simulations.

9.5.1 Site-specific channel models

Site-specific models are available for both rural and urban areas. In rural areas emphasis is placed on automatic detection of long excessive time dispersions. The task of predicting multipath signals can be subdivided into two steps. The first step consists of an algorithm to extract the relevant scattering areas. All known approaches, e.g. [9-7, 9-8, 9-9] take into account single scattering processes only. Hence every potential scatter area has to fulfil the LoS-condition to both transmitter and receiver. In a second step the path loss for each multipath signal has to be calculated. This calculation consists of three parts:

- propagation from transmitter to the scattering surface,
- process of scattering at the surface,
- propagation from the scattering surface to the receiver.

Digital terrain databases consisting of raster data with a resolution of 50 m to 200 m containing terrain height and land use information are sufficient for rural areas.

In urban areas ray-tracing or ray-launching techniques are applied to predict multipath signals based on high-resolution building databases, e.g. [9-9, 9-10, 9-11, 9-12]. Both raster and vector data formats are used. Due to the complexity of the environment, multiple-scattering and diffraction processes in transversal propagation planes must be considered.

A detailed overview of models for both environments can be found in [9-6]. Methods for channel characteristics from 3D propagation models are described in [9-9, 9-13].

9.5.2 Site general channel models for system simulation

Models for the mobile radio channel are vital for the study of radio systems. These models have to reproduce the typical characteristics observed in measurement data from a number of different

representative environments. Two such models have been developed with the European research programs COST207 [9-14] and COST259 [9-4].

9.5.2.1 COST207 time delay profiles

COST207 [9-14] provided a collection of suggested channels for testing rural and urban (hilly and not hilly) environments, with implementations of 6 or 12 taps. The basic elements (settings) for the channel simulation are:

- tap delay values following different profiles;
- tap mean power and Rayleigh distribution (eventually, for the first ray, a Rice distribution is used);
- Doppler Spectrum types: Classical [9-3], Gaussian (two different types) and Rice (Classical + direct ray).

COST207 models have been used as a reference for many measurements and utilized in a number of theoretical and performance studies, mainly for, but not restricted to, GSM.

9.5.2.2 COST259 directional channel models

In order to take into account the directivity of the radio channel the COST259 project has developed directional channel models (COST259-DCM) [9-4]. These models can be seen as an extension and further development of the COST207 delay profiles.

To account for the variety of extremely different topographical and electrical features of the different propagation environments COST259 has defined a 3-level structure, providing a framework from which channel models can be deduced.

At the top level, a first distinction has been made by cell type. For each cell type, a number of radio environments (REs) have been identified. RE stands for a whole class of propagation conditions that exhibit similar or typical features that can be related to the surroundings in which a communication system operates. The topographical features of an RE are given by a number of external parameters, such as the frequency band, the average height of BS (base station) and MS (mobile station), their average distance, average building heights and separations, etc. Furthermore, it has been defined whether the propagation path has line-of-sight (LoS) or non-line-of-sight (NLoS).

The propagation conditions encountered in each RE are characterized statistically by a set of probability density functions (PDFs) and/or statistical moments. Since the members of this set characterize propagation conditions of the entire RE, they are referred to as global parameters (GPs). They serve as key channel parameters that provide the necessary information for the basic system design decisions on modulation technique, burst length, coding scheme, etc.

The third level of COST259-DCM consists of propagation scenarios, which are defined as random realizations of incidence conditions. The latter are specified by random local parameters (LPs). A possible set of LPs may be given by the parameters of the waves incident at the location of the Rx antenna, i.e. their number, complex amplitude, delay, and incidence direction, or equivalently, by

describing the location of the BS, MS, and the scattering objects interacting with the electromagnetic field. The statistical properties of the LPs are given by the set of global parameters defined in the 2nd level of COST259-DCM.

9.6 References

- [9-1] COX, D. C. and LECK, R. P. [1975] Correlation bandwidth and delay spread multipath propagation statistics for 910 MHz urban mobile radio channels. *IEEE Trans. Comm.* COM-23, p. 1271-1280.
- [9-2] BELLO, P. A. [1963] Characterisation of randomly time-variant linear channels. *IEEE Trans. Comm.* Vol. COM-11, p. 360-393.
- [9-3] JAKES, Wm. C. (ed) [1974] *Microwave Mobile Communications*. Wiley, New York, United States of America.
- [9-4] COST 259 [March 2001] *Wireless Flexible Personalised Communications*. Final Report, Ed. Luis M. Correia, Wiley, New York, United States of America.
- [9-5] BLANZ, J. J. and JUNG, P. [1998] A flexibly configurable spatial model for mobile radio channels. *IEEE Trans. Comm.* COM-46, p. 367-371.
- [9-6] COST 231 [1999] Digital mobile radio towards future generation systems. Final Report, Office Official Publ. Eur. Commission, EUR 18957, ISBN 92-828-5416-7.
- [9-7] LIEBENOW, U. and KUHLMANN, P. [1996] A three-dimensional wave propagation model for macrocellular mobile communication networks in comparison with measurements. 45th IEEE Vehicular Technology Conference Record, Atlanta, United States of America, 28 April-1 May, p. 1623-1627.
- [9-8] DAVIDSEN, K. and DANIELSEN, M. Predicting impulse responses in mountainous areas. PIMRC '94 Conference Record, The Hague, Netherlands, p. 25-27.
- [9-9] KÜRNER, Th., CICHON, D. and WIESBECK, W. [September 1993] Concepts and results for 3D digital terrain based wave propagation models – an overview. *IEEE J. Selected Areas in Comm.*, Vol. 11, p. 1002-1012.
- [9-10] GSCHWENDTNER, G., WÖLFLE, B., BURK, F. and LANDSTORFFER, M. [1995] Ray tracing vs. ray launching in 3D-microcell modelling. Proc. European Personal and Mobile Communications Conference EPMCC'95, Bologna, Italy, 24-26 November, p. 74-79.
- [9-11] RIZK, K., WAGEN, J.-F. and GARDIOL, F. [September 1994] Ray, tracing based path loss prediction in two micro cellular environments. In Personal, Indoor and Mobile Radio Conference PIMRC'94 Conf. Record, p. 384-388, The Hague, The Netherlands.
- [9-12] BERTONI, H. L., HONCHARENKO, W., MACIEL, L. R. and XIA, H. H. [1994] UHF propagation prediction for wireless personal communications. *Proc. IEEE*, Vol. 83, **9**, p. 1333-1359.
- [9-13] KÜRNER, Th., CICHON, D. and WIESBECK, W. [March 1996] Evaluation and characterisation of the VHF/UHF propagation channel based on a 3-D-wave propagation model. *IEEE Trans. Ant. Prop.*, Vol. 44, **3**, p. 393-404.
- [9-14] COST 207 [1989] Digital land mobile radio communications. Final Report, Office Official Publ. Eur. Commission., ISBN 92-825-9946-9.

BIBLIOGRAPHY

The following is a list of suggested references for use as reference material on radiowave propagation in a terrestrial land mobile environment:

ITU-R texts

See Section 1.3.

Books

- BARCLAY, L. W., CRAIG, K. H., BACON, D. F. and HEWITT, M. T. (Eds.) [2002] *Propagation of Radiowaves 2nd Edition*. The Institution of Electrical Engineers.
- BECKMANN, P. and SPIZZICHINO, A. [1987] *The Scattering of Electromagnetic Waves from Rough Surfaces*. 503 pp., Artech, Norwood, United States of America.
- BLAUNSTEIN, N. [2000] *Radio Propagation in Cellular Networks*. Artech.
- BOITHIAS, L. [1987] *Radio Wave Propagation*. McGraw-Hill.
- CÁTEDRA, M. F. and PÉREZ-ARRIAGA, J. [1999] *Cell Planning for Wireless Communications*. Artech House.
- HESS, G. C. [1997] *Handbook of Land Mobile Radio Coverage*. Artech.
- JAKES, Wm. C. (ed) [1974] *Microwave Mobile Communications*. New York, Wiley.
- LEE, Wm. C. Y. [1995] *Mobile Communications Design Fundamentals*. 2nd ed., McGraw Hill.
- LEE, Wm. C. Y. [1982] *Mobile Communications Engineering*. 464 pp., McGraw-Hill.
- PARSONS, J. D. [1992] *The Mobile Radio Propagation Channel*. 2nd ed., Wiley.
- PICQUENARD, A. [1974] *Radio Wave Propagation*. Wiley.
- SHIBUYA, S. [1987] *A Basic Atlas of Radio-Wave Propagation*. Wiley, p. 264.
- SIWIAK, K. [1998] *Radiowave Propagation and Antennas for Personal Communications*. 2nd ed., Artech.
- SKOMAL, E. N. [1978] *Man-Made Radio Noise*. Van Nostrand Reinhold.
- SKOMAL, E. N. and SMITH Jr., A. A. [1985] *Measuring the Radio Frequency Environment*. Van Nostrand Reinhold.

Data-sets, online

GLOBE Task Team and others (Hastings, David A., Paula K. Dunbar, Gerald M. Elphingstone, Mark Bootz, Hiroshi Murakami, Hiroshi Maruyama, Hiroshi Masaharu, Peter Holland, John Payne, Nevin A. Bryant, Thomas L. Logan, J.-P. Muller Gunter Schrier and John S. MacDonald), eds., 1999. *The Global Land One-kilometer Base Elevation (GLOBE) Digital Elevation Model, Version 1.0*. National Oceanic and Atmospheric Administration, National Geophysical Data Center, 325 Broadway, Boulder, Colorado, 80305, U.S.A. Digital database on the World Wide Web (URL: <http://www.ngdc.noaa.gov/seg/topo/globe.shtml>) and CD-ROMs.

Monographs and reports

- ACHATZ, R. *et al.* [Sept. 1998] Man-made noise in the 136-138 MHz VHF meteorological satellite band. NTIA Report 98-355, U.S. Department of Commerce, National Telecommunications and Information Administration, Boulder CO, NTIS Accession Number PB 99 127 052.
- CAUSEBROOK, J. H. and DAVIES, B. [1971] Tropospheric radiowave propagation over irregular terrain: the computation of field strength for UHF broadcasting. BBC Research Report, No. 43.
- COST 207 [1989] Digital Land Mobile Radio Communications. Final Report, Office Official Publ. Eur. Commission., ISBN 92-825-9946-9.
- COST 231 [1999] Digital mobile radio towards future generation systems. Final Report, Office Official Publ. Eur. Commission., EUR 18957, ISBN 92-828-5416-7.
- COST 259 [March 2001] Wireless flexible personalised communications. Final Report, Ed. Luis M. Correia, Wiley.
- HASTINGS, D. A. and DUNBAR, P. K. [1999] Global land one-kilometer base elevation (GLOBE) digital elevation model. Documentation Volume 1.0. Key to Geophysical Records Documentation (KGRD) 34. National Oceanic and Atmospheric Administration, National Geophysical Data Center, 325 Broadway, Boulder, Colorado, 80305, United States of America.
- HUFFORD, G. A., LONGLEY, A. G. and KISSICK, W. A. [April 1982] A guide to the use of the ITS irregular terrain model in the area prediction mode. NTIA Rep. 82-100. NTIS Accession Number PB 82 217 977.
- LONGLEY, A. G. [April 1978] Radio propagation in urban areas. OT Rep. 78-144. NTIS Accession Number PB 281 932.
- LONGLEY, A. G. and RICE, P. L. [1968] Prediction of tropospheric radio transmission loss over irregular terrain – a computer method. ESSA Tech. Report ERL 79-ITS 67. NTIS Accession Number AD 676 874.
- RICE, P. L., LONGLEY, A. G., NORTON, K. A. and BARSIS, A. P. [1965] Transmission loss predictions for tropospheric communications circuits. NBS Technical Note 101; two volumes; issued 7 May, 1965. NTIS Accession Numbers AD 687 820 and AD 687 821.
- SPAULDING, A. D. and DISNEY, R. T. [June, 1974] Man-made radio noise Part 1: Estimates for business, residential, and rural areas. U.S. Department of Commerce, OT Report 74-38. NTIS Accession Number COM 75 10798.
- SPAULDING, A. D. and STEWART, F. G. [January 1987] An updated noise model for use in IONCAP. U.S. Department of Commerce, NTIA Report 87-212. NTIS Accession Number PB 87 165 007.
- TIA [1999] Wireless communications systems performance in noise- and interference-limited situations recommended methods for technology-independent modeling, simulation, and verification. TIA document TSB-88A. Telecommunications Industries Association.

Conference and journal papers

- AGUIRRE, S. [1994] Radio propagation into buildings at 912, 1 920, and 5 990 MHz using microcells. 3rd ICUPC Record, p. 129-134.
- ANDERSON, H. R. [September 1993] A ray-tracing propagation model for digital broadcast systems in urban areas. *IEEE Trans. Broadcasting*, 39(3), p. 309-317.

- ANDERSON, H. R. [November 1993] Digital terrain database structures and accuracy requirements for propagation modelling. Colloquium on Terrain Modelling and Ground Cover Data for Propagation Studies, IEE Digest No. 1993/212, p 6/1-6/5.
- BADSBERG, M., ANDERSEN, J. B. and MOGENSEN, P. [January 1995] Exploitation of the Terrain Profile in the Hata Model. COST 231 TD(95)009.
- BELLO, P.A. [1963] Characterisation of randomly time-variant linear channels. *IEEE Trans. Comm.*, Vol. COM-11, p. 360-393.
- BERTONI, H. L., HONCHARENKO, W., MACIEL, L. R. and XIA, H. H. [1994] UHF propagation prediction for wireless personal communications. *Proc. IEEE*, 83(9), p. 1333-1359.
- BETHE, H. A. [1944] Theory of diffraction by small holes. *Phys. Rev.*, Vol. 66, p. 163-182.
- BLANZ, J. J. and JUNG, P. [1998] A flexibly configurable spatial model for mobile radio channels. *IEEE Trans. Comm.* COM-46: 367-371.
- BROWN, G. S. and CURRY, W. J. [1982] A theory and model for wave propagation through foliage. *Radio Sci.*, 17(5), September-October, p. 1027-1056.
- BULLINGTON, K. [October 1947] Radio propagation at frequencies above 30 megacycles. *Proc. IRE*, 35(10), p. 1122-1136.
- BULITUDE, R. J. C. and BEDAL, G. K. [1989] Propagation characteristics on microcellular urban mobile radio channels at 910 MHz. *IEEE J. Selected Areas Comm.*, 7(1).
- COX, D. C. and LECK, R. P. [1975] Correlation bandwidth and delay spread multipath propagation statistics for 910 MHz urban mobile radio channels. *IEEE Trans. Comm.* COM-23: 1271-1280.
- DADSON, C. E. [1979] Radio network and radio link surveys derived by computer from a terrain data base. AGARD Conf. Proc., p. 25-1 to 25-17.
- DALKE, R. *et al.* [August 1998] Measurement and analysis of man-made noise in VHF and UHF bands. IEEE 1997 Wireless Comm. Conf. Record, p. 427-431.
- DALKE, R. *et al.* [1998] Statistics of man-made noise at 137 MHz. RAWCON Conf. Record, p. 229-233.
- DANIELSEN, M. [October 1991] Mobile telephone with 100 percentage coverage of the mountainous Faroe Islands. 6th World Telecom Forum, Tech. Symp., Proc., p. 219-223.
- DAVIDSEN, K. and DANIELSEN, M. [1994] Predicting impulse responses in mountainous areas. PIMRC '94 Conf Record, The Hague, Netherlands, p. 25-27.
- DAVIDSON, A. L. *et al.* [February 1997] Measurement of building penetration into medium buildings at 900 and 1500 MHz. *IEEE Trans. Veh. Tech.*, 46(1), p. 19-23.
- DE TOLEDO, A. F. and TURKMANI, A. M. D. [1992] Propagation into and within buildings at 900, 1800, and 2300 MHz. 42nd IEEE Veh. Tech. Conf. Record, p. 633-36.
- DEMASSO, E. *et al.* [April 1993] Indoor propagation measurements application to mobile channel modelling. IEE Conf. Pub. 370, p. 146-9.
- DEYGOUP, J. [July 1966] Multiple knife-edge diffraction of microwaves. *IEEE Trans. Ant. Prop.*, 14(4), p. 480-489.
- DIETZ, J. *et al.* [May 1973] Examination of the feasibility of conventional land-mobile operation at 950 MHz. FCC OCE Report R7202.

- DISNEY, R. T. [1972] Estimates of man-made noise levels based on the Office of Telecommunications ITS data base. IEEE Int'l. Comm. Conf. Record, Order No. 72CH0622-1-COM, 20-13/20-19.
- DOUGHERTY, H. T. and MALONEY, L. J. [February 1964] Application of diffractions by convex surfaces to irregular terrain situations. *Radio Sci.*, 68D(2), p. 239-250.
- DRIESEN, P. F. [1992] Multipath delay characteristics in mountainous terrain at 900 MHz. 42nd IEEE Veh. Tech. Conf. Record, p. 520-523.
- DURANTE, J. M. [1973] Building penetration loss at 900 MHz. 23rd IEEE Veh. Tech. Conf. Record.
- EDWARDS, R. and DURKIN, J. Computer prediction of services for v.h.f. mobile radio networks. *Proc. IEE*, 116(9), p. 1493-1500.
- EPSTEIN, J. and PETERSON, D. W. [May 1953] An experimental study of wave propagation at 850 Mc. *Proc. IRE*, 41(5), p. 595-611.
- FRIIS, H. T. [May 1946] A note on a simple transmission formula. *Proc. IRE*, 34(5), p. 254-256.
- FRIIS, H. T. [July 1944] Noise figures of radio receivers. *Proc. IRE*, 32(7), p. 419-422.
- GAHLEITNER, R. and BONEK, E. [1994] Radio wave penetration into urban buildings in small cells and microcells. 44th IEEE Veh. Tech. Conf. Record, p. 887-91.
- GREEN, J. A. and PULLEN, I. R. [1995] Building penetration loss measurements for digital analog broadcasting. IEE Coll. on Propagation in Bldgs, Digest No 1995/134, p. 1/1-1/6.
- GROßKOPF, R. [May 1994] Prediction of urban propagation loss. *IEEE Trans. Ant. Prop.*, 42(5), p. 658-665.
- GSCHWENDTNER, G. W. B., BURK, F. and LANDSTORFFER, M. [1995] Ray tracing vs. ray launching in 3D-microcell modelling. Proc. European Personal and Mobile Communications Conference EPMCC'95, Bologna, Italy, 24-26 November, p. 74-79.
- HACKING, K. [March 1970] U.H.F. propagation over rounded hills. *Proc. IEE*, 117(3), p. 499-511.
- HAGN, G. H. [1980] VHF radio system performance model for predicting communications operational ranges in irregular terrain. *IEEE Trans. Comm.*, Vol. 28, 9, p. 1637-1644.
- HASHEMI, H. [July 1993] The indoor radio propagation channel. *Proc. IEEE*, 81(7), p. 943-68.
- HATA, M. [1980] Empirical formula for propagation loss in land mobile services. *IEEE Trans. Veh. Tech.*, 29(3), p. 317-325.
- HOLLOWAY, C. L., PERINI, P. L., DELYSER, R. R. and ALLEN, K. C. [August 1997] Analysis of composite walls and their effects on short-path propagation modeling. *IEEE Trans. Veh. Tech.*, 46(3), p. 730-738.
- IEEE Vehicular Technology Society Committee on Radio Propagation [February 1988] Coverage Prediction For Mobile Radio Systems Operating In The 800/900 MHz Frequency Range. *IEEE Trans. Veh. Tech.*, 37(1).
- IKEGAMI, F. [March 1991] Theoretical prediction of mean field strength for urban mobile radio. *IEEE Trans. Ant. Prop.*, 39(3), p. 299-302.
- KIDNER, D. B. and SMITH, K. H. [November 1993] Data structures for terrain modelling and ground cover data. Colloquium on Terrain Modelling and Ground Cover Data for Propagation Studies, IEE Digest No 1993/212, p. 7/1-7/9.

- KOZONO, S. and WATANABE, K. [October 1977] Influence of environmental buildings on UHF land mobile radio propagation. *IEEE Trans. Comm.*, 25(10), 1133-1143.
- KÜRNER, T. *et al.* [August 1997] The influence of land usage on UHF wave propagation in the receiver near range. *IEEE Trans. Veh. Tech.*, 46(3), p. 739-747.
- KÜRNER, Th., CICHON, D. and WIESBECK, W. [September 1993] Concepts and Results for 3D digital terrain based wave propagation models – an Overview. *IEEE J. Sel. Comm.*, Vol. 11, p. 1002-1012.
- KÜRNER, Th., CICHON, D. and WIESBECK, W. [March 1996] Evaluation and characterisation of the VHF/UHF propagation channel based on a 3-D-wave propagation model. *IEEE Trans. Ant. Prop.*, 44(3), p. 393-404.
- LAFORTUNE, J.-F. and LECOURS, M. [May 1990] Measurement and modelling of propagation losses in a building at 900 MHz. *IEEE Trans. Veh. Tech.*, 39(2), p. 101-108.
- LEVY, M. F. [1993] Ground cover data and diffraction models. Colloquium on terrain modelling and ground cover data for propagation studies, IEE Digest No 1993/212, November, p. 3/1-3/4.
- LIEBENOW, U. and KUHLMANN, P. [1996] A three-dimensional wave propagation model for macrocellular mobile communication networks in comparison with measurements. 45th IEEE Veh. Tech. Conf. Record, Atlanta, United States of America, 28 April – 1 May, p. 1623-1627.
- LIENARD, M. *et al.* [1994] Theoretical and experimental study of radio coverage in tunnels using radiating cables. *Ann. Telecommunication*, 49(3-4), p. 143-53.
- LO, T. *et al.* [October 1994] A new approach for estimating indoor radio propagation characteristics. *IEEE Trans. Ant. Prop.*, 42(10), p. 1369-76.
- LOO, C. and SECORD, N. [November 1991] Computer models for fading channels with applications to digital transmission. *IEEE Trans. Veh. Tech.*, 40(4), p. 700-707.
- LÓPEZ, G. C. [March 1984] An analysis of simplified solutions for multiple knife-edge diffraction. *IEEE Trans. Ant. Prop.*, 32(3), p. 297-301.
- LORENZ, R. W. [1980] Field strength prediction method for a mobile telephone system using a topographical data bank. Intl. Conf. on Radio Spectrum Conservation Techniques, p. 6-10, Table 1.
- LÖW, K. [August 1988] UHF measurements of seasonal field-strength variations in forests. *IEEE Trans. Veh. Tech.*, 37(3), p. 121-124.
- MAEYAMA, T. *et al.* [February 1993] Analysis of mountain-reflected signal strength in digital mobile radio communications. *IEICE Trans. Comm.*, E76-B(2), p. 98-102.
- MEDEISIS, A. and KAJACKAS, A. [2000] Adaptation of the universal propagation prediction models to address the specific propagation conditions and the needs of spectrum managers. Ant. Prop. (AP 2000), Millenium Conf., 9-14 April, Davos.
- MEDEISIS, A. and KAJACKAS, A. [2000] On the use of the universal Okumura-Hata propagation prediction model in rural areas. 51st IEEE Conf. Veh. Tech. (VTC 2000 Spring) Conf. Record, 15-18 May, Tokyo.

- MIDDLETON, J. [November 1993] A comparison between UHF field strength measurements and predictions using different resolution terrain databases. Colloquium on Terrain Modelling and Ground Cover Data for Propagation Studies, IEE Digest No. 1993212, p. 5/1-5/6.
- MILLINGTON, G., HEWITT, R. and IMMIRZI, F. S. [1961] Double knife-edge diffraction in field strength predictions. *Proc. IEE.*, 1962, 109C(16), p. 419-429.
- MOHR, W. [May 1993] Wideband propagation measurements of mobile radio channels in mountainous areas in the 1 800 MHz frequency range. 43rd IEEE Veh. Tech. Conf. Record, p. 49-52.
- OKUMURA, Y. *et al.* [September-October 1968] Field strength and its variability in VHF and UHF land mobile radio service. *Rev. Elec. Comm. Lab.*, 16(9-10), p. 825-873.
- PALMER, F. H. [1978] The CRC VHF/UHF propagation program: Description and comparison with field-measurements. AGARD Conf. Proc., p. 49-1 to 49-15.
- PIAZZI, L. and BERTONI, H. L. [May 1999] Achievable accuracy of site-specific path-loss predictions in residential environments. *IEEE Trans. Veh. Tech.*, 48(3), p. 922-930.
- PIAZZI, L. and BERTONI, H. L. [August 1998] Effect of terrain on path loss in urban environments for wireless applications. *IEEE Trans. Ant. Prop.*, 46(8), p. 1138-1147.
- RICE, L. P. [January 1959] Radio transmission into buildings at 35 and 150 Mc. *BSTJ*, V.38, p. 197-210.
- RIZK, K., WAGEN, J.-F. and GARDIOL, F. [1994] Ray tracing based path loss prediction in two micro cellular environments. Personal, Indoor and Mobile Radio Conference PIMRC'94 Conf. Record, p. 384-388, The Hague, The Netherlands, 18-23 September.
- RUBINSTEIN, T. N. [September 1998] Clutter losses and environmental noise characteristics associated with various LULC categories. *IEEE Trans. Broad.*, 44(3), p. 286-293.
- SAINDON, J.-P. and CHOW, S. [April 1993] Propagation of radio waves in underground tunnels and underground radio systems. IEE Conf. Pub. 370, p. 155-8.
- SEIDEL, S. Y. and RAPPAPORT, T. S. [February 1992] 914 MHz path loss prediction models for indoor wireless communications in multifloored buildings. *IEEE Trans. Ant. Prop.*, 40(2), p. 207-17.
- SEKER, S. S. [February 1992] VHF/UHF radiowave propagation through forests: modelling and experimental observations. IEE Proc.-H, 139(1), p. 72-78.
- SOARES DE ASSIS, M. [March 1971] A simplified solution to the problem of multiple diffraction over rounded obstacles. *IEEE Trans. Ant. Prop.*, 19(3), p. 292-5.
- STRUTT, J. (Lord Rayleigh) On the resultant of a large number of vibrations of the same pitch and arbitrary phase. *Philosophy Mag.*, 10, 1880, p. 73.
- SUZUKI, H. [July 1977] A statistical model for urban radio propagation. *IEEE Trans. Comm.*, 25(7), p. 673-680.
- TANAKA, T. and AKEYAMA, A. [1990] Modeling of propagation delay profile in urban areas surrounded by mountains. IEEE Ant. Prop. Int'l. Symp. Digest, p. 1804-1807.
- TANIS, W. J. and PILATO, G. J. [1993] Building penetration characteristics of 880 MHz and 1 922 MHz radio waves. 43rd IEEE Veh. Tech. Conf. Record, p. 206-209.
- TEWARI, R. K. *et al.* [April 1990] Radio wave propagation through rain forests of India. *IEEE Trans. Ant. Prop.*, 38(4), p. 433-448.

- TURKMANI, A. M. D. and DE TOLEDO, A. F. [December 1993] Modelling of radio transmissions into and within multistorey buildings at 900, 1 800, and 2 300 MHz. *IEE Proc.-I*, 140(6), p. 462-470.
- VAN DER POL, B. and BREMMER, H. [1937] The diffraction of electromagnetic waves from an electrical point source round a finitely conducting sphere, with application to radiotelegraphy and the theory of the rainbow. *Phil. Mag.*, XXIV, p. 141-176 (Part 1) and p. 825-862 (Part 2).
- VOGEL, W. and GOLDHIRSH, J. J. [December 1986] Tree attenuation at 869 MHz derived from remotely piloted aircraft measurements. *IEEE Trans. Ant. Prop.*, 34(12), p. 1460-1464.
- VOGLER, L. E. [1964] Calculation of groundwave attenuation in the far diffraction region. *Radio Sci.*, 1964, 68D(7), p. 819-826.
- WALFISCH, J. and BERTONI, H. L. [December 1988] A theoretical model of UHF propagation in urban environments. *IEEE Trans. Ant. Prop.*, 36(12), p. 1788-1796.
- WALKER, E. H. [November 1983] Penetration of radio signals into buildings in the cellular radio environment. *BSTJ*, 62(9), p. 2719-2734.
- WELLS, P. I. [November 1977] The attenuation of UHF radio signals by houses. *IEEE Trans. Veh. Tech.*, 26(4), p. 358-362.

APPENDIX A

PRACTICAL EXAMPLES

A.1 Example of testing and tuning generalized empirical point-to-area models (see also § 4.1.2)

The following section addresses the testing and tuning of generalized propagation prediction models and describes the process in its simplest form. Therefore, this example should be used as a guide only, for use in restricted circumstances, by users with little or no previous experience and by those who have no access to sophisticated measurement and propagation planning tools.

However, even in this simplest form, the described example may help to significantly improve the precision of a generalized empirical propagation prediction model (or choose the most appropriate model from several available, before applying them in an area of unknown propagation character).

A.1.1 Model testing (see also § 4.1.2.2)

The first step is the selection of test (reference) transmitter(-s) and receiver. If there is no possibility of using a dedicated test transmitter, then it is advisable to make use of existing transmitters, such as operational base stations of land mobile systems in the area of interest. On the receiving side, it is possible to use calibrated hand-held RF field monitors or even the subscriber units of those operational systems under test with field monitoring functions. It is important to place the antenna of the receive unit at an appropriate height; i.e. 1.5-3 m for the land mobile services.

Once the equipment is selected, it is advisable to sketch a field plan for measurements. This may be conveniently done using a map of an appropriate scale. On this map the measurement routes should be outlined as well as measurement points for static measurements. In the following example, it is assumed that static measurements are carried out, because mobile measurements would require access to the mobile monitoring station, and if the latter is available it is usually equipped with all necessary automated measurement functions.

One real example of such a plan for rural area measurements is given below in Fig. A.1.

Note, that it may be very convenient to use a base station that is installed at the crossing of several roads going in various directions. Then the measurements may be done along those roads, as shown in the example in Fig. A.1. But care should be taken that the measurement paths do not leave the main lobe(s) of the base station's antenna pattern if the base station is equipped with directional antennas.

All measurement results should be recorded in a table against the distance from the test transmitter. This also allows an immediate comparison of averaged measured field strength with the results obtained using one or more propagation models. It may be useful to use conventional spreadsheet software for a basic automation of this exercise. One real reduced example of such records is shown in Table A.1.

FIGURE A.1

A real example of planning measurement routes around the test transmitters



TABLE A.1

A real example of measurement record, comparing modelling and measurement results

Location:	Xxxx	Station:	GSM	Hbs (m):	68								
Direction:	Yyyy	Azimuth:	100.0	Hbs_eff(m):	73								
		Frequency:	951.000	erp (dBW):	25								
Area type: Rural, slightly hilly terrain with little vegetation													
Modelling results:				Experimental results:				Measured set:					
Points:		P.370	Lee	Ok-Hata	Average	Deviation	Set	Confid.	R1	R2	R3	R4	R5
km		dB(μ V/m)				dB		+/ - dB		dB(μ V/m)			
5		65.6	79.5	45.1	65.0	1.9	10	1.2	64.8	63.8	67.8	65.3	60.8
10		50.5	66.4	35.3	42.7	3.2	10	2.0	42.8	44.8	44.3	46.3	45.3
15		41.7	58.7	29.5	49.1	0.8	10	0.5	49.8	48.3	48.8	49.8	49.3
20		35.4	53.3	25.4	36.7	1.1	10	0.7	37.3	36.8	35.8	36.3	38.3
25		30.6	49.1	19.5	27.3	3.0	8	2.1	31.8	30.8	26.8	21.8	26.8

The example in Table A.1 was reduced to display data for five distance points only. Normally the measurements should be taken in at least 15-20 distance points, evenly spread along the intended coverage range.

Along with tabular representation shown in Table A.1, a graphical representation may be very illustrative, as shown previously in Fig. 4.2.

A.1.2 Choosing the best model (see also § 4.1.2.2)

Once the measurements are completed in several representative coverage areas, then the model best fitting measurement results may be impartially selected using the least squares criterion (LSC), as shown in expression (4-2). An example is given below of the application of equation (4-2) to compare three models with measurement set from Table A.1.

- a) LSC as applied to measurement results in Table A.1 against the Recommendation ITU-R P.370 model:

$$LSC_{P370}^{areaX} = (65.0 - 65.6)^2 + (42.7 - 50.5)^2 + (49.1 - 41.7)^2 + (36.7 - 35.4)^2 + (27.3 - 30.6)^2 = 126.85$$

- b) LSC as applied to measurement results in Table A.1 against the Lee model:

$$LSC_{Lee}^{areaX} = (65.0 - 79.5)^2 + (42.7 - 66.4)^2 + (49.1 - 58.7)^2 + (36.7 - 53.3)^2 + (27.3 - 49.1)^2 = 1614.9$$

- c) LSC as applied to measurement results in Table A.1 against the Okumura-Hata model:

$$LSC_{OH}^{areaX} = (65.0 - 45.1)^2 + (42.7 - 35.3)^2 + (49.1 - 29.5)^2 + (36.7 - 25.4)^2 + (27.3 - 19.5)^2 = 1023.46$$

The above results demonstrate that for this particular example of set of measurements the Recommendation ITU-R P.370 model provided the best approximation, because it scored the lowest in the least squares analysis. Then by summarizing the performance of the selected models in all propagation areas tested, it is possible to conclude which of the models provides the best fit of experimental results more often than the others.

However, it should be stressed that in order to obtain statistically reliable results, much more extensive sets of data should be used for analysis than shown in this particular illustrative example.

A.1.3 Model tuning (see also § 4.1.2.3)

Precision of the selected generalized empirical model may be further enhanced for particular propagation conditions by means of model tuning, as described in § 4.1.2.3 of this Handbook. An illustrative example is provided below on the practical application of such tuning to the Okumura-Hata model (4-3), using the same reduced set of measurement results as shown in Table A.1.

Okumura-Hata model, for example, can be tuned by the method presented in Section 4.1.2.3 of this Handbook by making use of expressions (4-6) and (4-7). It should be also noted that the parameter x_i in equation (4-6) equals $\log(R_i)$, where R is distance in the same values as used in the model. So, for the set of distances in Table A.1 {5, 10, 15, 20, 25}, it would produce a set of $R = \{0.7, 1, 1.2, 1.3, 1.4\}$. Applying equation (4-6) to the measurement and modelling results from Table A.1 one would obtain the following:

$$\tilde{K} = \frac{(0.7^2 + 1 + 1.2^2 + 1.3^2 + 1.4^2) \cdot (65 + 42.7 + 49.1 + 36.7 + 27.3) - (0.7 + 1 + 1.2 + 1.3 + 1.4) \cdot (0.7 \cdot 65 + 1 \cdot 42.7 + 1.2 \cdot 49.1 + 1.3 \cdot 36.7 + 1.4 \cdot 27.3)}{5 \cdot (0.7^2 + 1 + 1.2^2 + 1.3^2 + 1.4^2) - (0.7 + 1 + 1.2 + 1.3 + 1.4)^2} \approx 95.96$$

$$\tilde{\gamma}_{SYS} = \frac{5 \cdot (0.7 \cdot 65 + 1 \cdot 42.7 + 1.2 \cdot 49.1 + 1.3 \cdot 36.7 + 1.4 \cdot 27.3) - (0.7 + 1 + 1.2 + 1.3 + 1.4) \cdot (65 + 42.7 + 49.1 + 36.7 + 27.3)}{5 \cdot (0.7^2 + 1 + 1.2^2 + 1.3^2 + 1.4^2) - (0.7 + 1 + 1.2 + 1.3 + 1.4)^2} \approx -46.25$$

The above results should be then substituted into equation (4-7). The remaining variables in equation (4-7) describe the parameters of the system under test, in accordance with their definition in the original description of the Okumura-Hata model (equation (4-3)). For this particular example the values from Table A.1 are used accordingly, thus obtaining from equation (4-7) the resulting values of tuned parameters of the empirical propagation prediction model:

$$\tilde{E}_0 = 95.96 - 25 + 6.16 \cdot \log(900) - 13.82 \cdot \log(73) - ((1.1 \cdot \log(900) - 0.7) \cdot 1.5 - (1.56 \cdot \log(900) - 0.8)) \approx 63.4$$

$$\tilde{\gamma} = -\frac{-46.25}{44.9 - 6.55 \cdot \log(73)} \approx 1.4$$

The latter results allow one to conclude that, in a given area, the propagation of radiowaves can be modelled empirically, using the selected Okumura-Hata model (equation (4-3)) with the values of empirical parameters $E_0 = 63.4$ and $\gamma = 1.4$. However, as described in § 4.1.2.3 of this Handbook, it would be advisable to perform such calculation of empirically-tuned parameters in several areas with similar propagation conditions so as to obtain averaged values of E_0 and γ for more general use in a particular country or region (see example in Table 4.1).

Again, it should be stressed that, in order to obtain statistically reliable results, much more extensive sets of data should be used for analysis than that used in this particular example from Table A.1.

APPENDIX B

UNIT CONVERSIONS

B.1 Propagation losses versus field strength

Although, when presenting various models in the text of the Handbook, there are interchangeable references either to the propagation loss modelling or to the field strength prediction, it should be clearly understood that these models provide modelling of the same phenomenon. The propagation losses (usually denoted as L) are linked directly to the received power or field strength by accounting for the actual power radiated into the space by transmitter.

For example, the transmission loss calculated in decibel units may be easily converted into the received power (PR) at the input of the receiver through a logarithmic expression:

$$P_R = P_T + G_T + G_R - L_{ST} - L_{SR} - L$$

where:

P_T : power at the output of transmitter, on logarithmic scale

G_T : gain of transmitting antenna

G_R : gain of receiving antenna

L_S : system losses at the transmitter, e.g. feeder losses

L_{SR} : system losses at the receiver

L : modelled propagation losses.

When it is sufficient to calculate the power or field strength at the reception point before passing into the receiving system, then it is not necessary to account for receiver parameters G_R and L_{SR} in the above expression.

For more detailed description of the relations between propagation losses, signals and system parameters, please see Recommendation ITU-R P.341 – The concept of transmission loss for radio links [B-1].

B.2 Decibel units and logarithmic scale

Very often in radiocommunications, power and other electrical parameters are expressed in decibel units. This allows one to use simple summation instead of more complex multiplication operations. Additionally, its logarithmic scale allows for more simple and uniform representation of an extremely wide dynamic range of radio signal parameters.

It should be noted that the decibel (denoted as dB) itself does not represent the absolute value of the parameter but rather its relation to some reference value. So, for example, the ratio between the output and input powers, p_{out} and p_{in} respectively (gain, G_p), may be described in dB units as follows:

$$G_p = 10 \log_{10} \left(\frac{p_{out}}{p_{in}} \right) \quad \text{dB}$$

For voltages or currents the expression for dB changes due to the fundamental fact that power is proportional to a square of voltage or current. This square transfers into a double multiplier in front of logarithm:

$$G_U = 20 \log_{10} \left(\frac{u_1}{u_0} \right) \quad \text{or} \quad G_I = 20 \log_{10} \left(\frac{i_1}{i_0} \right) \quad \text{dB}$$

Described in this way, the same value of dB means the same relation between two signals, irrespective of whether it was measured using power or voltage/current properties of those signals.

Although decibels themselves represent a ratio between the two parameters, decibels are often transformed to mean the absolute values, when a certain value is used as a reference. For example, for expressing an absolute power the so called “dBW” parameter is often used, which means power of the signal as referred to 1 W:

$$P = 10 \log_{10} \left(\frac{p}{1 \text{ W}} \right) \quad \text{dBW}$$

It may be noted here that very often the original quantities are denoted with lower case letters (such as p in the above expression), while their logarithmic equivalents are denoted with the corresponding capital letters (such as P above).

For example, the power of the transmitter equal to 25 W may be expressed in decibel units as being equal to:

$$10 \log_{10} \left(\frac{25 \text{ W}}{1 \text{ W}} \right) \approx 14 \text{ dBW}$$

Other similar logarithmic expressions for absolute values, that are most commonly used in radiocommunication practice, are shown below as derived from different reference bases:

- for powers where dBW is too large:

$$P = 10 \log_{10} \left(\frac{p}{1 \text{ mW}} \right) \quad \text{dBm}$$

- for amplitude of a received signal:

$$U = 20 \log_{10} \left(\frac{u}{1 \mu\text{V}} \right) \quad \text{dB}\mu\text{V}$$

- for the electric field strength of radio signal:

$$E = 20 \log_{10} \left(\frac{e}{1 \mu\text{V/m}} \right) \quad \text{dB}(\mu\text{V/m})$$

Other decibel-derived units also exist. The reference value used for their establishment may be distinguished by the suffix attached to the dB sign. Sometimes such use of a reference base is extended to the description of absolute gain. For example in radiocommunications “dBi” and “dBd” are often used, which describe the gain of antenna as related respectively to an isotropic radiator or to a half-wave dipole, noting that 0 dBd = 2.15 dBi.

When applied in calculations, the gains expressed in dB (including dBi value of antenna gain) all have the same logarithmic base and may be aggregated arithmetically. For example, when calculating radiated power one may obtain: 14 dBW of transmitter power plus 10 dBi of transmitting antenna gain minus 3 dB of feeder losses produce 21 dBW of e.i.r.p. (equivalent isotropically radiated power).

B.3 Unit conversions

The conversion of logarithmic decibel units of the same kind (e.g. power or field strength), that describe absolute values may be carried out by simple conversion to a different reference base. For example, to convert dBW to dBm, it should be noted first that $0 \text{ dBW} = 1 \text{ W} = 1000 \text{ mW}$, then the conversion may be easily calculated:

$$0 \text{ dBW} = 10 \cdot \log_{10} \left(\frac{1000 \text{ mW}}{1 \text{ mW}} \right) = 30 \text{ dBm}$$

Using the above expression, one can convert from dBW to dBm by simply adding 30 dB, or from dBm to dBW by subtracting 30 dB. For example $14 \text{ dBW} = 44 \text{ dBm}$ and $-55 \text{ dBm} = -85 \text{ dBW}$.

For other cases, when it is necessary to change between the units of a different nature, special conversion formulae should be used; e.g. as described in Recommendation ITU-R P.525 – Calculation of free-space attenuation [B-2]. The most frequent case met in propagation modelling is the need to convert the value of a given field strength into the isotropically received power at a given location or vice versa. This may be obtained using the following conversion formula:

$$P_R = E - 20 \cdot \log f - 167.2$$

where:

P_R : isotropically received power (dBW)

E : electric field strength (dB($\mu\text{V}/\text{m}$))

f : frequency (GHz).

With f in MHz, add 60 dB to the constant (i.e. -107.2). To calculate P_R in dBm, add 30 dB to the constant (i.e. -137.2).

B.4 References

- [B-1] Recommendation ITU-R P.341 – The concept of transmission loss for radio links. International Telecommunication Union, Geneva.
 - [B-2] Recommendation ITU-R P.525 – Calculation of free-space attenuation. International Telecommunication Union, Geneva.
-



* 2 1 4 4 7 *

Printed in Switzerland
Geneva, 2002
ISBN 92-61-09971-8